PHYSICAL REVIEW
LETTERS

VOLUME 6 MAY 1, 1961 NUMBER 9

THERMAL CONDUCTIVITY OF LIQUID He^3†

A. C. Anderson,* G. L. Salinger, and J. C. Wheatley‡
Department of Physics, University of Illinois, Urbana, Illinois
(Received April 13, 1961)

The thermal conductivity of liquid He^3 has been measured in the temperature range from 0.026°K to 0.2°K and at pressures near 10 cm Hg by measuring the temperature difference across a column of liquid through which a constant flow of heat is maintained. The conductivity is found to increase as temperature is decreased, attaining a temperature dependence of T^{-1} below 0.04°K.

The cell used for these measurements was a cylinder, 0.50 cm i.d. by 0.025 cm wall thickness, constructed of paper impregnated with Epibond 104.[1] Two resistance thermometers were made by coating RS-12 Shielding Micropaint[2] on Epibond 104-impregnated paper rings 0.10 cm long by 0.30 cm diameter. Electrical leads of 0.003-in. diameter niobium wire supported the resistors so that they were concentric with the cell wall. The distance L between resistors was 1.10 cm. The resulting value, corrected for thermal contraction, for the ratio L/A, where A is the cross-sectional area of the He^3 column, was 5.59 cm^{-1}. Each end of the cell was closed with a plug of Epibond 104 containing about 3500 Formex-insulated 0.0024-in. diameter copper wires. The final 0.4 cm of each wire was free to extend into the He^3, thus providing a He^3-copper contact area of about 27 cm^2. He^3 entered the cell through a 1/64 in. o.d. by 0.003 in. wall, 70-30 cupro-nickel tube molded into the upper plug.

The wires emerging from the ends of the cell were formed into "foils" of 100 wires each. Those from the upper plug made direct thermal contact with the heat sink, 97 g of chromium potassium alum. The lower set of foils made direct thermal contact to 9.4 g of ~0.16-cm thick cerium magnesium nitrate crystals (CMN). These crystals constituted a thermometer for which the absolute temperature was equal to the ballistically measured magnetic temperature. The thermal time constant of the CMN was always less than that of the cell.

The heater consisted of a 100-ohm, 6-in. length of 0.002-in diameter Evanohm wire[3] woven into the lower plug in such a manner as to insure uniform heating in a plane normal to the axis of the cell. The cell was heated from below to avoid heat transfer by convection.

Resistances were measured using a pair of ac Wheatstone bridges[4] operated at 33.3 cps. At the lowest temperatures the measuring power of 10^{-14} watt to the thermometers produced no observable heating effects. The resistors were maintained below 1°K for the duration of the experiment. Thermal equilibrium times were 5000 sec at 0.03°K, 2500 sec near 0.07°K, and 6000 sec at 0.2°K. The increase at low temperatures resulted from the increasing He^3-copper thermal boundary resistance while that at the highest temperature was due to the properties of He^3 alone.

The thermal conductance of the cell wall was measured using the CMN to determine a temperature drop across the empty cell for a given heat flow. The wall contributed 1% to the total conductance at 0.2°K and a negligible correction below 0.1°K.

Measurements of the CMN temperature and of

the resistances were made during alternate periods with the heater on and off, sufficient time being allowed during each period to obtain thermal equilibrium. The smoothed data with heater off provided a relation between resistance and temperature for each thermometer. These relations, together with the change in resistance with the heater on and off, gave, for each resistor, a value for the increase in temperature, during heating, above that of the heat sink. The difference between these values for the two resistors was taken to be the temperature drop ΔT between them. The conductivity K was calculated from the relation

$$K = (\dot{Q}/\Delta T)(L/A), \qquad (1)$$

where $\dot{Q}$ is the heating rate. Typical heating rates ranged from 0.2 erg/sec at 0.03°K to 1.2 ergs/sec at 0.2°K. The calculated thermal conductivities were independent of power.

The results of this experiment are shown in Fig. 1. Below 0.04°K the smooth curve on the figure represents the relation

$$K = (48/T) \text{ ergs/cm sec}, \qquad (2)$$

which agrees with the data to within experimental error. The data at 0.2°K agree within experimental error with an extrapolation of the conductivity as measured by Lee and Fairbank[5] at 0.24°K and above. The latter measurements

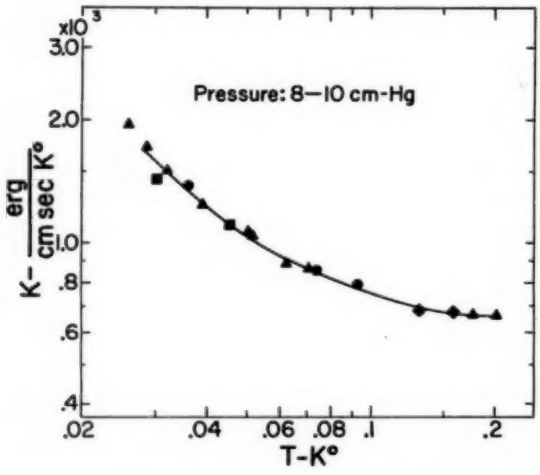

FIG. 1. Log-log plot of the thermal conductivity of He^3 vs the temperature. The points on this graph represent averaged experimental data. The various symbols represent different runs.

have been criticized by Jeener and Seidel,[6] who suggest that at 0.25°K the flow of heat from the walls of the cell into the He^3 might decrease the "measured" conductivity by 30% or more from the true value. However, we have analyzed the experiments of Lee and Fairbank along similar lines, using a range of reasonable estimates for the thermal boundary resistance, and conclude that the experimental agreement for values of K given by cells of different length is strong evidence that the effect pointed out by Jeener and Seidel is not as serious as was originally thought to be the case.

At the lowest temperatures we made an independent determination of the temperature dependence of K and of the thermal boundary resistance by using the temperature change of the CMN with the heater on and off. It is a good assumption in our apparatus that this temperature difference during heating occurred entirely across the cell. If it is assumed that K varies at T^{-1} and the boundary resistance as T^{-3},[7] the total thermal resistance of the cell may by written

$$\Delta T/\dot{Q} = a/T^3 + bT. \qquad (3)$$

Figure 2 shows a plot of $(\Delta T/\dot{Q})T^3$ vs T^4 for $T < 0.04$°K; the data are consistent with the above assumptions. Above 0.05°K the values of $(\Delta T/\dot{Q})T^3$ fall below an extrapolation of the line shown. The individual temperature drops between resistance thermometers and the ends of the cell were similarly treated and are also shown on Fig. 2. From the slopes of the three curves we obtain the thermal resistance of all the He^3, that between the upper resistor and the upper boundary, and that between the lower resistor and the lower boundary. By subtraction we obtain the thermal resistance of the column of He^3 between the two resistors. The resultant thermal conductivity is

$$K = (51/T) \text{ ergs/cm sec}, \qquad (4)$$

in good agreement with Eq. (2). From the intercepts of the three curves in Fig. 2 we obtain the thermal resistance of both boundaries in series, the upper boundary, and the lower boundary. The sum of the upper and lower boundary resistances agrees to within 2% with the independently obtained total resistance. The resultant boundary resistance between He^3 and the Formex-insulated wires is approximately $7\times10^{-6}(AT^3)^{-1}$ $(K°)^4$ cm² sec/erg, where A is the area of contact. This is twice the resistance reported in

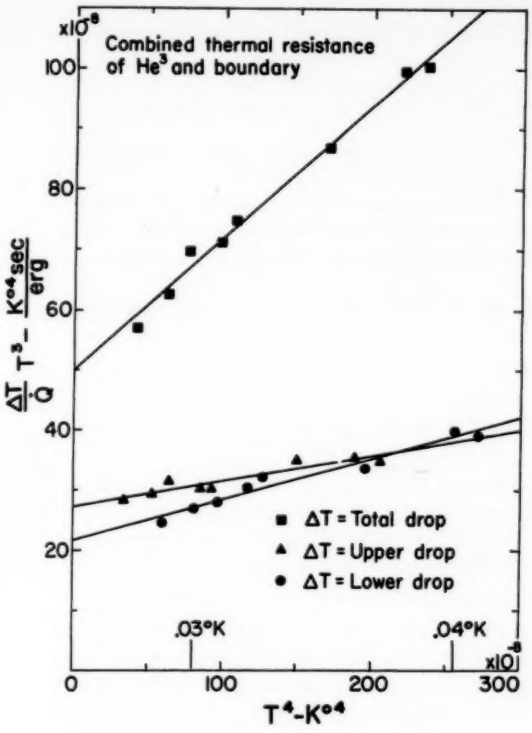

FIG. 2. Plot of $(\Delta T/\dot{Q})T^3$ vs T^4, where ΔT, the temperature difference produced by a heat flow $\dot{Q}$, is much less than T, the average temperature. Curves are shown for ΔT equal, respectively, to the temperature drop across the entire cell, to that between the upper resistance thermometer and the heat sink, and to that between the lower resistance thermometer and the heat source.

reference 7.

Abrikosov and Khalatnikov[8] derive an expression for the thermal conductivity of He^3 based on the Landau theory of a Fermi liquid.[9] An estimate of K can be made[8] by assuming that the scattering probability for two quasi-particles is given by $w(\theta,\varphi)=2\pi f^2/\hbar$, where for definition and evaluation of the quantity f and for notation we refer to reference 8. Evaluating Eq. (8.10) of reference 8, we find

$$K=(13/T)\ \text{ergs/cm sec}. \qquad (5)$$

This is smaller than the observed coefficient by a factor of four. In the numerical work we used the latest empirical values for density,[10] specific heat,[7] and velocity of sound.[11]

If $w(\theta,\varphi)$ were independent of φ and of spin interactions, the ratio D/K, where D is the diffusion coefficient as calculated by Hone,[12] should be independent of w and dependent experimentally only on the value of the susceptibility. Using the low-temperature susceptibility as given by Anderson, Hart, and Wheatley[13] and the theoretical expressions[8,11] for D and K, we find

$$D/K=2\times10^{-6}\ \text{cm}^3\ \text{K}^\circ/\text{erg}, \qquad (6)$$

at 0.03°K. The observed value at 0.03°K is 1×10^{-6} cm³ K°/erg, where the empirical value for D is taken from reference 13. The difference between theory and experiment may be explained by the collision probability being dependent on φ, by different spin dependences of the w applicable to D and K, by the Fermi liquid concept being inapplicable to He^3 at 0.03°K (D appears to have a $T^{-3/2}$ temperature dependence,[13] in disagreement with theory), or by some unknown experimental errors in the temperature scales of the diffusion and conductivity experiments.

The thermal conductivity formula given in reference 8 can be expressed in terms of a relaxation time, τ_K, by the formula $K=\frac{1}{3}v_0^2\tau_K C$, where v_0 is the velocity at the Fermi surface and C is the specific heat per unit volume. Below 0.04°K the experimental data are consistent with a relaxation time $\tau_K=(6\times10^{-13}/T^2)$ sec $(\text{K}^\circ)^2$. At 0.03°K one finds $\hbar/k\tau_K=0.012$°K, where $\hbar$ is Planck's constant divided by 2π and k is Boltzmann's constant, indicating that the quasi-particle concept is probably valid at these low temperatures.

---

†This work has been supported by the U. S. Atomic Energy Commission, The Alfred P. Sloan Foundation, and the Office of Naval Research. It is being submitted by A. C. Anderson in partial fulfillment of the requirements for the Ph. D. degree at the University of Illinois.

*National Science Foundation Fellow.

‡A. P. Sloan Fellow.

[1]Furane Plastics, Inc., 4516 Brazil Street, Los Angeles 39, California.

[2]Micro-Circuits Company, New Buffalo, Michigan. We are indebted to Mr. Bradley of this firm for suggesting the addition of carbon black to RS-12 to obtain a larger temperature coefficient of resistance.

[3]Wilbur B. Driver Company, Newark, New Jersey.

[4]C. Blake, C. E. Chase, and E. Maxwell, Rev. Sci. Instr. 29, 715 (1958). This circuit was modified by using a Hewlett-Packard 200CD oscillator and a phase-sensitive detector, the circuit for which was suggested to us by D. M. Ginsberg. Although the

electrical circuits were well shielded, Joule heating of the resistors at low temperatures by $\sim 10^8$ cps FM and TV signals made measurements inaccurate, so data were obtained when the transmitters were off.

[5]D. M. Lee and H. A. Fairbank, Phys. Rev. 116, 1359 (1959).

[6]J. Jeener and G. Seidel, Proceedings of the Seventh International Conference on Low-Temperature Physics, August 29, 1960, edited by G. M. Graham and A. C. Hollis Hallett (University of Toronto Press, Toronto, Canada, 1961), p. 483.

[7]A. C. Anderson, G. L. Salinger, W. A. Steyert, and J. C. Wheatley, Phys. Rev. Letters 6, 331 (1961).

[8]A. A. Abrikosov and I. M. Khalatnikov, Reports on Progress in Physics (The Physical Society, London, 1959), Vol. 32, p. 329.

[9]L. D. Landau, J. Exptl. Theoret. Phys. U.S.S.R. 30, 1058 (1956) [translation: Soviet Phys. – JETP 3, 920 (1957)].

[10]R. H. Sherman and F. J. Edeskuty, Ann. Phys. 9, 522 (1960).

[11]H. L. Laquer, S. G. Sydoriak, and T. R. Roberts, Phys. Rev. 113, 417 (1959).

[12]Daniel Hone, Phys. Rev. 121, 669 (1961).

[13]A. C. Anderson, H. R. Hart, Jr., and J. C. Wheatley, Phys. Rev. Letters 5, 133 (1960).

"CORKSCREW"—A DEVICE FOR CHANGING THE MAGNETIC MOMENT OF CHARGED PARTICLES IN A MAGNETIC FIELD*

Richard C. Wingerson

Department of Nuclear Engineering and Research Laboratory of Electronics
Massachusetts Institute of Technology, Cambridge, Massachusetts

(Received March 15, 1961; revised manuscript received April 12, 1961)

Consider the motion of a charged particle in the magnetic configuration shown in Fig. 1. A properly designed helical field source (a "Corkscrew") can perturb an initially uniform axial field in such a way that there will be a monotonic increase (or decrease) in the transverse energy component of certain particles traversing the structure. The necessary design condition is that the force resulting from the interaction of the axial particle velocity with the transverse component of the field perturbation be always approximately in the direction of the transverse particle velocity. It follows that there must be a close match between the local pitch of the Corkscrew and that of the modified helical particle trajectory. This condition may be expressed as

$$p(z) = -2\pi m v_z(z)/qB_0, \qquad (1)$$

where B_0 is the unperturbed axial field, m, q, and v_z are the mass, charge, and axial velocity of the particle, and $p(z)$ is the Corkscrew pitch length at position z (p is negative for the left-handed structure of Fig. 1). The helical field perturbation has no over-all effect on the axial field; therefore, a change in the transverse particle energy necessitates a change in magnetic moment. The trajectory in Fig. 1 could apply to an ion moving from left to right or to an electron moving from right to left.

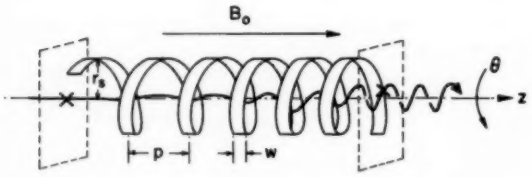

FIG. 1. Schematic diagram of a Corkscrew showing a resonant particle trajectory.

The Corkscrew may permit trapping of a high-energy beam injected axially into a magnetic mirror device. A positive particle following a path as shown in Fig. 1 could be reflected by a magnetic mirror somewhere to the right. On its return, the particle trajectory would have a handedness opposite to that of the Corkscrew, and, therefore, the particle would encounter a series of perturbations alternating in direction at a frequency higher than the cyclotron frequency. These perturbations should cancel to first order, so a mirror to the left would again reflect the particle, and trapping would appear to have been achieved. The Liouville theorem, of course, demands that some mechanism exist for particle loss. The unique feature of the Corkscrew is that this loss mechanism cannot be the same as the trapping mechanism. Trapping is achieved by what is essentially a strong resonance effect. Loss must occur by a random "scatter" effect whose exact nature has not as yet been determined. This nonreciprocal charac-

ter of the Corkscrew is in sharp contrast to axially symmetric nonadiabatic systems previously investigated[1] in which particle loss can occur along paths that are mirror images of paths leading to trapping.

The resonance effect of the Corkscrew has been demonstrated in an experiment wherein an electron beam on the axis of a solenoid was passed through an iron helix. The resulting helical beam was then reflected from a magnetic mirror with mirror ratio 1.8; this indicated that over half the beam energy was in the transverse component. The iron helix was formed from bar stock 1/8 in. thick, 30 in. long, and with width cut to a sine curve 1/2 in. at the center and zero at the ends. The bar was wound onto a cylinder of 1-in. diameter with turns spaced to give a central pitch of 7/8 in. and an over-all length of 4 in. The symmetric structure was necessary to eliminate end effects, and only the exit half was effective in "winding up" the electron beam. The measured ratio of transverse to longitudinal field was approximately 0.15 maximum on axis. For combinations of beam voltage (up to 1 kv) and magnetic field which gave a proper pitch length, reflection occurred from the mirror. Detuning either voltage or magnetic field permitted the beam to pass through the mirror. Reversing the direction of the magnetic field so that the handedness was wrong eliminated the resonance effect, and no beam reflection could be obtained for any value of particle pitch length.

An approximate analytic treatment of the Corkscrew yields the following results, which are presented without complete derivation. The scalar magnetic potential for an infinite helical current-carrying ribbon of constant pitch and radius is given in cylindrical coordinates as

$$\phi_m = I\left\{\frac{z}{p}+\frac{1}{n}\sum_{n=1}^{\infty}\left(\frac{2\pi r_s}{p}\right)K_n'\left(\frac{2n\pi r_s}{p}\right)\left[\frac{\sin(n\pi w/p)}{n\pi w/p}\right]\times\sin\left[n\left(\frac{2\pi z}{p}+\theta\right)\right]I_n\left(\frac{2n\pi r}{p}\right)\right\}, \quad (2)$$

where the K_n' and I_n are Bessel functions, I represents current in the ribbon, and the origin for z and θ is taken at a radial line passing through the center of the ribbon. Pitch length p, ribbon width w, and source radius r_s are shown in Fig. 1. In a practical Corkscrew, a bifilar helix with currents opposed would be desirable because this decouples the helical perturbation from the main axial field. Then, all even n terms vanish from the summation. If we make $w = p/k$ (k an integer), every kth term vanishes. For $k = 3$, the magnetic potential can be expressed very well as

$$\phi_m = +3.3I\left(\frac{r_s}{p}\right)K_1'\left(\frac{2\pi r_s}{p}\right)\sin\left(\frac{2\pi z}{p}+\theta\right)I_1\left(\frac{2\pi r}{p}\right). \quad (3)$$

The application of this equation to a helix of finite length and variable pitch should be qualitatively correct. The perturbation due to an iron helix in an initially uniform axial field is not significantly different.

The equations of motion can be solved under restricted conditions. Define a "phase angle," α, from the equation of motion,

$$\dot{\vec{v}}_z = (q/m)(\vec{v}_\perp \times \vec{b}_\perp) = (q/m)|v_\perp||b_\perp|\sin\alpha, \quad (4)$$

where $\vec{b}_\perp = -\nabla\phi_m$. Use of the ϕ_m from Eq. (3) gives a dependence of $b_\perp$ on pitch length, and Eq. (1) further relates this to v_z. Thus one may write

$$b_\perp = b_0 f(v_z), \quad (5)$$

where $f(v_z)$ is assumed normalized to 1 at $z = 0$. Equation (4) can be solved by taking α = constant (resonance), relating v_z and $v_\perp$ by the conservation of energy, and making a judicious choice of $f(v_z)$ which facilitates solution while still approximating the dependence from Eq. (3). For $v_\perp = 0$ and $v_z = v_0$ at $z = 0$, series expansions of the solution take the form

$$\frac{v_0}{v_z} = 1+\tfrac{1}{2}\left(\frac{qb_0\sin\alpha}{mv_0}z\right)^2+\cdots. \quad (6)$$

Equations (1), (3), and (6) provide an adequate basis for preliminary Corkscrew design.

An interesting coupling appears to exist between Corkscrew influence on the motion of a particle in real and velocity space. If one considers a perturbation given by Eq. (3) on an initially uniform axial field, it can be seen that a particle off axis and in resonance will see a variation in axial field that in the moving frame of reference looks like a steady gradient of field. This observation can be formalized by use of the equation for ∇B drift from guiding center theory.[2] The result is $r^2 v_z \approx$ constant, where r is the guiding center position of the particle in the coordinate system of Eq. (3). The crudeness of the analogy leading to this result makes the value of the exponent questionable. This type of coupling, however, suggests that a Corkscrew might bunch

particles in velocity space at the expense of a diffusion in real space, without violating the requirement for conservation of volume in phase space.

A particle in resonance will experience a form of phase stability. It follows from previous definitions that

$$\dot{\alpha} = (2\pi v_z/p) - \dot{\theta}, \tag{7}$$

and for the structure of Fig. 1

$$\dot{\alpha} \approx -(2\pi v_z/p) + (q/m)B_0. \tag{8}$$

Consideration of Eqs. (4) and (8) shows that phase stability exists for $-\frac{1}{2}\pi < \alpha < \frac{1}{2}\pi$, since if v_z is too large $\dot{\alpha}$ is negative and v_z moves toward larger negative values. The converse is also true. Differentiation of Eq. (8) and elimination of velocity factors by use of Eqs. (4) and (8) leads to a second-order equation for α. The equation is oscillatory for small α and contains a damping term which is positive for p increasing in the direction of z motion and negative for p decreasing. This derivation is very approximate, but it points up a possible area of difficulty in Corkscrew design and further illustrates the complexity of the device.

There are two ways in which Liouville's theorem might be satisfied when the Corkscrew is used as a trapping device. Essentially random scatter of a particle by the field perturbations may cause real space diffusion leading to a radial drift, or may cause velocity space diffusion leading to loss from the mirror loss cone. Equations (4) and (8) suggest the origins of these effects. An axial particle entering a Corkscrew-mirror system as in Fig. 1 will be caught in the stable phase, and v_z will decrease monotonically. This constitutes the trapping pass. On its second or return pass through the Corkscrew, the particle will have a negative v_z, $\dot{\alpha}$ will be large, and $\dot{v}_z$ will average near zero. This situation will occur on every pass for which $v_z < 0$, and the scatter effect will be small. On the third pass, v_z will again be positive, $\dot{\alpha}$ will be small and at some point during the traverse will pass through zero. The cancellation argument used on the second pass will not hold, and it is uncertain just what will happen. If there is no preferred value of α for the $\dot{\alpha} = 0$ condition, then an essentially random scatter in both real and velocity spaces might be expected. If v_z merely oscillates as α changes, then the phase at the exit of the Corkscrew would influence the amount of scatter. If a sufficiently strong mechanism of phase stability exists, it is even possible that the particle would be caught and held in the favorable phase associated with the first pass. At worst there does not seem to be any loss mechanism that could produce an effect amounting to more than a small fraction of the resonance trapping effect. Hopefully, the difference between trapping and loss mechanisms will permit particle containment times to be increased arbitrarily by suitable modification of the basic Corkscrew configuration.

---

*This work was supported in part by the U. S. Army Signal Corps, the Air Force Office of Scientific Research, and the Office of Naval Research; and in part by the National Science Foundation.

[1]K. D. Sinel'nikov, B. N. Rutkevich, and V. D. Fedorchenko, J. Tech. Phys. U.S.S.R. 30, 249 (1960) [translation: Soviet Phys.– Tech. Phys. 5, 229 (1960)].

[2]L. Spitzer, Jr., Physics of Fully Ionized Gases (Interscience Publishers, Inc., New York, 1956), p. 7.

PHONON MASERS AND THE PHONON BOTTLENECK*

C. Kittel†
Department of Physics, University of California, Berkeley, California
(Received April 3, 1961)

It was suggested some years ago by Van Vleck[1] that in some circumstances the lattice phonons cannot always carry off all the power delivered to them by a paramagnetic system, with one-phonon direct coupling. Orbach[2] has estimated under representative conditions the steady-state temperature differences of the spin, direct phonon, and heat bath systems. These differences were not impressively large, showing that the phonons are not necessarily a serious bottleneck.

The conditions for a grave phonon bottleneck are not unrelated to the basic condition for phonon maser action, with paramagnetic ions radiating phonons. The argument of Townes[3] can be readily adapted from the electromagnetic problem to the phonon problem. We consider a solid of volume V containing per unit volume N paramagnetic ions in their upper state and zero in their lower state. We suppose that a single phonon mode of frequency ω and quality factor Q lies within the linewidth $\Delta\omega$ of the paramagnetic transition. All Raman processes are neglected. The electron-phonon coupling is assumed to be described by a spin-strain Hamiltonian,[4]

$$\mathcal{H} = G_{\mu\nu} S_\mu S_\nu e_{\mu\nu}, \qquad (1)$$

linear in the strain components $e_{\mu\nu}$. This form has been demonstrated, particularly by the work of Shiren and Tucker, to account in a consistent way for the observations on direct spin-phonon interactions. The largest value of the coupling constant G reported by Shiren[5] is $\sim 10^{-13}$ erg, for Fe^{2+} in MgO; the smallest, for Mn^{2+} in MgO, is $\sim 10^{-16}$ erg. The estimates in reference 4 were made with $G = 3\times 10^{-14}$ erg.

The initial rate at which the spin system transfers energy to the isolated mode ω is of the order of

$$\hbar\omega(2\pi/\hbar)e^2|G|^2(1/\hbar\Delta\omega)NV,$$

while the rate at which the phonon energy decays is

$$\tfrac{1}{2}Ce^2V(\omega/Q),$$

where C is the elastic modulus. The condition for the buildup of stimulated phonon emission is that the gain should exceed the loss, or that

$$N > C\hbar\Delta\omega/(4\pi|G|^2Q).$$

If we take $C = 10^{12}$ ergs/cm^3, $\Delta\omega = 2\pi\times 10^7$ sec^{-1}, $G = 10^{-14}$ erg, and $Q = 100$, then for maser action $N > 0.5\times 10^{18}$ cm^{-3}. This is the value by which the concentration in the upper state must exceed that in the lower state, but our argument has assumed (for simplicity) that the latter is itself negligible. It therefore appears feasible to obtain a phonon bottleneck leading to maser action.

I am indebted to Professor Y. Rocard and Professor P. Aigrain for the hospitality of the Ecole Normale Supérieure, where these calculations were made. Dr. N. S. Shiren kindly furnished the estimates of the spin-strain coupling constants.

---

*Supported in part by the National Science Foundation.

†Professor of Physics in the Miller Institute for Basic Research in Science.

[1]J. H. Van Vleck, Phys. Rev. 59, 724 (1941).

[2]R. Orbach, Proc. Roy. Soc. (London) (to be published).

[3]J. P. Gordon, H. J. Zeiger, and C. H. Townes, Phys. Rev. 99, 1264 (1955); C. H. Townes (unpublished) has independently suggested that an ultrasonic maser was feasible.

[4]C. Kittel, Phys. Rev. Letters 1, 5 (1958); a relation between $|G|^2$ and T_1T is also given in this Letter.

[5]N. S. Shiren (private communication).

HYPERFINE FIELD AND ATOMIC MOMENT OF IRON IN FERROMAGNETIC ALLOYS

C. E. Johnson, M. S. Ridout, T. E. Cranshaw, and P. E. Madsen
Atomic Energy Research Establishment, Harwell, England
(Received February 1, 1961; revised manuscript received April 10, 1961)

Mott and Stevens[1] and Lomer and Marshall[2] have proposed models of the ferromagnetic alloys of the iron group metals, based on the assumption that for dilute alloys a rearrangement of electrons occurs around solute atoms only, while to a first approximation the electronic structure of the matrix atoms remains unaltered from that in the pure metal. Each atom carries a localized magnetic moment which contributes directly to the total saturation moment and to the magnetic part of the neutron scattering cross section, and indirectly to the hyperfine field H_n. Marshall[3] has shown that the hyperfine field in a pure ferromagnetic metal should be proportional to the magnetization. This has been confirmed experimentally for cobalt[4] and for iron[5] by varying the temperature, but the absolute agreement between theory and measurement is poor.[6] The Mössbauer effect[7] provides a method for measuring H_n for iron in alloys which may be used to test the localized models and to investigate the relation between hyperfine field and atomic moment.

We have measured the Mössbauer absorption spectrum at room temperature over the whole range of Fe-Co and Fe-Ni alloys for the 14.4-kev γ radiation of Fe^{57}. The source was prepared by electroplating Co^{57} onto copper foil, followed by diffusion by annealing. Rapid electron spin exchange resulted in a single line which had the natural width associated with the lifetime of the emitting state: The line was shifted by 0.20 mm/sec with respect to the center of the iron spectrum. The alloys were prepared by arc-casting spectroscopically standardized materials supplied by Johnson Matthey, Ltd., and were cold rolled into foils about 1 mil thick. Alloys containing 30% or less iron were enriched in Fe^{57} by plating and annealing. Data for pure cobalt and nickel were obtained with Co^{57} sources plated onto foils of each metal, using stainless steel as a monoenergetic absorber.[8] Motion of the source was provided by a moving coil vibrator driven by an amplifier and a triangular wave generator. A moving iron transducer gave a voltage proportional to the source velocity, and this waveform was fed back to the input of the amplifier, so that the velocity of the source closely followed the input waveform. Counts were fed into a single-channel pulse-height analyzer to select the 14.4-kev radiation, and the output pulses were modulated with the velocity waveform and fed into a 100-channel kicksorter. The resulting spectrum[9] showed six lines arising from the Zeeman splitting of the nuclear levels of Fe^{57}, and the hyperfine field was computed from their separations. The spectra for the alloys showed no appreciable line broadening or shifts compared with the pure iron spectrum. Hence, the variations in hyperfine field due to local inhomogeneities are small (less than 3%), and there is no large change in s-electron density at the iron nuclei due to alloying.

The variation of the magnetic field at iron nuclei in the alloys, expressed as a fraction of the field in metallic iron, is shown in Fig. 1, where $H_n(x)/H_n(0)$ is plotted against the excess electron number x over that of iron. A remarkable feature is the general similarity in form with the corresponding region of the Slater-Pauling curve[10] for the saturation moments: For both alloy systems H_n and the saturation moment show a maximum near $x = 0.3$. Even for small additions of solute it seems that large changes in the hyperfine field of the iron atoms result, in contrast to the localized theories.

If it is assumed that the hyperfine field is proportional to the atomic moment in the alloys, then the moment on iron is given by $\mu(\mathrm{Fe}) = 2.22 H_n(x)/H_n(0)$ Bohr magnetons. The field on cobalt nuclei in Fe-Co alloys has been determined from low-temperature specific heat measurements by Arp, Edmonds, and Petersen,[11] and in contrast to the field on iron nuclei it shows no maximum but increases steadily from 217×10^3 gauss in pure cobalt to about 320×10^3 gauss in iron. From these data a curve for $\mu(\mathrm{Co})$ may be derived, taking the moment in pure cobalt to be 1.71 Bohr magnetons. If these moments are averaged so that $\bar{\mu} = (1-c)\mu(\mathrm{Fe}) + c\mu(\mathrm{Co})$, where c is the cobalt concentration, $\bar{\mu}$ is found to lie on a curve which is close to the Slater-Pauling curve.

There are no data on the hfs of nickel in Fe-Ni alloys, but Shull and Wilkinson[12] have measured the atomic moments in some of these alloys by neutron diffraction. For ordered Ni_3Fe they find $\mu(\mathrm{Fe}) = 2.8$, whereas our data, combined with the

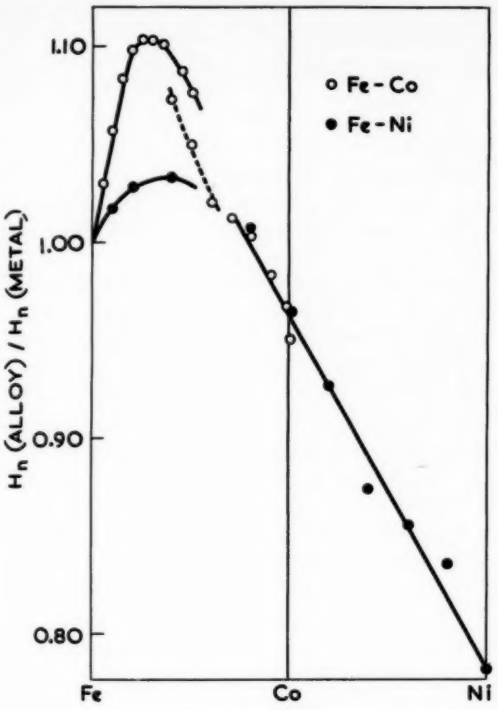

FIG. 1. The magnetic field at iron nuclei in Fe-Co and Fe-Ni alloys relative to the field in metallic iron, plotted as a function of electron number. The data in the range $Fe_{0.8}Ni_{0.2}$ to $Fe_{0.5}Ni_{0.5}$ where the Curie points are low have been corrected to take account of incomplete saturation at room temperature. Points for Co and Ni agree well with the results given by Wertheim.[8] Alloys near $Fe_{0.5}Co_{0.5}$ are very brittle and difficult to roll and the points on the dashed curve were taken with small and cracked specimens. Alloys were also prepared in this range by electroplating and they gave higher values for H_n which lie on the continuous curve.

assumption that atomic moment is proportional to H_n, give about 1.8. This implies that the proportionality between atomic moment and H_n is not strictly valid in alloys. The discrepancy could be explained by a contribution to H_n which depends on the nickel as well as the iron moments, e.g., if the component due to the conduction electron polarization were a function of the average moment $\bar{\mu}$. Since $\bar{\mu}$ for Ni_3Fe is smaller than that for iron and H_n is negative,[13] this explanation requires the polarization to be negative in accord with a suggestion of Anderson and Clogston[14] and with measurements of the field at tin nuclei in alloys with iron.[15] An estimate of the effect of such a term in the Fe-Co alloys shows that, owing to the smaller variation of $\bar{\mu}$ throughout the series, it would not destroy the agreement between $\bar{\mu}$ derived from hfs and saturation magnetization data.

We thank Dr. W. Marshall and Dr. W. M. Lomer for many valuable discussions, Dr. J. H. Stephen for performing the electroplating, and Dr. E. Bretscher for his generous support.

[1]N. F. Mott and K. W. H. Stevens, Phil. Mag. 2, 1364 (1957).
[2]W. M. Lomer and W. Marshall, Phil. Mag. 3, 185 (1958).
[3]W. Marshall, Phys. Rev. 110, 1280 (1958).
[4]A. M. Portis and A. C. Gossard, J. Appl. Phys. 31, 205S (1960).
[5]D. E. Nagle, H. Frauenfelder, R. D. Taylor, D. R. F. Cochran, and B. T. Matthias, Phys. Rev. Letters 5, 364 (1960).
[6]S. S. Hanna, J. Heberle, G. J. Perlow, R. S. Preston, and D. H. Vincent, Phys. Rev. Letters 4, 513 (1960).
[7]R. L. Mössbauer, Z. Physik 151, 124 (1958).
[8]G. K. Wertheim, Phys. Rev. Letters 4, 403 (1960).
[9]S. L. Ruby, L. M. Epstein, and K. H. Sun, Rev. Sci. Instr. 31, 580 (1960).
[10]See, e.g., C. Kittel, Introduction to Solid-State Physics (John Wiley & Sons, Inc., New York, 1953), Chap. XII.
[11]V. Arp, D. Edmonds, and R. Petersen, Phys. Rev. Letters 3, 212 (1960).
[12]C. G. Shull and M. K. Wilkinson, Phys. Rev. 97, 304 (1955).
[13]In collaboration with Dr. G. J. Perlow we have shown that the sign of the field is negative for $Fe_{0.2}Ni_{0.8}$ as well as for iron.
[14]P. W. Anderson and A. M. Clogston, Bull. Am. Phys. Soc. 6, 124 (1961).
[15]A. J. F. Boyle, D. St. P. Bunbury, and C. Edwards, Phys. Rev. Letters 5, 553 (1960).

SUPERCONDUCTIVITY OF Nb_3Sn IN PULSED FIELDS OF 185 KILOGAUSS*

V. D. Arp, R. H. Kropschot, and J. H. Wilson
National Bureau of Standards, Cryogenic Engineering Laboratory, Boulder, Colorado
and
W. F. Love and R. Phelan
Department of Physics, University of Colorado, Boulder, Colorado

(Received April 10, 1961)

We have observed the superconductivity of a Nb_3Sn wire in pulsed magnetic fields of 185 kgauss. When extrapolated to negligible measuring current, the critical field of this specimen appears to be about 188 kgauss at 1.6°K.

The wire was prepared by the NBS Metallurgy Division. They followed the procedure outlined by Kunzler et al.,[1] except that the wire was swaged rather than drawn to final diameter (0.50 mm). The 12-cm long specimens were annealed in a vacuum for 16 hours at 1000°C, after which the sample ends were etched in $2H_2SO_4 + 2HNO_3 + HF$ and then immediately tinned in a bath of molten indium. Current and potential leads were attached using indium solder. The sample was oriented parallel to the field of a pulsed magnet having an i.d. = 1.4 cm and a length of 6.4 cm. Current and potential leads to the sample were thus completely outside of the magnet.

The magnetic field as a function of time is shown as the upper trace in Fig. 1. The field rises to a peak of 185 kgauss in 7 msec. The lower trace in the figure is the voltage across the sample with a small steady current flow. However, most of the data were obtained using square current pulses of 2 msec or less duration initiated after controlled time delays from the start of the field pulse. This procedure reduces the undesirable effects of Joule heating in the current leads. A transient voltage signal is seen at the beginning of the trace when the field pulse is initiated. Superconductivity is destroyed when the voltage finally reappears. We interpret the continuously increasing voltage with time as a spread of the normal region to the outer ends of the wire where the applied field is small.

The results of a number of such measurements are plotted in Fig. 2. The results are limited by the maximum of 23 amperes obtainable from the current source which was used. This corresponds to a current density in the core of approximately 10^5 amp per cm^2. The noise on the sample potential leads during the field pulse is

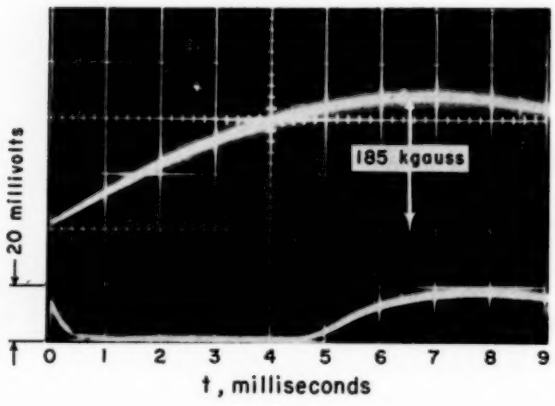

FIG. 1. Upper trace: magnetic field as a function of time. Lower trace: sample voltage as a function of time with 3-amp current.

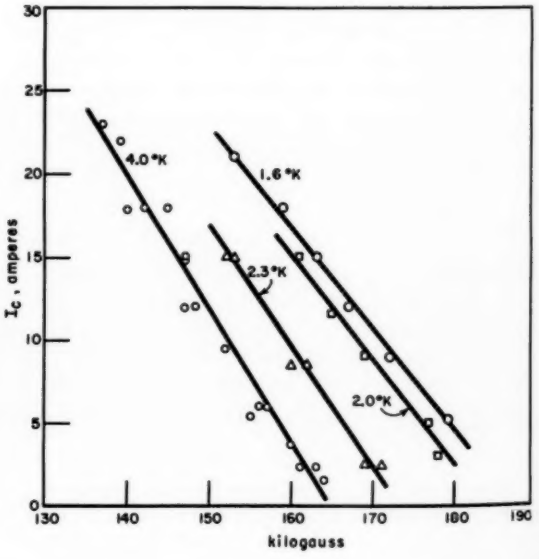

FIG. 2. Critical current versus magnetic field.

the order of 0.5 millivolt, so that the sensitivity of this pulse method of determining sample resistance is about 10^4 times less than the dc method used by Kunzler.

We have made an estimate of eddy current heating in the sample during the field pulse. Above the lambda point (2.17°K) the sample might warm by as much as 1°K. Below the lambda point the high heat transfer rate to superfluid helium should restrict the temperature rise to less than 0.5°K. The temperatures indicated in Fig. 2 are those of the helium bath. The shift in critical field from just above to just below the lambda point indicates that heat exchange to the bath has a measurable but not important effect on the data.

The attenuation of the pulsed field through the niobium sheath can be calculated from equations given by Kosevich.[2] It turns out to be the order of 1 gauss and so is completely negligible.

The great interest in Nb_3Sn wire is, of course, for use in superconducting magnets. In this application it is necessary to know the critical field transverse to the current flow, rather than parallel to it as in our experiment. For a "soft" perfectly diamagnetic specimen the transverse critical field (which restores the first trace of resistance) is one half of the longitudinal critical field. For a hard superconductor, in which flux penetration is nearly complete, these two critical fields are nearly the same. The measurements reported here certainly set an upper limit on the critical field for transverse measurements on this specimen. Kunzler[1] reports that the critical current in their samples scales with diameter in a manner intermediate between that of soft and that of hard superconductors. We are continuing our measurements, and hope to obtain transverse critical fields in the near future.

J. G. Anderson and C. J. Pierce have been very helpful in setting up the apparatus for this experiment. We thank L. L. Wyman of the NBS Metallurgy Division for supplying the wire. We appreciate the suggestion of P. Aron and T. Hitchcock of the Lawrence Radiation Laboratory for the acid etch in order to make good electrical contacts.

---

*This work was supported in part by the U. S. Atomic Energy Commission and the Army Research Office.

[1]J. E. Kunzler, E. Buehler, F. S. Hsu, and J. H. Wernick, Phys. Rev. Letters 6, 89 (1961).

[2]A. M. Kosevich, J. Exptl. Theoret. Phys. U.S.S.R. 33, 735 (1958) [translation: Soviet Phys.—JETP 6, 564 (1958)].

ULTRASONIC CYCLOTRON RESONANCE IN GALLIUM

B. W. Roberts

General Electric Research Laboratory, Schenectady, New York

(Received April 5, 1961)

Mikoshiba[1] suggested that a cyclotron resonance of metallic electrons could be induced by ultrasonic waves in which the attenuation of the sound waves should be a maximum whenever the frequency of the sound wave is an integral multiple of the cyclotron frequency, $\omega = n\omega_c$. This type of resonance has been seen in the semimetal bismuth[2] but not in any true metal, because the condition required—that $\omega\tau$ be greater than unity—has not been met. This requirement makes severe demands on metal purity; for example, at 100 Mc/sec an electron mean free path of approximately one cm is required to obtain $\omega\tau = 5$.

Single crystals of the metal Ga, kindly prepared and supplied by Kramer and Foster,[3] have been shaped by careful machining techniques into oriented ultrasound specimens about 1 cm in thickness. The electronic grade Ga from which the crystals were grown had a room temperature to 4.2°K resistivity ratio of about 50 000 determined by dc four-probe methods.

Standard ultrasonic pulse techniques[4] were used with a single transducer for transmission and detection. The bonding agent was a silicone fluid with viscosity of 20 000 centistokes.

In Fig. 1 the reflected pulse amplitude is plotted as a function of field for a longitudinal, 115-Mc/sec sound wave traveling along the c_0 axis at 1.6°K. Two types of resonance behavior are present. The first consists of a geometric resonance with a maximum (indicated by a minimum in the pulse amplitude) at 80 oe and additional members of the series occurring at equal intervals of $(1/H)$. About 30 maxima have been ob-

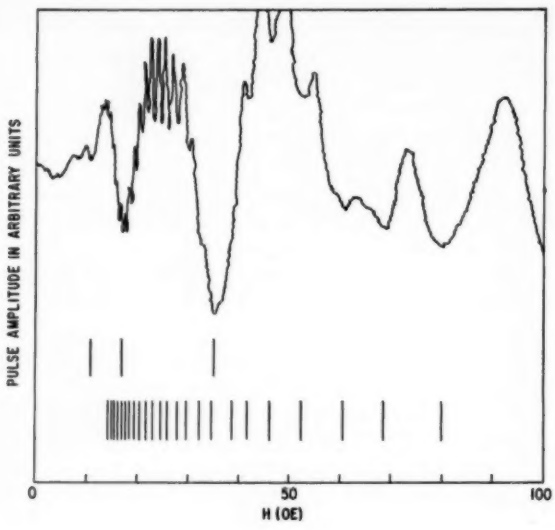

FIG. 1. Reflected ultrasound pulse in Ga as a function of magnetic field. $f = 115$ Mc/sec. $T = 1.5°K$. Upper reference marks indicate ultrasonic cyclotron resonance maxima. Lower reference marks indicate observed geometric resonance maxima.

served, including those which exist above 80 oe. Geometric resonance occurs when the electron orbit dimensions match the sonic wavelength and subsequent maxima are predicted nearly by $\Delta(1/H) = (\lambda/2)(e/c)(1/\hbar k)$, where $\hbar k$ is the electron momentum. The unusually large number of maxima observed in this experiment indicate that the resonance arises from a well-defined extremal portion of the Fermi surface and that electrons in the material have an unusually long mean free path.

The second resonance behavior, the cyclotron resonance, has maxima indicated at 35, 17, and 11 oe. A smoothed curve through the cyclotron resonance maxima but ignoring the geometric resonance maxima is shown in Fig. 2(b); the data here are plotted as attenuation relative to the attenuation at $H = 0$, and they are compared with the predictions of Cohen, Harrison, and Harrison[5] in Fig. 2(a). Both the experimental and theoretical curves are for longitudinal ultrasonic waves, the theoretical curve for $\omega\tau = 10$ and the experimental one for $\omega\tau \sim 5$. Marked similarity exists, although the third maximum is less pronounced in the experimental observations, probably because of the lower $\omega\tau$.

In order to verify that the maxima attributed to the cyclotron resonance and those attributed to the geometric resonance were actually due to those causes, the experiment was repeated with a shear wave produced with an AC-cut quartz transducer. The frequency of the shear wave (116 Mc/sec) was approximately equal to that of the longitudinal, but because its velocity is only 2.4×10^5 cm/sec compared to the longitudinal velocity of 4.7×10^5 cm/sec, the wavelength of the transverse waves was less than that of the longitudinal. The first two maxima of the cyclotron resonance were found to persist at the same H values, while marked changes occurred in the geometric resonance.

The presence of the maximum at only 11 oe in the cyclotron resonance series indicates an orbit circumference of about mcv_f/eH or 0.8 cm, where v_f is the Fermi velocity. Also, if we consider the requirements for the geometric reso-

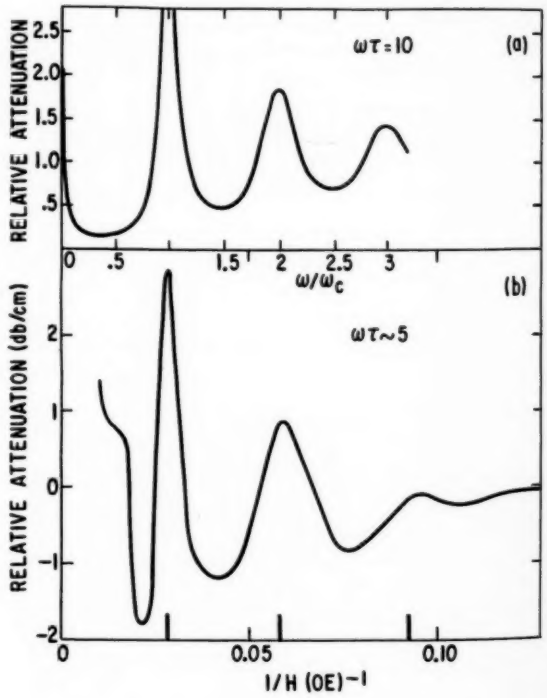

FIG. 2. (a) Predicted relative attenuation for ultrasonic cyclotron resonance after Cohen, Harrison, and Harrison.[5] (b) Observed curve in Ga single crystal derived from data in Fig. 1.

nance series with about 30 maxima, we find that the orbit circumference must be about $30\pi\lambda = 0.4$ cm. The maxima of both phenomena sharpened and the background attenuation shifted as the temperature was reduced from 4.2°K to 1.5°K, suggesting that the resistivity of the Ga was changing. Using these measurements and extrapolating the resistivity measurements of Olsen-Bär and Powell,[6] one finds that $\rho_{1.5°K}$ must be of the order of 10^{-12} ohm cm. Recent measurements by Weisberg and Josephs[7] also indicate that very low resistivity values may occur in Ga samples at 1.26°K. These four observations suggest that a mean free path, l, of order 1 cm is obtained in these Ga crystals at 1.5°K. Associated values of $\omega\tau \sim 5$ and $ql \sim 1500$ follow, where q equals $2\pi/\lambda$. The condition for geometric resonance is $ql > 1$ and is much less stringent than the condition for observing cyclotron resonance.

The topology of the Fermi surface is yet to be established, but the geometric resonance presented here suggests an extremal dimension (1.3×10^{-20} g cm/sec) consistent with regions of electrons in the seventh zone as predicted by the nearly free electron model.[8] The effective electronic mass, m^*, derived from the cyclotron resonance for the same orientation is $0.8_4 m_0$.

Further study of the Ga Fermi surface topology and related effective masses is under way.

I thank my colleagues, T. G. Castner, Jr., F. E. Dickey, and H. R. Hart, Jr., for encouragement and suggestions in equipment design, L. M. Osika for assistance in crystal orientation, and Dr. Kramer and Dr. Foster, Alcoa Research Laboratories, for provision of the samples.

[1]N. Mikoshiba, J. Phys. Soc. Japan 13, 759 (1958).
[2]D. H. Reneker, Phys. Rev. 115, 303 (1960).
[3]R. A. Kramer and L. M. Foster, Alcoa Research Laboratories, New Kensington, Pennsylvania.
[4]B. W. Roberts, Phys. Rev. 119, 1889 (1960).
[5]M. H. Cohen, M. J. Harrison, and W. A. Harrison, Phys. Rev. 117, 937 (1960).
[6]M. Olsen-Bär and R. W. Powell, Proc. Roy. Soc. (London) A209, 548 (1951).
[7]L. R. Weisberg and R. M. Josephs, Bull. Am. Phys. Soc. 5, 430 (1960).
[8]W. A. Harrison, Phys. Rev. 116, 555 (1959).

GENERATION-RECOMBINATION NOISE IN p-TYPE GOLD-DOPED GERMANIUM

L. J. Neuringer and W. Bernard
Research Division, Raytheon Company, Waltham, Massachusetts
(Received April 10, 1961)

Preliminary estimates of the capture cross sections of free holes by the 0.041-ev donor level and the 0.145-ev acceptor level in p-type gold-doped germanium have been obtained from measurements of the generation-recombination noise spectrum in the range 10^4-10^7 cps. At 97°K the Fermi level of the sample studied was located midway between the two gold levels, such that the noise spectrum simultaneously exhibited relaxation times characteristic of both levels. A two-impurity level model appropriate to the gold-doped germanium system was employed to predict the observed noise in terms of the capture cross sections. Good agreement was obtained between theory and experiment, using values for the total cross sections of $\sigma_A = 1.55 \times 10^{-12}$ cm^2, $\sigma_D = 3.75 \times 10^{-18}$ cm^2. To our knowledge this work represents the first experimental observation of two-level generation-recombination noise in gold-doped germanium and the development of a theory capable of accounting for all of the observed noise in interacting two-level systems of this type.

Generation-recombination noise in semiconductors arises from the modulation of the conductivity by the random thermal fluctuation of charge carriers between the valence (or conduction) band and the impurity levels. Thus, for an extrinsic semiconductor the time-dependent second moment $\langle \Delta J(0) \Delta J(t) \rangle$ of the current fluctuations is simply related to the corresponding moment $\langle \Delta p_V(0) \Delta p_V(t) \rangle$ of the fluctuations in the valence band population:

$$\langle \Delta J(0) \Delta J(t) \rangle = (J^2/p_V^2) \langle \Delta p_V(0) \Delta p_V(t) \rangle , \quad (1)$$

where J is the average current and p_V the equilibrium valence band population. The generation-recombination noise spectrum $G(f)$ is the Fourier transform of Eq. (1).

Van Vliet[1] has developed a general prescription for obtaining the free carrier fluctuations in multilevel systems by computing the linear

response of the various level populations to the thermodynamically conjugate applied Fermi potentials and has applied this technique to several simple systems and to the Shockley-Read model. We shall adopt the more straightforward approach of calculating the free carrier fluctuations directly, which is, of course, equivalent to the fluctuation-dissipation theorem of Callen and co-workers.[2] The model of p-type gold-doped germanium we consider is indicated in Fig. 1, which shows the impurity level scheme, and also the Fermi level as a function of temperature for the sample studied, as given by Klein and Debye.[3] The shallow acceptor level is assumed to be completely ionized at 97°K, so that only two independent variables need be considered. These we take to be the hole populations p_V and p_D of the valence band and gold donor level, respectively. The customary assumption is made regarding the interaction of the gold levels, wherein the number $N_{Au}{}^0$ of neutral gold atoms corresponds simultaneously to the number of ionized donor states and the number of filled acceptor states.

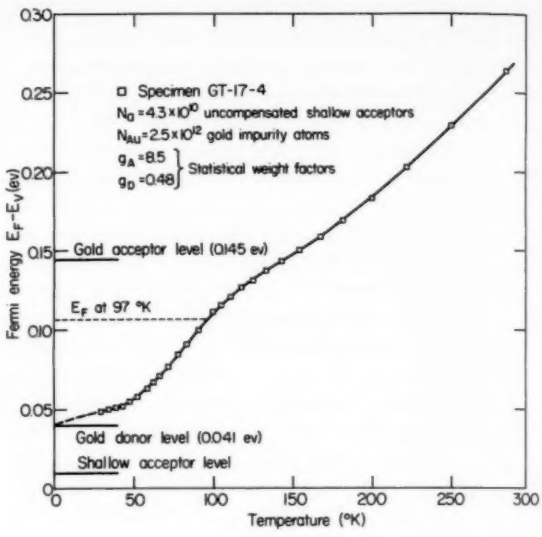

FIG. 1. Energy level scheme for Au-doped p-type germanium.

The linear kinetic equations for the displacements Δp_V and Δp_D of the hole populations of the valence band and donor level, respectively, have the form

$$d\Delta p_V(t)/dt = -A_{VV}\Delta p_V(t) - A_{VD}\Delta p_D(t), \quad (2)$$

$$d\Delta p_D(t)/dt = -A_{DV}\Delta p_V(t) - A_{DD}\Delta p_D(t), \quad (3)$$

where the A_{ij} are functions of the equilibrium statistics and the capture cross sections σ_A and σ_D. The lifetimes are the usual roots of the secular determinant obtained from these equations. $\Delta p_V(t)$ is taken to be a linear combination of decaying exponentials,

$$\Delta p_V(t) = C_1 e^{-t/\tau_1} + C_2 e^{-t/\tau_2}, \quad (4)$$

the expansion coefficients being determined by the initial conditions. The free carrier fluctuation moment $\langle \Delta p_V(0)\Delta p_V(t)\rangle$ is obtained from Eq. (4) by multiplying through by $\Delta p_V(0)$ and averaging over the equilibrium system. Substituting this result into Eq. (1) and taking the Fourier transform yields the noise spectrum in the form

$$G(f) = 4\frac{J^2}{p_V{}^2(\tau_1 - \tau_2)}\left\{\frac{\tau_1{}^2[(1-\tau_2 A_{VV})\langle(\Delta p_V)^2\rangle - \tau_2 A_{VD}\langle\Delta p_V \Delta p_D\rangle]}{1+(2\pi f\tau_1)^2} - \frac{\tau_2{}^2[(1-\tau_1 A_{VV})\langle(\Delta p_V)^2\rangle - \tau_1 A_{VD}\langle\Delta p_V \Delta p_D\rangle]}{1+(2\pi f\tau_2)^2}\right\}. \quad (5)$$

The fluctuation moments $\langle(\Delta p_V)^2\rangle$ and $\langle\Delta p_V \Delta p_D\rangle$ appearing in Eq. (5) can be computed from the free energy, according to the equilibrium fluctuation theory of Greene and Callen,[4] by solving the equations

$$\sum_k \frac{\partial^2 F}{\partial p_i \partial p_k}\langle \Delta p_k \Delta p_j\rangle = kT\delta_{ij}. \quad (6)$$

The free energy appropriate to the interacting gold levels in germanium is

$$F = -p_V E_V - kTp_V \ln\frac{N_V}{p_V} - p_D E_D - kT\ln\frac{g_D{}^{p_D}(N_{Au}{}^0 + p_D)!}{p_D!\,N_{Au}{}^0!} - (N_{Au}{}^0 + p_D)E_A - kT\ln\frac{g_A{}^{(N_{Au}{}^0+p_D)}(N_{Au})!}{(N_{Au}{}^0+p_D)!\,(N_{Au}-N_{Au}{}^0-p_D)!}. \quad (7)$$

That Eq. (7) is correct can be verified by showing

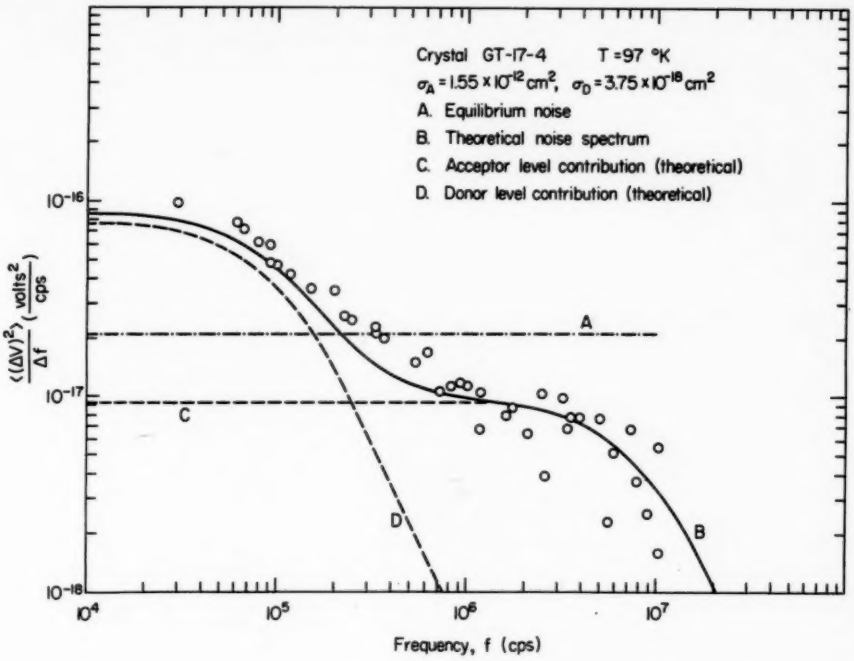

FIG. 2. Generation-recombination noise spectrum.

that it is consistent with Klein's calculation[3] of the equilibrium level populations using the grand canonical potential.

The experimental noise spectrum, obtained by standard techniques similar to those employed by van der Ziel and co-workers,[5] is shown by the circles in Fig. 2. These data have been corrected for the equilibrium noise, indicated by Curve *A*, and certain high-frequency characteristics of the apparatus. Two characteristic relaxation times, corresponding roughly to the two gold levels, are clearly evident. The increased scatter of the data in the high-frequency range can be attributed to the low generation-recombination noise level relative to the equilibrium noise. The best fit of Eq. (5) to the experimental points, corresponding to the total hole capture cross sections $\sigma_A = 1.55 \times 10^{-12}$ cm^2 and $\sigma_D = 3.75 \times 10^{-18}$ cm^2, is shown by solid Curve *B*. These values are in qualitative agreement with those obtained independently using other techniques. For example, the field-effect studies of Rupprecht[6] yield the cross sections $\sigma_A = 4.85 \times 10^{-13}$ cm^2, $\sigma_D = 6.70 \times 10^{-19}$ cm^2.

From Fig. 2, the quantitative agreement between theory and experiment is seen to be quite good, especially for the acceptor level contribution, Curve *C*. The significance of the small discrepancy associated with the donor level contribution, Curve *D*, is not as yet clear. Aside from experimental causes, such a discrepancy might arise either from the incidental presence of copper, which has an acceptor level at ~0.04 ev, or from the contribution of excited gold donor states to the generation-recombination process. Further studies are planned on additional crystals as they become available, as are investigations of the temperature dependence of the noise spectrum. We wish to thank G. Rupprecht of this laboratory for lending us this particularly appropriate crystal and to acknowledge the experimental assistance of E. Wang during the early phases of the work.

[1]K. M. van Vliet, Phys. Rev. 110, 50 (1958).

[2]H. B. Callen and T. A. Welton, Phys. Rev. 83, 34 (1951); H. B. Callen and R. F. Greene, Phys. Rev. 86, 702 (1952).

[3]C. A. Klein and P. P. Debye, Proceedings of the International Conference on Semiconductors, Prague, 1960 (to be published).

[4]R. F. Greene and H. B. Callen, Phys. Rev. 83, 1231 (1951).

[5]A. van der Ziel (private communication).

[6]G. Rupprecht, Proceedings of the International Conference on Semiconductors, Prague, 1960 (to be published).

CYCLOTRON RESONANCE OBSERVATIONS IN CADMIUM

J. K. Galt, F. R. Merritt, and P. H. Schmidt
Bell Telephone Laboratories, Murray Hill, New Jersey
(Received March 30, 1961)

We have observed cyclotron resonance effects in single-crystal samples of cadmium at 1.3°K, or below, and at both 24 000 Mc/sec and 72 000 Mc/sec. We have done the experiment with the magnetic field, B_{dc}, along each of the three principal axes [$\langle 0001\rangle$, $\langle 11\bar{2}0\rangle$, and $\langle 10\bar{1}0\rangle$] and with it both parallel and perpendicular to the sample surface in each case. The effective masses observed range from 0.35 to about 1.5, and are somewhat similar to those observed in zinc, for which preliminary results have previously been reported.[1,2]

The experiments were done using a technique previously reported,[3] and will, therefore, be described only briefly. The crystallographically oriented plane surface of a disk sample is made to form part of the wall of a cylindrical cavity, and a signal proportional to the variation in the power absorption coefficient of the sample surface is observed as a function of applied magnetic field. The radiation incident on the sample is substantially circularly polarized; the part of the radiation with the undesired circular polarization is 15%, or less, in power density of that with the desired circularity.

Single-crystal boules of cadmium were grown from zone-refined raw material in vacuum, using the Bridgman method. Samples cut from these boules showed residual resistance ratios $[R_{300°K}/R_{4.2°K}] \cong 30000$. The boules were oriented by means of x-ray techniques, and disk-shaped samples were then cut from them with an acid string saw.

Figure 1(a) shows data taken with B_{dc} along the $\langle 10\bar{1}0\rangle$ twofold axis and parallel to the sample surface. Two signals are observed. One is a well-resolved oscillation of the Azbel'-Kaner type[4] whose resonance field corresponds to an

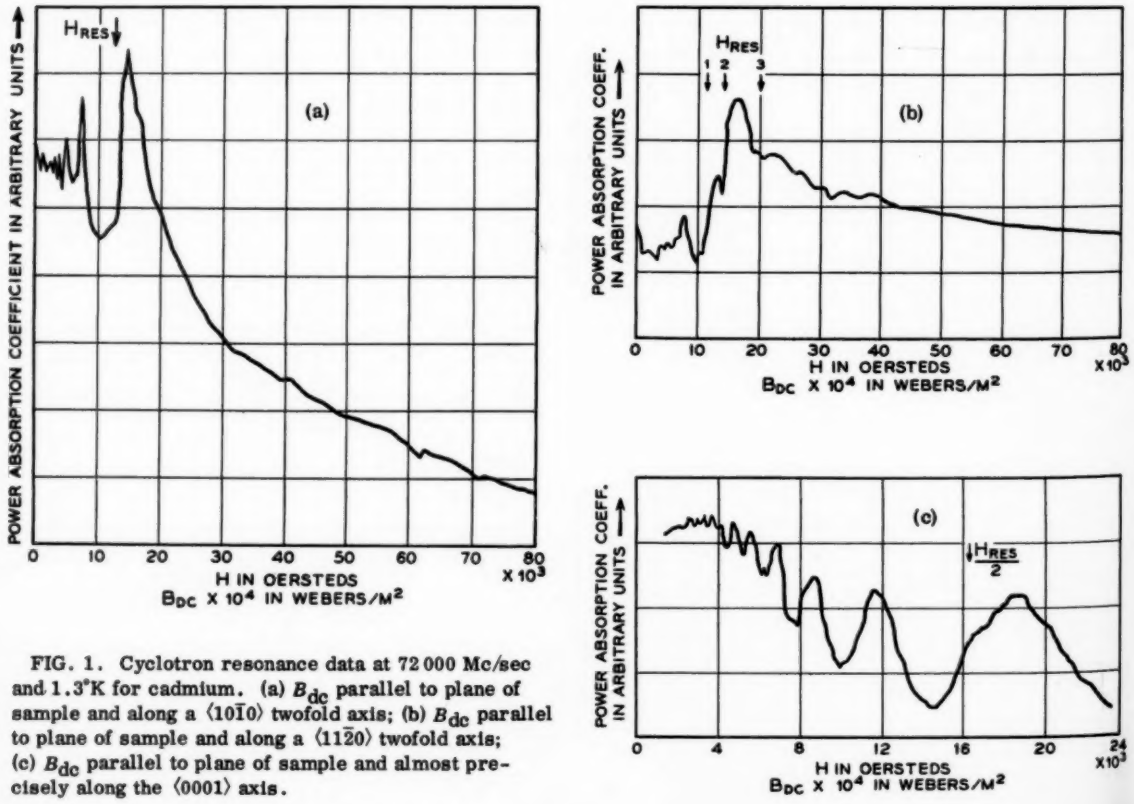
H_RES
(a)
POWER ABSORPTION COEFFICIENT IN ARBITRARY UNITS
0 10 20 30 40 50 60 70 80 X10³
H IN OERSTEDS
B_DC X 10⁴ IN WEBERS/M²
H_RES
1 2 3
(b)
POWER ABSORPTION COEFF. IN ARBITRARY UNITS
0 10 20 30 40 50 60 70 80 X10³
H IN OERSTEDS
B_DC X 10⁴ IN WEBERS/M²
(c)
H_RES/2
POWER ABSORPTION COEFF. IN ARBITRARY UNITS
0 4 8 12 16 20 24 X10³
H IN OERSTEDS
B_DC X 10⁴ IN WEBERS/M²

FIG. 1. Cyclotron resonance data at 72 000 Mc/sec and 1.3°K for cadmium. (a) B_{dc} parallel to plane of sample and along a $\langle 10\bar{1}0\rangle$ twofold axis; (b) B_{dc} parallel to plane of sample and along a $\langle 11\bar{2}0\rangle$ twofold axis; (c) B_{dc} parallel to plane of sample and almost precisely along the $\langle 0001\rangle$ axis.

effective mass $m^* = (0.51 \pm 0.02)m_0$. The other is a much broader signal which suggests to us the presence of a distribution of effective masses which begins at about $m^* = 0.35\,m_0$ and goes up to $m^* = 0.6\,m_0$ and perhaps further.

Figure 1(b) shows data taken with B_{dc} along the $\langle 11\bar{2}0\rangle$ twofold axis and parallel to the sample surface. Here three signals of the Azbel'-Kaner type are discernible, and there is some evidence for an additional signal from a distribution of masses which extends up from about $0.7\,m_0$. The three oscillatory signals interfere with each other so that relatively few harmonics are resolved, but the fundamental resonance fields indicated by arrows in Fig. 1(b) give effective masses $m^* = (0.40 \pm 0.02)m_0$, $m^* = (0.51 \pm 0.02)m_0$, and $m^* = (0.76 \pm 0.04)m_0$.

The data obtained with B_{dc} near the $\langle 0001\rangle$ axis and parallel to the sample surface show great anisotropy. When B_{dc} is sufficiently close to $\langle 0001\rangle$, one oscillatory signal corresponding to a mass $m^* = (1.23 \pm 0.05)m_0$ occurs. Data at the lower magnetic fields corresponding to this condition are shown in Fig. 1(c), although even here the presence of a second signal can be detected. As B_{dc} deviates from $\langle 0001\rangle$, three signals occur; one shows masses which increase rapidly to $1.5\,m_0$ in a degree or so, suggesting that open orbits occur at larger angles, one continues to show a mass near $1.25\,m_0$, and the third shows masses which drop slowly to around $1.1\,m_0$ when B_{dc} is about 8 degrees from $\langle 0001\rangle$.

Figure 2 shows data obtained with B_{dc} along the $\langle 11\bar{2}0\rangle$ axis and normal to the sample surface. These data are obtained under anomalous skin effect conditions, and a satisfactory detailed theory is not available. Nevertheless, a general increase in absorption occurs at the higher fields, and we conclude that the relevant charge carriers are electrons, since this absorption is so much stronger on the side for which electrons resonate (fields labeled negative). The other outstanding feature of the data is a sharp change in absorption which occurs at the field for resonance of carriers of $m^* = 0.51\,m_0$. A smaller but similar change occurs at half this field. This signal is not well understood, but is now thought to be associated with the presence of a group of minority electrons. It has also been suggested that it is a conduction electron spin resonance.[2] A similar effect is observed when this experiment is done with B_{dc} parallel to $\langle 10\bar{1}0\rangle$, but not when B_{dc} is parallel to $\langle 0001\rangle$. We do not show other data observed with the field normal to the sample surface for lack of space.

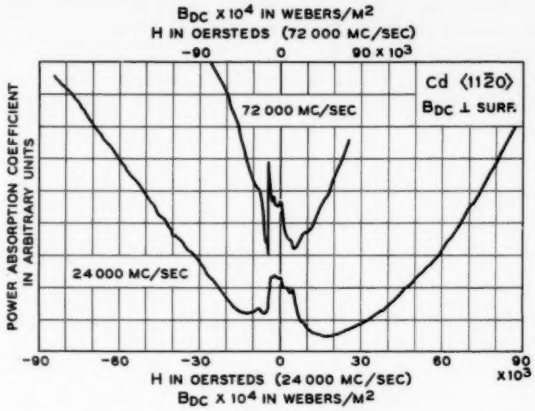

FIG. 2. Cyclotron resonance data at 72 000 Mc/sec and 24 000 Mc/sec at 1.3°K for cadmium with magnetic field normal to sample surface and along a $\langle 11\bar{2}0\rangle$ twofold axis. Field scales are adjusted so that cyclotron resonance fields for both curves are on the same vertical line. Electrons resonate on the negative-field side of the figure, holes on the positive-field side.

Harrison[5] has proposed an approximate band structure in cadmium in which the hole band has a complicated shape which might give rise to the distribution of masses indicated by some of our data, and in which the electron band has discrete sections which might give rise to the discrete masses observed here when B_{dc} is along one of the twofold axes, especially since Fig. 2 indicates that these masses are electrons. More detailed comparisons lead to some difficulties, and it seems likely that two of the signals observed with B_{dc} near $\langle 0001\rangle$ are associated with holes. Quantitatively, Harrison predicts an effective mass $m^* = 0.14\,m_0$ which we do not observe. Berlincourt[6] observes such a mass from temperature dependence of the de Haas–van Alphen effect. We are not able at present to understand the discrepancy between this result and ours; we have done experiments near the orientation mentioned by Berlincourt and failed to see such a resonance. We expect to continue this work with a view toward resolving these problems.

The authors wish to thank J. H. Wernick for zone refining the cadmium used, and S. Millman and J. C. Phillips for comments on the manuscript.

---

[1] J. K. Galt, F. R. Merritt, W. A. Yager, and H. W. Dail, Jr., Phys. Rev. Letters 2, 292 (1959).

[2]J. K. Galt and F. R. Merritt, Conference on Fermi Surface in Metals, Cooperstown, New York, August, 1960 (to be published).

[3]J. K. Galt, W. A. Yager, F. R. Merritt, B. B. Cetlin, and A. B. Brailsford, Phys. Rev. 114, 1396 (1959).

[4]M. Ia. Azbel' and E. A. Kaner, Zhur. Eksp. i Teoret. Fiz. 30, 811 (1956) [translation: Soviet Phys.-JETP 3, 772 (1956)]; J. Phys. Chem. Solids 6, 113 (1958).

[5]W. A. Harrison, Phys. Rev. 118, 1190 (1960).

[6]T. G. Berlincourt, Phys. Rev. 94, 1172 (1954).

SUPERCONDUCTING TUNNELING ON BULK NIOBIUM

M. D. Sherrill and H. H. Edwards
General Electric Research Laboratory, Schenectady, New York
(Received April 11, 1961)

Superconducting tunneling experiments on bulk niobium-niobium oxide-lead film sandwiches indicate that the energy gap in bulk niobium is about $3.6kT_C$ which is in good agreement with the Bardeen-Cooper-Schrieffer[1] theory.

If two metals are separated by a thin dielectric (50 A), then a potential applied across them results in a current due to electron tunneling. Recent experiments by Giaever[2,3] and Nicol, Shapiro, and Smith[4] have shown that if either or both of the metals are superconducting films, then the tunneling current depends strongly upon the superconducting density-of-states functions. These experiments have provided direct measurements of superconducting energy gaps in films. Bardeen[5] has shown that the dependence of tunneling current on density of states for superconductors can be deduced if tunneling is treated as a many-particle problem.

In the present experiment, plates of commercial grade niobium were mechanically polished and then annealed at 1800°C in vacuum for about six hours. The residual gas pressure during annealing was about 10^{-5} mm Hg for some samples and about 5×10^{-7} mm Hg for others. This annealing procedure was adopted after early experiments on niobium not so treated indicated that the niobium was not superconducting at the surface.

These niobium plates were painted with collodion leaving a narrow unpainted strip at the center. Lead films were evaporated onto these substrates so that they crossed the unpainted strip at right angles, providing a region where the films were separated from the niobium only by the thin niobium oxide which had grown in air. The area of these junctions ranged from 2 mm^2 to 10 mm^2. Using an ammeter and a vacuum tube voltmeter, the tunneling current for these junctions was measured as a function of voltage.

Figure 1 shows the I vs V trace for a typical junction at 4.2°K. The niobium used for this sample was annealed in 5×10^{-7} mm Hg and was polycrystalline with crystallite sizes ranging from 0.2 mm to 1.5 mm across as evidenced by

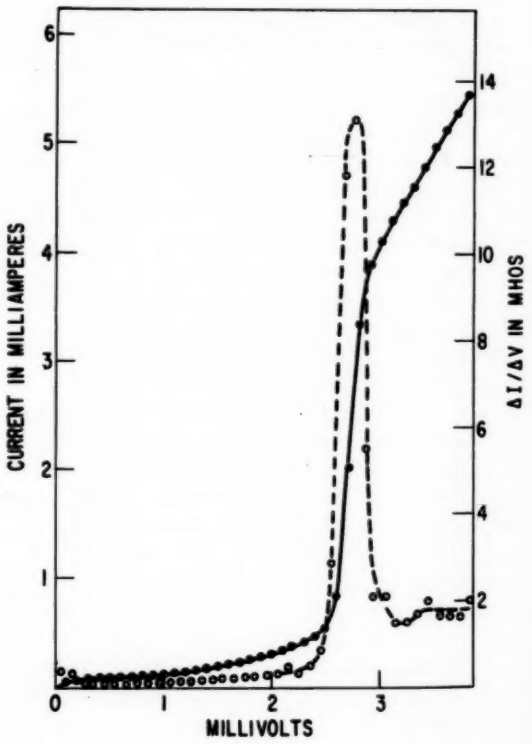

FIG. 1. The solid curve shows the current-voltage characteristic for a typical niobium-lead tunneling junction at 4.2°K. The dashed curve is the first difference ($\Delta I/\Delta V$) of the solid curve. The error in $\Delta I/\Delta V$ increases by a factor of ten over 1 ma.

the grain boundaries at the surface. In the temperature range 1.9°K to 4.2°K, no negative-resistance region was observed in this sample. This is because the energy gaps in the lead and niobium were nearly equal. There is, however, a small maximum in the slope at the origin and a large maximum at 2.75 mv. At 1.9°K the maximum at the origin was not observed and the large maximum had moved to 2.85 mv.

The position of this large maximum in the slope should be given by[2,3] $\epsilon_1+\epsilon_2$, where ϵ_1 and ϵ_2 are half the energy gaps in the two superconductors. Using previously determined values for the energy gap in lead ($2\epsilon_{Pb}=2.68$ mv $=4.3kT_c$),[3,4] we can now determine the value of the gap in bulk niobium.

$$1.9°\text{K: } 2\epsilon_{Nb}=3.02 \text{ mv}=3.59kT_c \quad (T_c=9.2°\text{K}).$$

Richards and Tinkham[6] obtained $2\epsilon=2.8kT_c$ for niobium from far-infrared reflection measurements. They pointed out, however, that it was possible that the surface layer of their sample did not have the value of the energy gap characteristic of bulk niobium.

The I vs V characteristics for several junctions displayed some indications that the energy gap was not the same for all parts of the junction. Almost all samples had a small minimum in the slope of the I vs V curve about 0.2 to 0.3 mv above the second maximum. In one sample this minimum became a small negative resistance region (0.11 mv broad at 3.0 mv) when cooled to 1.9°K. Figure 2 shows the data for another junction (annealed in 10^{-5} mm Hg) which has a small negative-resistance region corresponding to a very small energy gap for part of the junction.

Since these peculiarities were either absent or much less pronounced for niobium plates prepared in the better vacuum, the conclusion that they are due to anisotropies in the energy gap is not justified. Instead we tentatively conclude that they are probably caused by the poor quality of the niobium plate.

The authors thank V. L. Newhouse and Warren DeSorbo for their active interest and helpful suggestions during the course of these measurements.

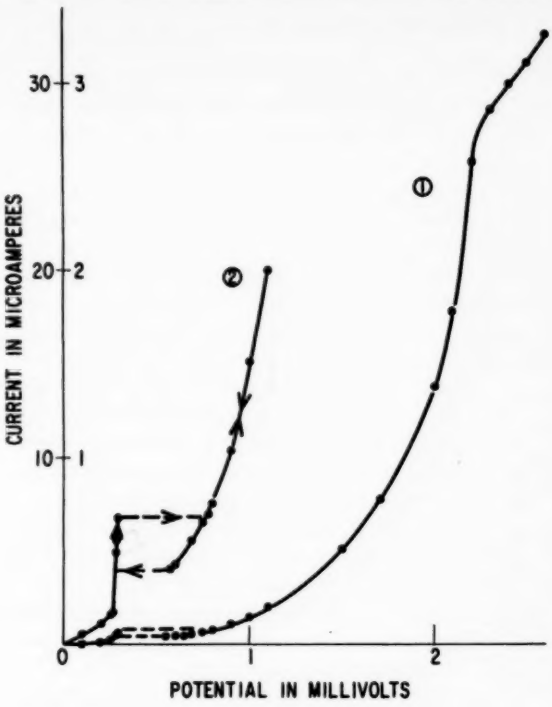

FIG. 2. The current-voltage relationship for the most atypical junction studied. Curve 2 shows the data of curve 1 plotted to an expanded current scale.

[1]J. Bardeen, L. N. Cooper, and J. R. Schrieffer, Phys. Rev. 108, 1175 (1957).
[2]I. Giaever, Phys. Rev. Letters 5, 147 (1960).
[3]I. Giaever, Phys. Rev. Letters 5, 464 (1960).
[4]J. Nicol, S. Shapiro, and P. Smith, Phys. Rev. Letters 5, 461 (1960).
[5]J. Bardeen, Phys. Rev. Letters 6, 57 (1961).
[6]P. L. Richards and M. Tinkham, Phys. Rev. 119, 575 (1960).

EXCHANGE-ORDERING AND OBSERVATION OF FORBIDDEN SPIN RESONANCE TRANSITIONS IN CRYSTALLINE ORGANIC RADICALS*

R. S. Rhodes, J. H. Burgess, and A. S. Edelstein
Department of Physics, Stanford University, Stanford, California
(Received December 22, 1960; revised manuscript received April 10, 1961)

In examining the electron spin resonance spectrum of polycrystalline samples of the organic free radicals picryl-n-amino carbazyl (PAC),[1] 1-3-bisdiphenylene-2-phenyl allyl (BDPA),[2] and Wurster's blue perchlorate (WB)[1] at low temperatures and low frequencies, we have observed a resonance at $g=4$. We believe that this line may arise from a "forbidden" transition made possible by the dipolar interaction between spins. In the frequency range from 20 Mc/sec to 200 Mc/sec the g value is four to within 3% independent of temperature. At fixed temperature the ratio of the peak intensity of the $g=4$ resonance absorption to that of the $g=2$ absorption decreases with the increasing frequency. At fixed frequency the intensity ratio decreases with increasing temperature and vanishes above a temperature T^* characteristic of the particular free radical (see Figs. 1 and 2). The intensity ratio decreases with increasing values of the radio-frequency power. The width of the $g=4$ resonance appears to be essentially independent of temperature and is of the same order of magnitude as that of the $g=2$ resonance. In some cases there is evidence for a $g=6$ resonance in the form of a weak bump on the low-field side of the $g=4$ resonance.

Various types of measurement have shown that the electron exchange plays an important role in these free radicals. Estimates of the dipolar interaction (≈ 100 oersteds) indicate that the Larmor ($g=2$) resonances are strongly exchange-narrowed. Both the resonant and static magnetic susceptibility measurements shown in Fig. 2 give further evidence of exchange and show that the exchange coupling is antiferromagnetic. In each radical the susceptibility goes through a maximum at a temperature presumably indicative of the strength of the exchange coupling. At low temperatures the resonant susceptibilities of PAC and WB again increase with a greatly reduced effective spin density. This behavior may be attributable to magnetic dilution effects.[3]

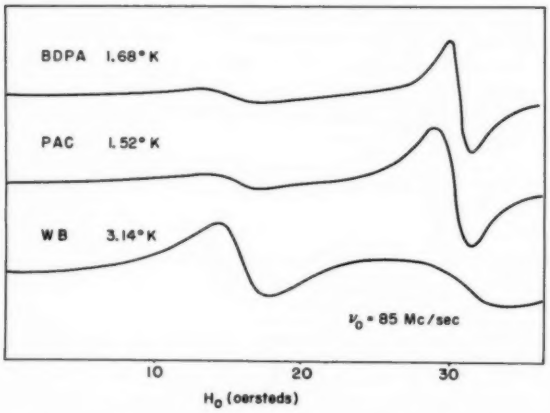

FIG. 1. Absorption spectra of BDPA, PAC, and WB in perpendicular radio-frequency and static magnetic fields. At fixed marginal oscillator frequency of 85 Mc/sec the static field, H_0, is increased from zero.

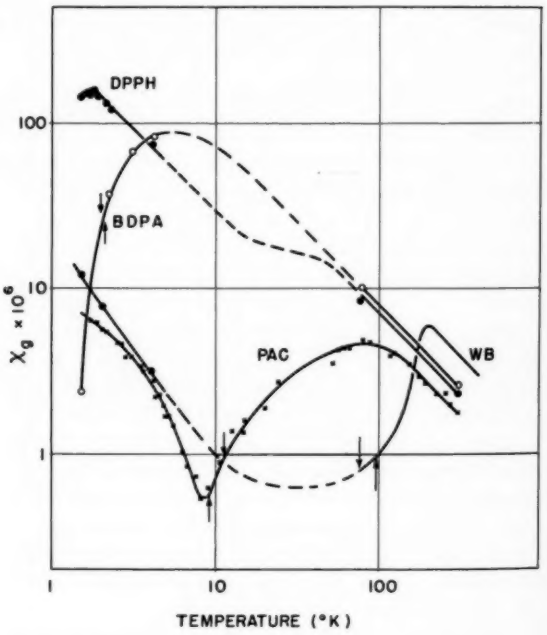

FIG. 2. Mass susceptibilities of free radicals vs temperature. The experimental points represent the intensity of the Larmor resonance at 25 Mc/sec (except WB at 10 kMc/sec). WB is reproduced from static susceptibility measurements by N. Elliott and M. Wolfsberg [Phys. Rev. 91, 435(A) (1953)]. DPPH is extrapolated in the 4°K - 77°K region with reference to L. S. Singer and E. G. Spencer [J. Chem. Phys. 21, 939 (1953)]. Arrows below curves indicate temperatures below which we have observed $g=4$ resonances. Arrows above curves indicate position of $g=2$ linewidth peaks.

Other evidence of exchange is provided by measurements of low-temperature specific heat, electron and proton relaxation times, and Knight shifts.[4]

It is significant that in all three radicals the maximum temperature T^* at which the $g=4$ absorption was observed falls below the peak in the susceptibility. Here the correlation time of the exchange "motion" has been sufficiently lengthened by spin ordering to broaden the Larmor line by a factor of two or more. Moreover, in BDPA at 85 Mc/sec, T^* is very near the temperature at which the width between derivative maxima of the Larmor line shows a sharp peak. Near 1.85°K, ΔH_{pp} reaches a sharp maximum several times the 300°K value, decreases rapidly, and then rises again as the temperature is lowered. The line also deviates from its normal Lorentz form in this region, the tails becoming more prominent.

From similar measurements on other free radicals picryl-n-amino carbazyl (PAC), Wurster's blue perchlorate (WB), and 1,1-bisdiphenyl-β-picryl hydrazyl (DPPH), it appears that the susceptibility maximum, Larmor linewidth peak, $g=4$ resonance pattern is common to all these substances. PAC exhibits a Larmor resonance intensity maximum near 70°K, a linewidth maximum near 12°K, and a $g=4$ resonance below 12°K. For WB the static and resonant susceptibility maximum, linewidth peak, and first appearance of $g=4$ resonance occur near 180°K, 80°K, and 100°K, respectively. In DPPH the resonance intensity maximum[5] occurs near 1.8°K. No linewidth peak or $g=4$ resonance was observed, presumably because the temperature was not low enough.

Resonances at $H_0/2$ have been observed before in copper acetate by Lancaster and Gordy, in cobalt ammonium sulfate by Bleaney and Ingram, and in iron and aluminum alums by Ubbink, Poulis, and Gorter[6] but no correlation with susceptibility was made. The static susceptibility of copper acetate does decrease rapidly below 300°K. Bleaney and Bowers[7] attribute these properties to pairs of exchange-coupled spins giving singlet and triplet levels. J is negative so that the singlet is the lower state. The resonance at $H_0/2$ is due to $\Delta M=2$ transitions within the triplet levels made possible by the crystalline electric field interaction. This model predicts a temperature dependence for the $g=4$ resonance intensity which is opposite to that which we observe in the free radicals. Moreover, the predicted susceptibility peak is not sharp enouth to fit the data.

The occurrence of resonances at fields harmonically related to the Larmor resonance field suggest the "forbidden" dipolar transitions discussed by Van Vleck.[8] However, the electron dipolar interactions in these free radicals is much too large to be regarded as a small perturbation on the Zeeman energy at the frequencies employed. Nevertheless, a perturbation method may be employed under the assumption that electron exchange averages the dipolar coupling, leaving a small secular interaction proportional to the exchange correlation time τ_e. On this model the appearance of the $g=4$ transition is expected only at low temperatures where linewidth and susceptibility data indicate that the exchange correlation time has become long. A proper theoretical treatment following Kubo and Tomita's general theory[9] is required for a detailed explanation of the effects of exchange in the width, intensity, and saturation properties of the $g=4$ resonance.[10]

We wish to express our appreciation to Dr. M. Mandel and Professor G. E. Pake for many helpful discussions and to Professor S. I. Weissman of Washington University for preparation of the WB sample.

*Supported by the Air Force Office of Scientific Research.

[1]D. J. E. Ingram, Free Radicals (Academic Press, Inc., New York, 1958).

[2]J. Vivo, thesis, University of Minnesota, 1956 (unpublished).

[3]H. Sato, A. Arrott, and R. Kikuchi, J. Phys. Chem. Solids 10, 19 (1959).

[4]J. P. Goldsborough, M. Mandel, and G. E. Pake, Proceedings of the Seventh International Conference on Low-Temperature Physics, edited by G. M. Graham and A. C. Hollis (University of Toronto Press, Toronto, 1960); R. Rhodes, thesis, Stanford University (to be published); M. E. Anderson, thesis, Stanford University (to be published).

[5]C. Jeffries of the University of California has observed a rapid decrease in the X-band absorption intensity of DPPH near 1.1°K (private communication).

[6]J. A. Ubbink, J. A. Poulis, and C. J. Gorter, Physica 16, 570 (1950).

[7]B. Bleaney and K. D. Bowers, Proc. Roy. Soc. (London) A214, 451 (1952).

[8]J. H. Van Vleck, Phys. Rev. 74, 1168 (1948).

[9]R. Kubo and K. Tomita, J. Phys. Soc. Japan 9, 888 (1954).

[10]A. Wright has indicated that if the external field H_0 is much larger than the dipolar and exchange fields, the effect of exchange is to broaden the $g=4$ resonance [Phys. Rev. 76, 1826 (1949)].

THEORY OF INTERBAND FARADAY ROTATION IN SEMICONDUCTORS

Benjamin Lax
Lincoln Laboratory,* Massachusetts Institute of Technology, Lexington, Massachusetts
and National Magnet Laboratory,† Massachusetts Institute of Technology, Cambridge, Massachusetts

and

Yuichiro Nishina
National Magnet Laboratory,† Massachusetts Institute of Technology, Cambridge, Massachusetts
(Received April 13, 1961)

In the experimental investigation of Faraday rotations in semiconductors, it has been observed that large changes in rotation occur at energies close to the energy gap.[1] In attempting to treat this in InSb, it has been recognized by Stephen and Lidiard[2] that the classical model of bound valence electrons is only qualitative in interpreting this phenomena. Consequently, Lax[3] has proposed a quantum mechanical approach to interpret this in terms of virtual interband transitions associated with the direct transition in this material. It can be shown that similar calculations can be made for the indirect and direct forbidden transitions to calculate the interband Faraday rotation and its dependency on wavelength.

Consider first the indirect case. It is known that the absorption coefficient for simple quadratic bands in the presence of a magnetic field, H, is given by the following expression[4]:

$$\alpha_i^{\pm}(\omega, H) = (A/\omega)\hbar^2\omega_{c1}\omega_{c2}\sum_{n_1 n_2} S(\omega - \omega_{12}^{\pm}), \qquad (1)$$

where $\omega_{12}^{\pm} = \omega_g + \omega_p + \omega_{c1}(n_1 + \frac{1}{2}) + \omega_{c2}(n_2 + \frac{1}{2}) \pm \Delta\omega_i$ Here $S(\omega - \omega_{12}^{\pm})$ is a step function. $\Delta\omega_i = \gamma_i H$ is the differential frequency shift for left and right circularly polarized waves which propagate along the magnetic field H. The superscripts $\pm$, respectively, correspond to left and right circular waves; ω_g is the frequency corresponding to the energy gap, ω_p to the phonon energy either in emission (+) or absorption (-). $\omega_{c1} = eH/m_1 c$ is the cyclotron frequency for the valence band and ω_{c2} for the conduction band. A is a constant which involves fundamental parameters, temperature, and matrix elements. We represent γ_i as a phenomenological parameter which can be evaluated for each transition in terms of the selection rules for interband transitions between Landau levels above the energy gap. For simplicity we shall assume that, to the first approximation, γ_i is the same for both left and right circularly polarized waves and is the same for all combinations of quantum numbers, n_1 and n_2. In the indirect transition where phonon absorption and emission are involved, the selection rules for orbital and magnetic quantum numbers are presumably not conserved.

According to the Kramers-Kronig relationship, the index of refraction at frequency ω is

$$n^{\pm}(\omega) = 1 + \frac{2c}{\pi}\int_0^{\infty} \frac{\alpha^{\pm}(\omega')d\omega'}{\omega'^2 - \omega^2}. \qquad (2)$$

Hence, the dispersion associated with the absorption coefficient $\alpha_i^{\pm}(\omega)$ in terms of the phase constant $\beta_i^{\pm}(\omega)$ is

$$\beta_i^{\pm}(\omega) = \beta_0 + 2A\pi^{-1}\omega\hbar^2\omega_{c1}\omega_{c2}\int_0^{\infty}\sum_{n_1 n_2}\frac{S(\omega' - \omega_{12}^{\pm})d\omega'}{\omega'(\omega'^2 - \omega^2)}$$
$$= \beta_0 + 4A(\pi\omega)^{-1}\hbar^2\omega_{c1}\omega_{c2}\sum_{n_1 n_2}\ln[\omega_{12}(\omega_{12}^2 - \omega^2)^{-1/2}], \qquad (3)$$

where $\omega_{12} = \omega_g + \omega_p + \omega_{c1}(n_1 + \frac{1}{2}) + \omega_{c2}(n_2 + \frac{1}{2})$, and $\beta_0 = \omega/c$.

The above expression applies in ω both below and above the energy gap. For the latter case, $\beta_i^{\pm}(\omega)$ should indicate the structure associated with the transition between each pair of magnetic levels n_1 and n_2. For a weak magnetic field, and at frequencies well below the energy gap, $\Delta\omega_i \ll \omega_{12}^{\pm} - \omega$. Then $\beta_i^{\pm}(\omega)$ may be expanded

with respect to $\Delta\omega_i$ and the Faraday rotation angle per unit length, θ_i, given by $\theta_i = (\beta_i^+ - \beta_i^-)/2$ gives the following result:

$$\theta_i = -\frac{2}{\pi} A\hbar^2 \omega_{c1}\omega_{c2}\omega \sum_{n_1 n_2} \frac{\Delta\omega_i}{(\omega_{12}^2 - \omega^2)\omega_{12}}. \quad (4)$$

For the frequency ω well below the gap, the summation merely represents the tail of the dispersion for each of the transitions and, hence, to the first approximation should not differ from the limit at zero magnetic field. Thus, the summation can be evaluated to this limit by integrating to obtain the expression for the Faraday rotation θ_i as follows:

$$\theta_i = -\frac{2}{\pi} A\hbar^2 \frac{\Delta\omega_i}{\omega}\left[\omega_g \ln\frac{\omega_g^2 - \omega^2}{\omega_g^2} + \omega \ln\frac{\omega_g + \omega}{\omega_g - \omega}\right], \quad (5)$$

where $\lim_{H\to 0}\omega_{12} = \omega_g$. The above expression approaches $-(2/\pi)A\hbar^2\Delta\omega_i \ln 2$ as $\omega \to \omega_g$, and asymptotically reduces to zero as ω becomes small compared to ω_g.

In a similar way we can evaluate the Faraday rotation due to the direct transition from the well-known absorption coefficient $\alpha_d^{\pm}(\omega, H)$,[4] where

$$\alpha_d^{\pm} = \tfrac{1}{2} B(\hbar\omega_c/\omega)\textstyle\sum_n (\omega - \omega_n^{\pm})^{-1/2}. \quad (6)$$

Here $\omega_n^{\pm} = \omega_g + (n + \frac{1}{2})\omega_C \pm \Delta\omega_d$; $B = 2e^2(2\mu)^{3/2} \times (\eta m^2 c)^{-1}\hbar^{-7/2}|\vec{P}_{12}\cdot\vec{e}|^2$, $\mu = m_1 m_2/(m_1 m_2)$ = reduced mass, $\omega_C = \omega_{C1} + \omega_{C2}$, m = free electron mass, η = index of refraction, and $\vec{P}_{12}$ = momentum matrix. The final result for frequency $\omega < \omega_g$ was found to be

$$\theta_d = \frac{B\hbar\omega_c}{4\omega}\sum_n \Delta\omega_d[2\omega_n^{-3/2} - (\omega_n + \omega)^{-3/2} - (\omega_n - \omega)^{-3/2}], \quad (7)$$

where $\omega_n = \omega_g + (n + \frac{1}{2})\omega_C$. In this case $\Delta\omega_d = \gamma_d H$ can be in principle evaluated for each transition, since the selection rules for the normal magnetic level structures have been worked out.[5] The sign of the value of γ_d for such direct transitions will then be determined by the admixture of orbital states as well as effective g values in the presence of spin-orbit coupling. We shall again assume that $\Delta\omega_d$ is the same for each transition. The summation was approximated by an integral over n in the limit of weak magnetic field, with the result

$$\theta_d = \tfrac{1}{2}B\hbar(\Delta\omega_d/\omega)[2\omega_g^{-1/2} - (\omega_g + \omega)^{-1/2} - (\omega_g - \omega)^{-1/2}]. \quad (8)$$

The above results in Eqs. (5) and (8) can readily give the semiquantitative explanation of the interband Faraday rotation observed by Hartmann and Kleman[1] in Ge where the direct and indirect energy gaps are close to one another. Assuming that $\Delta\omega_i$ is negative for a positive value of magnetic field, our result indicates that the Faraday rotation for the indirect transition has the same sign, i.e., positive, as that for free carrier. This sign is consistent with the experimental result.[1,3] $\Delta\gamma_d$ must be positive, since the interband Faraday rotation due to the direct transition is negative. Its magnitude becomes very large as the incident photon energy approaches the gap energy. Both from the theoretical and experimental curves in Figs. 1 and 2, which are

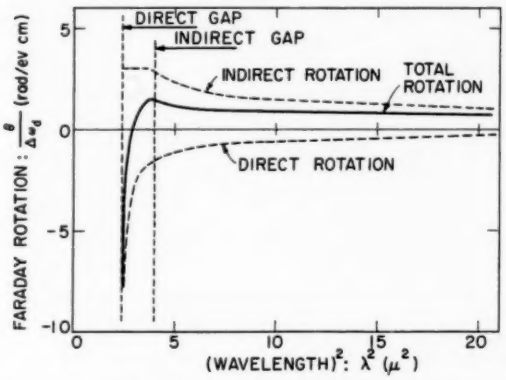

FIG. 1. Theoretical curve of Faraday rotation in intrinsic Ge at room temperature. The dashed lines are individual contributions of indirect and direct interband virtual transitions. The solid line is the combined total rotation. The magnitude of the dispersion was evaluated from the absorption coefficients for both transitions from the experimental data by W. C. Dash and R. Newman [Phys. Rev. 99, 1151 (1955)] at zero magnetic field.

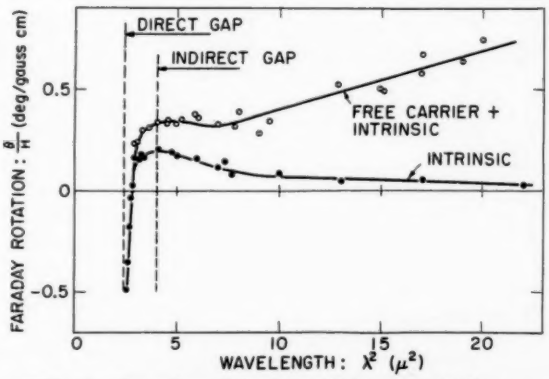

FIG. 2. Experimental curve of Faraday rotation in intrinsic Ge at room temperature by Hartmann and Kleman.[1]

similar in shape, it is apparent that a strong singularity in Faraday rotation must correspond to the direct transition consistent with the theoretical result of Eq. (8).

The forbidden direct transition can be treated in an analogous manner. The two bands have the same symmetry, so that no transition is allowed at $k=0$. In this case the absorption coefficient is given by the expression,

$$\alpha_f^{\pm} = \tfrac{3}{2}\left(\frac{\hbar\omega_c}{2}\right)^2 \frac{C}{\omega}\sum_n (n+1)[(\omega-\omega_1^{\pm})^{-1/2}+(\omega-\omega_2^{\pm})^{-1/2}], \tag{9}$$

where $\omega_1^{\pm}=\omega_g+(n+\frac{1}{2})\omega_C+\omega_{C1}\pm\Delta\omega_f$, (and similarly for $\omega_2^{\pm}$), and $C=\frac{2}{3}e^2(\eta m^2 c)^{-1}\hbar^{-7/2}|\vec{M}_{12}|^2(2\mu)^{3/2}$, $\vec{M}_{12}$ being the momentum matrix. Following the steps indicated previously, we obtain the result for the Faraday rotation angle per unit length:

$$\theta_f=\tfrac{3}{16}(\hbar\omega_c)^2(C/\omega)\textstyle\sum_n(\Delta\omega_f)(n+1)[\omega_1^{-3/2}-\frac{1}{2}(\omega_1+\omega)^{-3/2}-\frac{1}{2}(\omega_1-\omega)^{-3/2}+\omega_2^{-3/2}-\frac{1}{2}(\omega_2+\omega)^{-3/2}-\frac{1}{2}(\omega_2-\omega)^{-3/2}]. \tag{10}$$

In the limit of weak magnetic fields we obtain, by integrating Eq. (10),

$$\theta_f \cong \tfrac{3}{4}\hbar^2 C(\Delta\omega_f/\omega)[-2\omega_g^{1/2}+(\omega_g+\omega)^{1/2}+(\omega_g-\omega)^{1/2}]. \tag{11}$$

This result has some interesting application to p-type Ge, where such transitions have been observed between the split valence bands. The two prominent absorptions observed at room temperature at approximately 3 and 5 microns should give rise to peaks in the curve of Faraday rotation as shown in Fig. 3. These correspond to the transitions between $P_{1/2}$ and the degenerate $P_{3/2}$ bands. The sign of rotation is not known from theory. We have assumed $\Delta\omega_f$ to be positive, giving negative values of θ as shown in Fig. 3. However, experimental results will determine the sign. It is necessary to use doped samples to observe these transitions. Hence, the contribution from the free-carrier absorption would be superimposed. At low temperatures where many of the light-hole states are filled, only the transition to the heavy-hole states about 4 microns would be observable.[6] At such temperatures and in very high magnetic fields, it is possible that only a few transitions can be seen, so that the width of the peak in the Faraday rotation would be small, giving rise to fine structures. In this case the Faraday rotation should be expressed in terms of Eq. (10) rather than Eq. (11).

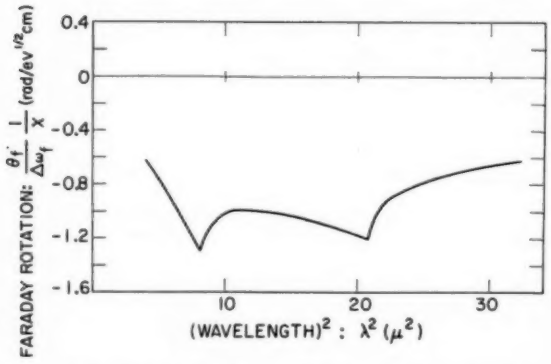

FIG. 3. Theoretical curve of Faraday rotation due to forbidden direct transitions in Ge at room temperature. The relative magnitudes of absorption coefficients and position of peaks were determined from the experimental curve of Kaiser, Collins, and Fan.[6] $\chi=\frac{3}{4}\hbar^2 C$ in Eq. (11).

The theory is only approximate, since it makes a number of assumptions. One assumption is that the bands are quadratic and extend to large k values without changing the curvature. This is incorrect since the dispersion or phase constant obtained by Kramers-Kronig relationship at zero magnetic field would diverge for the indirect and the forbidden direct transitions. This contradiction can be avoided by using the nonparabolic representation of the bands, when they are known, as in InSb. The wavelength dependence of the Faraday rotation would be modified for nonparabolic bands. The theory has also neglected the losses which can be taken into account phenomenologically in the final expressions. This

has been done for the direct interband transitions above the energy gap. For more accurate analysis of the Faraday rotation in p-type Ge, it is also necessary to take statistics into account since the dispersion must be weighted by the number of empty states. In spite of these assumptions, however, the above approximate results seem to be reasonable because they can explain the major features of the experimental observations, whereas the classical theory for bound electrons cannot. Lastly, in order to account for the proper sign of the interband Faraday rotation, it is necessary to consider in detail the individual magnetic levels of the two sets of the bands involved in transition, including spin, particularly in the presence or absence of spin-orbit splitting. The analysis would presumably account for the apparent difference between the observation in GaAs as contrasted to InSb and InAs.[1]

We would like to thank Dr. G. S. Heller, Dr. H. J. Zeiger, and Dr. L. M. Roth for helpful discussions in connection with this problem.

*This work was done in part at Lincoln Laboratory, operated with support from the U. S. Army, Navy, and Air Force.

†This work was done in part at the National Magnet Laboratory, operated with support by the Air Force through the Air Force Office of Scientific Research.

[1]S. D. Smith, T. S. Moss, and K. W. Taylor, J. Phys. Chem. Solids 11, 131 (1959); R. N. Brown and B. Lax, Bull. Am. Phys. Soc. 4, 133 (1959); A. K. Walton and T. S. Moss, J. Appl. Phys. 30, 951 (1959); B. Hartmann and B. Kleman, Arkiv Fysik 18, 75 (1960); M. Cardona, Phys. Rev. 121, 752 (1961).

[2]M. J. Stephen and A. B. Lidiard, J. Phys. Chem. Solids 9, 43 (1958).

[3]B. Lax and S. Zwerdling, Progress in Semiconductors, edited by A. F. Gibson (Heywood and Company, Ltd., London, 1960), Vol. 5, p. 224; B. Lax, Proceedings of the Prague Semiconductor Conference, August, 1960 (to be published).

[4]L. M. Roth, B. Lax, and S. Zwerdling, Phys. Rev. 114, 90 (1959).

[5]R. J. Elliott, T. P. McLean, and G. G. Macfarlane, Proc. Phys. Soc. (London) 72, 553 (1958); B. Lax, L. M. Roth, and S. Zwerdling, J. Phys. Chem. Solids 8, 311 (1959); E. Burstein, G. S. Picus, R. F. Wallis, and F. J. Blatt, J. Phys. Chem. Solids 8, 305 (1959), and Phys. Rev. 113, 15 (1959); S. Zwerdling, B. Lax, L. M. Roth, and K. Button, Phys. Rev. 114, 80 (1959).

[6]H. B. Briggs and R. C. Fletcher, Phys. Rev. 87, 1130 (1952); W. Kaiser, R. J. Collins, and H. Y. Fan, Phys. Rev. 91, 230(A) and 1380 (1953).

HYPERFINE INTERACTIONS IN THE GROUND STATE AND FIRST EXCITED STATE OF Dy^{161} IN DYSPROSIUM IRON GARNET*

R. Bauminger, S. G. Cohen, A. Marinov, and S. Ofer
Department of Physics, The Hebrew University, Jerusalem, Israel
(Received April 13, 1961)

The hyperfine Zeeman splittings in the recoil-free absorption spectrum[1] of the 26-kev γ rays from Dy^{161m} ($\tau_{1/2} \sim 3\times10^{-8}$ sec)[2] in Dy^{161} situated in dysprosium iron garnet (DIG) have been observed. This is possible since in the rare earth iron garnets ($5Fe_2O_3 \cdot 3M_2O_3$) the sublattice of rare earth ions below the Curie temperature shows a temperature-dependent spontaneous magnetization.[3] Nearly all the rare earth elements can be incorporated in iron garnets and since an appreciable recoil-free efficiency is expected at liquid air temperature for the γ transition from the first excited state of many rare earth nuclei, the method is of general application. Values for the effective magnetic field at the nucleous (H_{eff}) and the magnetic and quadrupole moments of the ground state and first excited state of Dy^{161} are derived. At 85°K a large nuclear quadrupole interaction has been observed, but at 300°K the quadrupole interaction is much smaller. This strongly temperature-dependent interaction is interpreted as being largely due to the average electric field gradient produced by the partially aligned orbitals of the $4f$ electron shell and correlated with the spontaneous magnetization (and H_{eff}) within each domain. This gradient will have an axis of symmetry parallel to H_{eff}.

The recoil-free absorption spectrum of polycrystalline DIG, isotopically enriched in Dy^{161}, was measured using a source of Dy^{161m} which showed an unsplit emission line of relatively narrow width. This was prepared as follows: 6.7-day Tb^{161} was separated by ion exchange

from neutron-irradiated Gd_2O_3 enriched in Gd^{160}, electroplated on copper from a solution of the chloride in pyridine, covered with evaporated copper, and the "sandwich" heated in hydrogen at about 900°C. With this source the linewidth of the unsplit recoil-free absorption spectrum in a dysprosium aluminum alloy at room temperature was about 4 mm/sec, which is, therefore, an upper limit to the source linewidth. The source (in all measurements at 300°K) was vibrated on a loud-speaker membrane at 65 cycles/sec and the absorption of the 26-kev radiation recorded automatically as a function of relative velocity as described elsewhere.[4]

Figure 1 shows the absorption spectrum obtained in DIG at 85°K. Well-resolved lines extending to velocities of about 10 cm/sec in each direction are seen. The positions of the peaks were confirmed in separate runs extending to smaller velocities. The Dy^{161} ground state is known to be 5/2- and the first excited state has been thought to be 5/2+.[5] The analysis of the results shown in Fig. 1(A) in terms of transitions between the Zeeman levels of the two nuclear states demands that both levels have a spin 5/2 and that the magnetic moments have opposite sign. The measurements of Park[6] indicate a negative magnetic moment for the ground state. It was assumed that each level was split according to the expression,[7]

$$W = mg_I\mu_n H_{\text{eff}} + \tfrac{1}{4}eqQ[3m^2 - I(I+1)]/[I(2I-1)].$$

Table I shows the identification of the transitions between the Zeeman levels. There are a

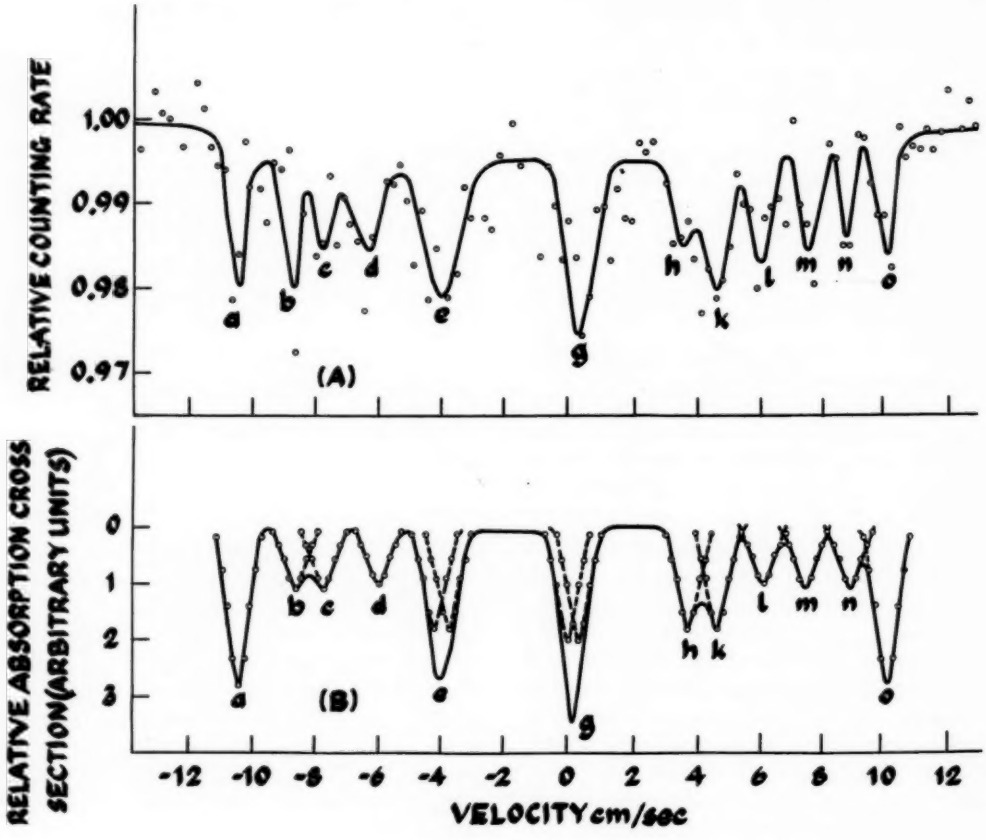

FIG. 1. (A) The absorption by dysprosium iron garnet at liquid air temperature of the 26-kev γ ray emitted at room temperature in the decay of Tb^{161}, diffused into copper, as a function of relative velocity between source and absorber. The statistical error on each point is about 0.3%. (B) Reconstructed spectrum assuming the results of the least-square analysis of the experimental peak energies, the theoretical relative transition probabilities, and a Gaussian line shape.

Table I. Identification of observed transitions between nuclear Zeeman levels at liquid air temperature.

Peaks observed	Transitions between Zeeman substates	Peaks observed	Transitions between Zeeman substates
a	$-5/2 \rightarrow -5/2$	h	$+1/2 \rightarrow +3/2$
b	$-3/2 \rightarrow -5/2$	k	$+3/2 \rightarrow +1/2$
c	$-5/2 \rightarrow -3/2$	l	$+3/2 \rightarrow +3/2$
d	$-3/2 \rightarrow -3/2$	m	$+3/2 \rightarrow +5/2$
e	$-3/2 \rightarrow -1/2$	n	$+5/2 \rightarrow +3/2$
	$-1/2 \rightarrow -3/2$	o	$+5/2 \rightarrow +5/2$
g	$-1/2 \rightarrow +1/2$		
	$+1/2 \rightarrow -1/2$		

total of 16 possible electric dipole transitions. The calculated Wigner coefficients determining the transition probabilities for two of the transitions ($+1/2 \rightarrow +1/2$, and $-1/2 \rightarrow -1/2$) are very small and they cannot be observed. The remaining transitions are all observed but at two positions in the spectrum two transitions overlap [e and g in Fig. 1(A)].

Table II shows the results of a least-squares analysis of the experimental peak energies giving $g\mu_n H_{\text{eff}}$ and $eqQ/4$ for both nuclear levels, and ΔE, the chemical shift between source and absorber.[8] Figure 1(B) shows the reconstructed spectrum obtained from these values, using the appropriate theoretical relative transition probabilities, and assuming a Gaussian line shape. The agreement between Figs. 1(A) and 1(B) is seen to be very satisfactory. Measurements in DIG at 300°K shows a similar but much narrower spectrum corresponding to a smaller H_{eff}; the analysis of the results at 300°K is also given in Table II.[9]

Using the value of (-0.37 ± 0.05) nm for the Dy^{161} ground-state magnetic moment obtained by Park,[6] we get $(+0.42 \pm 0.08)$ nm for the magnetic moment of the first excited state, $H_{\text{eff}}(85°K) = (3.5 \pm 0.55) \times 10^6$ oe, and $H_{\text{eff}}(300°K) = (7.5 \pm 1.5) \times 10^5$ oe. $H_{\text{eff}}(85°K)/H_{\text{eff}}(300°K)$ is then (4.6 ± 1), which is close to the value 4 for the ratio of the partial spontaneous magnetizations of the dysprosium sublattice at the two temperatures deduced by Pauthenet from magnetization measurements using the Néel model.[3] This illustrates again the proportionality between H_{eff} and spontaneous magnetization.[10,4] The experimental values for the magnetic moment and their signs for the two nuclear states are in agreement with the predictions of Nilsson's unified model.[5]

The results show a remarkably large quadrupole interaction ($eqQ_1/4 = +120$ Mc/sec) at 85°K and a relatively much smaller interaction at 300°K ($eqQ_1/4 < 20$ Mc/sec). This is interpreted as due largely to the average field gradient produced by the $4f$ electrons which should be partially aligned below the Curie temperatures. Assuming that J of the rare earth ion (the ground state of the Dy^{3+} is ${}^6H_{15/2}$) in the garnet is a good quantum number and neglecting crystalline field effects on the $4f$ shell,[11] then the electric field gradient

Table II. Summary of results for the hyperfine interactions and chemical shifts observed in dysprosium iron garnet at 300°K. Q_1 and g_1 correspond to the ground state of Dy^{161}; Q_2 and g_2 correspond to the 26-kev level of Dy^{161}.

Temperature (°K)	ΔE (Mc/sec)	$eqQ_1/4$ (Mc/sec)	$eqQ_2/4$ (Mc/sec)	$g_1\mu_n H_{\text{eff}}$ (Mc/sec)	$g_2\mu_n H_{\text{eff}}$ (Mc/sec)
85	8 ±10	120 ±30	90 ±30	-400 ±40	+455 ±40
300	12 ±10	<20	<20	-84 ±20	+97 ±20

produced by this mechanism will be equal to the Boltzmann average of the electric field gradient produced by the ion in the various J_z states. In the Weiss field approximation, eqQ will then be given by

$$eqQ = e^2Q\langle 1/r^3\rangle\, a \left[\sum_{J_z=-J}^{J_z=+J} [3J_z^2 - J(J+1)] \exp(-J_z g\beta H/kT)\right] \Bigg/ \left[J(2J-1) \sum_{J_z=-J}^{J_z=+J} \exp(-J_z g\beta H/kT)\right], \quad (1)$$

where a is the matrix element $\langle \sum_i (3\cos^2\theta_i - 1)\rangle$ for the ion in the state $J_z = J$, [12] and H is the temperature-dependent Weiss field.[13] The expression in brackets can be regarded as a modified Brillouin function giving the average of $[3J_z^2 - J(J+1)]$ instead of the average of J_z appearing in the usual Brillouin function

$$M/M_S = \left[\sum_{J_z=-J}^{J_z=+J} J_z \exp(-J_z g\beta H/kT)\right] \Bigg/ \left[J \sum_{J_z=-J}^{J_z=+J} \exp(-J_z g\beta H/kT)\right], \quad (2)$$

which should describe the dependence of the spontaneous magnetization of the dysprosium sublattice on temperature. The functions of the argument $x = g\beta H/kT$ have been computed for $J = 15/2$, and using Pauthenet's values for the spontaneous magnetization to fix x from Eq. (2) at 85°K and 300°K, Eq. (1) shows that $eqQ(85°K)/eqQ(300°K)$ should equal about 8, consistent with experiment. Moreover, taking $\langle 1/r^3\rangle = 74\times10^{+24}$ cm^3, [14] $a = 2/3$ (assuming LS coupling), [12] we obtain from the experimental value of $eqQ_1/4$ at 85°K, a value of about 2×10^{-24} cm^2 for Q_1. This lies between the value 3×10^{-24} cm^2 obtained for Q_1 from measurements of $B(E2)$ in Coulomb excitation[15] and the value 1.1×10^{-24} obtained by Park[6] from spin resonance experiments. We consider that further investigations leading to a knowledge of the necessary corrections to the simple treatment outlined above will permit accurate estimate of the electric field gradients and nuclear quadrupole moments.

We would like to thank M. Schieber from the Department of Electronics of the Weizmann Institute for preparing the DIG and A. Moustachi for help in chemical problems.

*Supported in part by the U. S. Air Force, Air Research and Development Command, through its European Office.

[1]R. L. Mössbauer, Z. Physik 151, 124 (1958).

[2]S. Ofer, P. Avivi, R. Bauminger, A. Marinov, and S. G. Cohen, Phys. Rev. 120, 406 (1960).

[3]R. Pauthenet, Ann. Phys. 3, 424 (1958).

[4]R. Bauminger, S. G. Cohen, A. Marinov, and S. Ofer, Phys. Rev. 122, 743 (1961).

[5]B. R. Mottelson and S. G. Nilsson, Kgl. Danske Videnskab. Selskab, Mat.-fys. Medd. 1, No. 8 (1959).

[6]J. G. Park, Proc. Roy. Soc. (London) A245, 118 (1958).

[7]This is an approximation to first order in the ratio of the quadrupole interaction (assumed to be axially symmetric) to magnetic interaction. The arguments presented in this Letter lead us to believe that q is predominantly axially symmetric and parallel to H_{eff}. To the extent that this is true, the use of the expression is justified even if the ratio of interactions is not small.

[8]O. C. Kistner and A. W. Sunyar, Phys. Rev. Letters 4, 412 (1960).

[9]The definition of the lines in Fig. 1(A) shows that there must be a fast thermal exchange between the various Stark levels of the Dy ion excited at 85°K. Nevertheless the linewidths are broader than those observed at 300°K, and this might be ascribed to a slower relaxation between the Stark levels at 85°K.

[10]D. E. Nagle, H. Frauenfelder, R. D. Taylor, D. R. F. Cochran, and B. T. Matthias, Phys. Rev. Letters 5, 364 (1960).

[11]A detailed theoretical treatment should take into account the possibility of partial decoupling of the orbital angular momentum from the aligned spin angular momentum under the combined influence of the exchange interactions acting on the spins and the crystal field interactions. There is some evidence for a partial quenching of the orbital magnetic moment in the garnets. (See reference 3.)

[12]K. W. Stevens, Proc. Phys. Soc. (London) A65, 209 (1952); a is equal to the factor α of Stevens, multiplied by $[3J^2 - J(J+1)]$, which in this case is equal to 105.

[13]We neglect the atomic core distortion factor which has not yet been calculated for rare earth states. [R. M. Sternheimer, Phys. Rev. 95, 736 (1954).]

[14]B. Bleaney, Proc. Phys. Soc. (London) A68, 937 (1955).

[15]N. P. Heydenburg and G. F. Pieper, Phys. Rev. 107, 1297 (1957).

EXCITATION OF H 2s BY ELECTRON IMPACT

D. G. Hummer and M. J. Seaton
Department of Physics, University College, London, England
(Received March 27, 1961)

The cross section, $Q_T(2s)$, for production of H 2s atoms by electron bombardment of ground-state atoms, has been measured by Lichten and Schultz[1] and by Stebbings, Fite, Hummer, and Brackmann.[2] The results obtained have been discussed by Lichten[3] and are discussed further in the present Letter.

In the LS experiment measurements were made for energies up to 45 ev. The shape of the curve appears to be determined accurately, but the absolute values are much less certain, the measured maximum cross section being $(0.28 \pm 0.14) \times \pi a_0^2$. The published results of LS are obtained on normalizing to the first Born approximation at energies of 30-40 ev; this gives a maximum cross section of $0.36 \pi a_0^2$. In the SFHB experiment measurements were made for energies up to 700 ev. For the determination of the curve shape the SFHB measurements are less accurate than those of LS, but, in the common energy range, the agreement between the two curve shapes is satisfactory. For their absolute values SFHB claim an accuracy much better than that claimed by LS, but Lichten[3] has correctly pointed out that the published values of SFHB must be multiplied by a factor of 1.5 to correct for an erroneous assumption made in the reduction of the data. With this correction the maximum SFHB cross section, $(0.16 \pm 0.01) \times \pi a_0^2$, is consistent with the absolute LS measurement but is not consistent with the LS cross section normalized to the first Born approximation.

In order to discuss the matter further we put $Q_T(2s) = Q_C(2s) + Q(2s)$, where $Q_C(2s)$ is the cross section for the process of excitation of $3p$ and higher states, followed by cascade to $2s$, and $Q(2s)$ is for direct excitation of $2s$. Putting $Q_C(2s) = \gamma Q(3p)$, LS obtain $\gamma = 0.21$ using an extrapolation formula for the higher states. Using Born cross sections[4] we obtain $\gamma = 0.23$. We calculate $Q(3p)$ on assuming that the correction factor by which the Born $3p$ cross section must be multiplied, as a function of $(E/\Delta E)$, is the same as the factor of $2p$ as determined experimentally.[5,6] Figure 1 shows results for $Q(2s)$ obtained from the SFHB measurements. The full-line curve is obtained from the LS results normalized on making a least-squares fit to SFHB.

In Fig. 1 we give the cross section obtained by Smith[7] from a solution of the $1s$-$2s$ coupled exchange equations. Lichten[3] argues that this calculation justifies the procedure of normalizing to the first Born approximation at 30-40 ev. The assumption made is that coupling to intermediate states can be neglected. The coupling most likely to be of importance is that between the $2s$ and $2p$ states. The calculations of Burke and Seaton[8] show that this coupling is fairly strong, but a better estimate of its effect is obtained from the second Born approximation calculations of Kingston, Moiseiwitsch, and Skinner.[9] Figure 1 shows the results they obtain on including the following states in the second Born summation: $(1s, 2s)$, $(2p)$, and $(1s, 2s, 2p)$. It is seen that allowance for coupling to $2p$ brings about a drastic reduction in the cross section.

We compare the second Born $(1s, 2s)$ curve, which represents an approximation to the solution of the $1s$-$2s$ nonexchange equations, with the curve from the exact solution of the $1s$-$2s$ exchange equations. For energies of about 30 ev it is seen that the effect of exchange is to bring about a considerable reduction in the cross section.[10] It may, therefore, be expected that a calculation allowing both for exchange and for coupling to $2p$ would give a cross section smaller than the second Born $(1s, 2s, 2p)$ and, hence, in better agreement with the SFHB results. At higher energies, greater than about 150 ev, the corrections to the first Born approximation are fairly small, and for these energies the SFHB results are in satisfactory agreement with the first approximation.

We conclude that there is no evidence for any discrepancy between the SFHB results and the most recent theoretical work.

---

[1] W. Lichten and S. Schultz, Phys. Rev. 116, 1132 (1959); referred to here as LS.

[2] R. F. Stebbings, W. L. Fite, D. G. Hummer, and R. T. Brackmann, Phys. Rev. 119, 1939 (1960); referred to as SFHB.

[3] W. Lichten, Phys. Rev. Letters 6, 12 (1961).

[4] R. McCarroll, Proc. Phys. Soc. (London) A70, 460

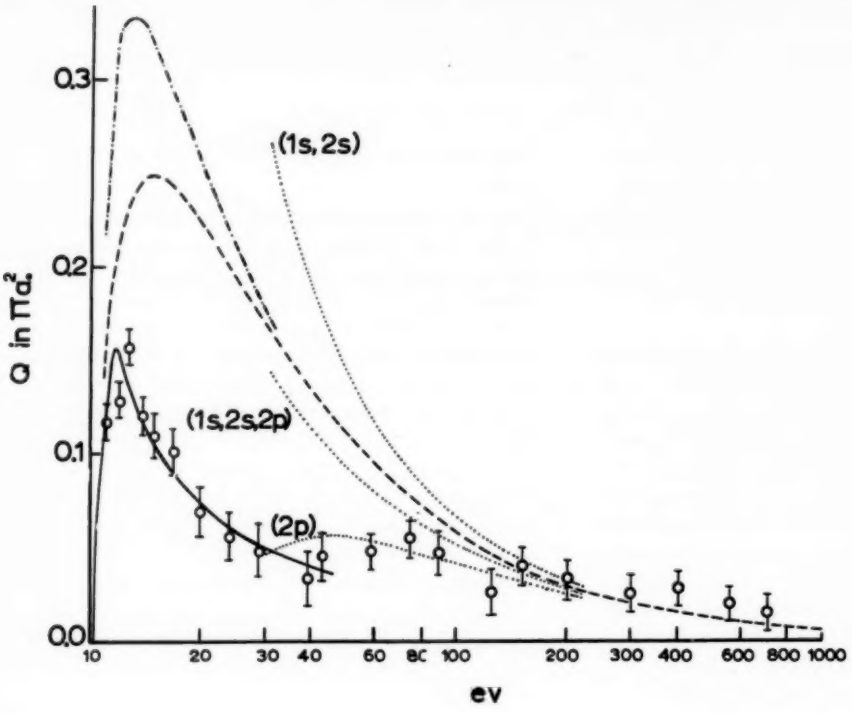

FIG. 1. The cross section for 1*s*-2*s* transitions by electron impact. The experimental points with error bars are from the measurements of SFHB and the full line curve is from the measurements of LS normalized to the SFHB results. The dashed curve is the first Born approximation, the dotted curves are the second Born approximation for various terms included in the summation, and the dot-dashed curve is from the solution of the 1*s*-2*s* exchange equations.

(1957).

[5]W. L. Fite and R. T. Brackmann, Phys. Rev. 112, 1151 (1958).

[6]W. L. Fite, R. F. Stebbings, and R. T. Brackmann, Phys. Rev. 116, 356 (1959).

[7]K. Smith, Phys. Rev. 120, 845 (1960). We have added a small correction, calculated in the first Born approximation, for $l \geq 3$.

[8]V. M. Burke and M. J. Seaton, Proc. Phys. Soc. (London) 77, 199 (1961).

[9]A. E. Kingston, B. L. Moiseiwitsch, and B. G. Skinner, Proc. Roy. Soc. (London) A258, 245 (1960). In the second Born calculations, fourth-order terms in the interaction are neglected in the expressions for the cross sections.

[10]Exact solutions of the 1*s*-2*s* nonexchange equations have been obtained by K. Smith, W. F. Miller, and A. J. P. Mumford, Proc. Phys. Soc. (London) 76, 559 (1960). This gives a cross section smaller than that obtained in the second Born (1*s*,2*s*) approximation but larger than that obtained from exact solutions of the 1*s*-2*s* exchange equations.

NEW ELEMENT, LAWRENCIUM, ATOMIC NUMBER 103

Albert Ghiorso, Torbjørn Sikkeland, Almon E. Larsh, and Robert M. Latimer
Lawrence Radiation Laboratory, University of California, Berkeley, California
(Received April 13, 1961)

Bombardments of californium with boron ions have produced alpha-particle activity which can only be ascribed to decay of a new element with atomic number 103. This activity at best amounts to only a few alpha counts per hour ($\sigma \approx 1$ microbarn), so it has not yet been possible to detect the mendelevium decay product to prove further the atomic number of the new activity. For the present, attribution of this activity to element number 103 must rest entirely on nuclear rather than chemical evidence.

The method used to produce and identify radiations from element 103 decay is shown schematically in Fig. 1 and is based on the one used for the element 102 experiment.[1] The 3-microgram californium target has an isotopic composition at present of 3.3% 249, 32.8% 250, 12.3% 251, and 50.8% 252.[2] It was electroplated in an area 0.10 inch in diameter onto nickel foil 50 microinches thick. The purification of the target, crucially important for the success of the experiment, consisted in careful use of ion exchange columns with specially purified reagents. The last step in the purging of undesirable lead and bismuth impurities was accomplished by heating the final target in vacuo by electron bombardment. Lead and bismuth impurities must be reduced because heavy-ion bombardment of these elements produces in high yield an alpha activity with an 8.8-Mev alpha-particle energy and a 25-second half-life which can obscure the lower energy alpha activity of element 103. The heavy-ion beam of either B^{10} or B^{11} was collimated so as to pass through the tiny target and typically was limited to 0.5 microampere dc to avoid melting the target foil. The transmuted atoms recoiled from the target into an atmosphere of helium. This gas flowed slowly through a nearby 0.050-inch orifice and carried the electrically charged transmutation products to a thin copper conveyor tape. This tape was periodically pulled a short distance to place the groups of collected atoms to positions successively in front of each of five solid-state Au-Si surface-barrier detectors. The pulses caused by passage of alpha particles into each detector were amplified, except for a few milliseconds during the beam bursts, by separate preamplifiers in the shielded bombardment area and then sent to a main counting area to be further amplified and analyzed. In the counting area, the pulses were passed through separate window amplifiers and then analyzed by two separate electronic systems. One system consisted of five separate 100-channel pulse ana-

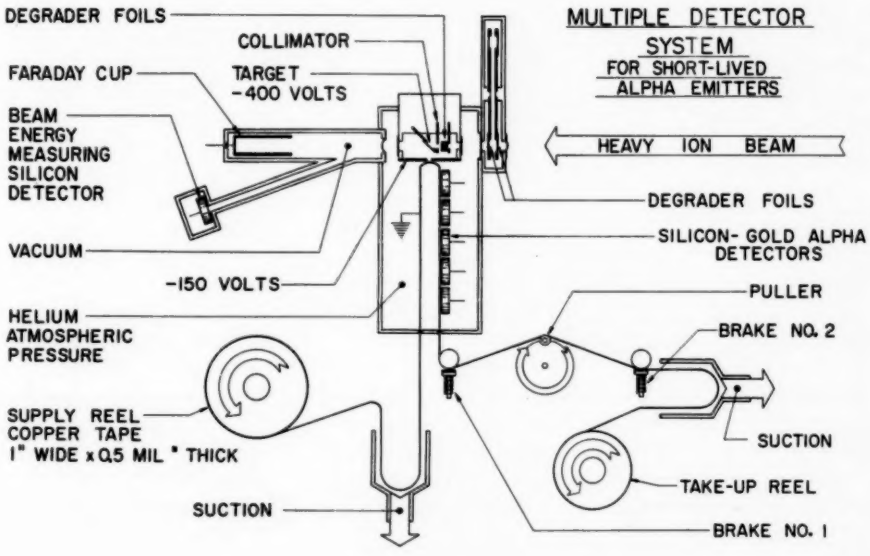

FIG. 1. Schematic diagram of apparatus.

lyzers, and the other consisted of a multiplex unit using five punched paper tape storage units. With the multiplex unit, it was possible to determine the time when each event occurred, since the conveyor tape was last advanced.

The silicon crystal detectors vitally necessary for the experiment were brought to the authors' attention by C. J. Borkowski and J. L. Blankenship of the Oak Ridge National Laboratory. With their very kind help, it has been possible in our laboratory to make silicon detectors suitable for these experiments. The present detectors are made of 800-1800 ohm-cm silicon, 6×10 mm, suitably etched and mounted, and are covered with a layer of gold about 20 micrograms per cm^2 thick. Initially, it was found that operation of these detectors was very erratic because of the helium atmosphere and the very intense beta radiation fields. The use of charge-sensitive preamplifiers reduced this effect, but it is still found that because of the circumstances of the experiment, it is necessary to replace the crystal detectors occasionally.

The energy of the boron ions was changed by degradation of the 10.3-Mev per nucleon beam in aluminum absorbers. Because the beam is so intensely concentrated, it was found that the amount of energy loss in a given absorber could change with time. To monitor the energy of the ions striking the target, another Si detector was calibrated against nuclear emulsions, and used at a small solid angle to measure the energy of those ions scattered forward at 20° by the Faraday cup window.

Calibration and study of the total system without beam was accomplished with either U^{230} recoil products collected onto the tape or with Po^{212} alpha particles from samples held in front of the detector assembly. Studies of the method with heavy-ion reactions were made by bombarding Sm^{147} to produce short-lived holmium alpha emitters or Pb and Bi to produce various alpha emitters with energy between 7 and 9 Mev.

In the bombardment of Cf with B ions, the activity attributed to element 103 consists of alpha particles with an energy of 8.6 Mev decaying with a half-life of 8±2 seconds. Also observed are alpha particles of 8.4 and 8.2 Mev with similar half-lives of about 15 seconds, which are probably due to element 102. Figure 2 shows an alpha-particle spectrum from the first detector obtained during the most recent set of runs. These activities have been observed repeatedly during many weeks of bombardment of the californium target with both B^{10} and B^{11} ions. Similar bombardments of Pb, Bi, Pu^{240}, and Am^{241} do not produce the new activities.

The mass number of the element 103 isotope is thought to be 257 for the following reasons. B^{11} bombardments of Cf^{250}, Cf^{251}, and Cf^{252} cause compound nucleus reactions which lead to 103^{257} by the emission of 4, 5, or 6 neutrons, while with B^{10} this same result is accomplished with 3, 4, or 5 neutrons. These are known from other experiments to be the most prominent neutron-out reactions of boron with the transuranium elements. Excitation functions with B^{11} and B^{10} ions for production of the 8.6-Mev alpha activity are consistent with the above deduction.

These excitation functions were, of necessity, very broad because the same activity could be produced by several reactions; consequently, these data could not rule out conclusively (B, *pxn*) reactions which would produce light isotopes of element 102. The final proof was then accomplished by accentuating the element 102 produc-

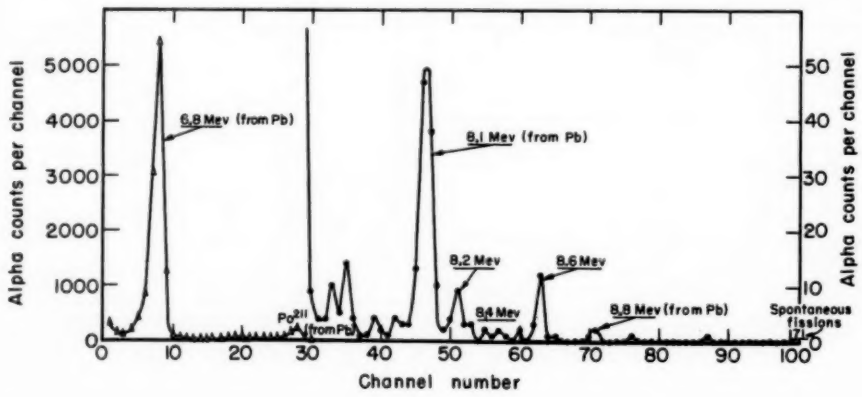

FIG. 2. Cf+B^{11}. Alpha spectrum from first detector. Summation of Runs Nos. 139-148. Total bombardment = 5.0 μa hr. Cycle time = 15 seconds.

tion by bombarding the californium target with C^{12} ions. It was found that the 8.6-Mev activity was decreased by more than a factor of 2, and the 8.2-Mev activity (thought to be mostly 102^{255}) was increased by a factor of about 20. This was to be expected for the element assignments given. Experiments with Pu^{240} had shown that the (C^{12}, αxn) cross sections would be larger, while the (C^{12}, pxn) cross sections would be smaller in comparison with the boron bombardments of californium. Possible light isotopes of mendelevium that could be produced and conceivably might emit alpha particles in the 8.2-8.6 Mev region were ruled out by bombardments of Am^{243} with C^{12} ions.

In honor of the late Ernest O. Lawrence, we respectfully suggest that the new element be named lawrencium with the symbol Lw.

The element 103 experiment has been in the process of development for almost three years, and its successful culmination has been due in no small part to the help of all of our colleagues. We would like to express our appreciation particularly to the following: to F. Grobelch for his tireless assistance in innumerable ways, both with the accelerator and the experimental equipment; to J. Gavin, the HILAC operators, its engineering and maintenance personnel for their patient production of the many hundreds of hours of boron beam operation; to C. Corum for his always ingenious mechanical designs which were the backbone of the experiment; to S. G. Thompson, L. Phillips, R. Gatti, F. McCarthy, and T. Parsons for their separation of the californium from the "napkin-ring" material; to R. Garrett for her continuous capable assistance; to A. Wydler for his very able multiplex design and construction; to W. Goldsworthy for his competent amplifier designs; to W. Stockton for his indispensable silicon detectors; and to B. Isaacs and S. Hargis for their very good-natured help in the data processing. Special acknowledgment is due to the Health Chemistry Department under P. Howe for its skillful handling of a very difficult radioactivity protection problem. We are also indebted to F. Asaro, I. Perlman, and G. T. Seaborg for helpful discussions regarding interpretation of these experiments.

[1]A. Ghiorso, T. Sikkeland, J. R. Walton, and G. T. Seaborg, Phys. Rev. Letters 1, 18 (1958).

[2]We are indebted to M. C. Michel for the mass analysis.

TWO-PHOTON DE-EXCITATION OF THE 0+ LEVEL IN Zr^{90}

Hans Ryde, Pedro Thieberger,* and Torsten Alväger†
Nobel Institute of Physics, Stockholm, Sweden

(Received February 21, 1961; revised manuscript received March 27, 1961)

Recently great interest has been focused on the second-order radiation process in which the de-excitation of a nuclear level takes place by the simultaneous emission of two photons, two conversion electrons, or one photon and one conversion electron, in competition with a single-quantum transition. The effect has been theoretically treated by various authors[1-6] and experimentally studied by several workers.[7-11] These processes are described as taking place via virtually reached, intermediate levels of higher excitation energy and a continuous energy distribution of the emitted radiation is expected. The total energy of each pair of quanta is the same as the energy available for the single-quantum transition.

To study the two-photon de-excitation experimentally under favorable circumstances, a transition has to be chosen in which the single-quantum emission is forbidden or strongly hindered. In the decay of the 1.73-Mev 0+ level to the 0+ ground state in Zr^{90} all electromagnetic radiation is, to the first order, absolutely forbidden. The only modes of decay are then internal conversion ($E0$ transition), internal pair formation, or two-photon de-excitation. The radioactive decay of the Y^{90} nucleus by beta emission to levels in Zr^{90} with a half-life of 64 hours has been thoroughly studied by, among others, Yuasa et al.[12] They report that the main beta transition to the ground state of Zr^{90} has a maximum energy of 2.26 Mev and that a weak beta component feeds the 1.73-Mev level with a relative intensity of 2.2×10^{-4}. The internal pair formation in the decay of this level takes place with a relative intensity of about

5×10^{-5} of the total beta decay.[13] The decay of the 0+ level in Zr^{90} has been treated theoretically with respect to double-quantum emission by Eichler and Jacob.[5]

In the present experiments a Sr^{90} sample obtained from fission products was used. Sr^{90} decays with a half-life of about 28 years to the ground state of Y^{90} by a low-energy beta transition. Y^{90} is thus fed continuously and decays in the way described above. This fact makes it possible to study the Y^{90} decay without making decay corrections, for the time used in these experiments.

The electromagnetic radiation from the source was detected by two 3-in. × 3-in. NaI(Tl) crystals, while the beta particles were stopped by aluminum absorbers. As it was considered to be essential to make the possibilities for the detection of the simultaneously emitted two photons an optimum by working with large solid angles, the crystals were placed at 180° to each other. The scattering of the radiation from one crystal to the other was reduced by 5 cm of lead between them. The source was placed in the middle of the lead shield with a conical collimator to each crystal. This arrangement made the solid angle through which each crystal was seen from the source as large as about 25% of 4π. The pulses from the two detectors were summed and then fed to a 100-channel pulse-height analyzer, which was gated only when the two pulses appeared within the resolving time (about 30 nanoseconds) of a fast coincidence circuit.[14] Coincidence pulses due to Compton backscattering from one crystal to the other were avoided by a suitably chosen discriminator setting for the pulses from each detector.

The coincidence spectrum of the annihilation radiation from the internal pair formation was recorded in a separate run to get an intensity reference. The discriminator level was in this case set at about 400 kev. The summation of pairs of annihilation quanta gives rise to a peak at about 1 Mev. The number of counts recorded in this peak is proportional to the intensity of the internal pair formation process. The external pair formation due to the emitted bremsstrahlung from the intense beta decay is proved to be negligible in a test experiment. Having the same source and the same geometry as in the main experiment, 15 000 coincidences per hour were recorded in the 1-Mev peak.

In the main experiment the discriminator levels were set at about 600 kev. Consequently, use has been made of the two-photon energy spectrum only between 600 kev and 1100 kev. This fraction is estimated to be 45% of the total, assuming an $E1E1$ transition.[5] Besides the coincidence spectrum a random coincidence spectrum was also recorded by introducing a suitable delay for the pulses from one of the detectors. Further, a background spectrum was obtained by running a measurement without the sample but with the detectors, absorbers, and collimator in the same position as in the main runs. The number of chance coincidences in the background measurement is negligible.

Figure 1 shows the result of the experiments performed so far. For each point shown the contributions from random and background coincidence have been subtracted. Following this procedure the disturbing effects due to radioactive impurities in the collimator, absorbers, and detectors are eliminated. Thus, the spectrum shown in Fig. 1 originates exclusively from coincidences in the source. It may be mentioned that several independent coincidence measurements all have resulted in spectra having similar structure to that shown in Fig. 1, with the indicated peak at an energy of about 1.7 Mev.

According to Ford[15] there is no reason to believe that there should exist an intermediate level between the two 0+ levels, which otherwise could explain the sum peak obtained. Thus, if the peak at 1.7 Mev is assumed to be due to double-quantum emission, it is possible to estimate from these experimental results the probability for this process compared with that for internal pair formation. As an average value, 8 coincidences per hour are obtained, which may be due to two-photon de-excitation in the source used. Adopting a mean value of the photopeak efficiency for the 3-in. × 3-in. NaI(Tl) crystals in the energy region in question,[16] a ratio of about

$$P_{\gamma\gamma}/P_{e^-} = 1.6\times10^{-3}$$

is obtained for the probability for two-photon emission ($P_{\gamma\gamma}$) compared with that for internal conversion (P_{e^-}). The number of two-photon de-excitations per disintegration would then be about 2.7×10^{-7}.

A careful search for activities, which, if they were present as impurities in the sample, could give rise to a peak at about 1.7 Mev has been made through the whole periodic table. The conditions are fulfilled in the decay of RaC. The alpha activity from the sample was measured in an alpha-ion chamber to be less than 10^{-8} of the

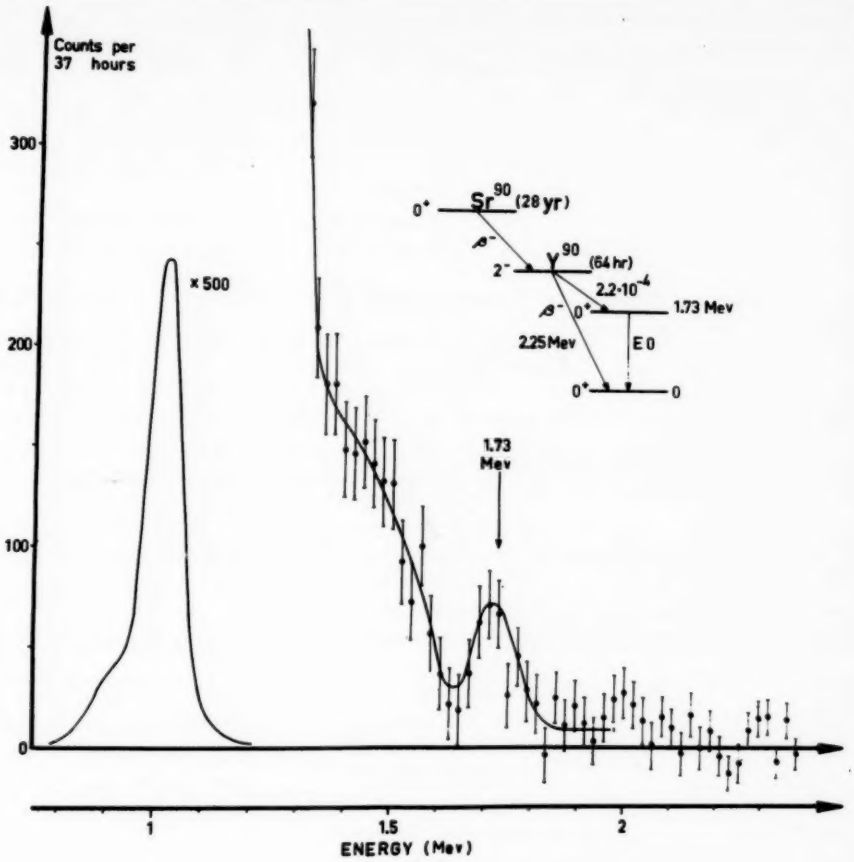

FIG. 1. Gamma-ray spectrum recorded by summing coincident pulses due to the decay of Y^{90}. For each point the contributions from random and background coincidences have been subtracted. For comparison the 1.02-Mev peak due to annihilation radiation following internal pair formation is also shown.

Sr^{90} beta activity, which thus excludes this source of error.[17] Another possibility would be the decay of Eu^{154}, but it is considered reasonable to assume the amount of Eu^{154} in the sample to be negligible, as the independent fission yield for this shielded nucleus is probably extremely low and as the chemical procedure gives a favorable decontamination factor.

It can be concluded from the measurements presented here, that the probability for two-photon de-excitation of the 0+ level in Zr^{90} is, in any case, at least forty times lower than that obtained from a rough theoretical estimate,[5] in which a higher state responsible for the transition is assumed to lie just above the 1.73-Mev level. The assumption of having the possible intermediate levels at an energy very large compared with 1.73 Mev leads in turn to a much lower theoretical limit for the probability of double-quantum emission. Our results seem to indicate that this second assumption is the better one, a fact which may also be indicated, as is pointed out in reference 5, by the existence of the giant resonance in photonuclear reactions.

---

*On leave from the Instituto de Física, San Carlos de Bariloche, Argentina.

†Present address: Argonne National Laboratory, Argonne, Illinois.

[1]M. Goeppert-Mayer, Ann. Physik 9, 273 (1931).

[2]R. G. Sachs, Phys. Rev. 57, 194 (1940).

[3]R. H. Dalitz, Proc. Roy. Soc. (London) A206, 521 (1951).

[4]J. R. Oppenheimer and J. S. Schwinger, Phys. Rev. 56, 1066 (1939).

[5]J. Eichler and G. Jacob, Z. Physik 157, 286 (1959).

[6]J. Eichler, Z. Physik 160, 333 (1960).

[7]T. Alväger and H. Ryde, Arkiv Fysik 17, 535 (1960); Phys. Rev. Letters 4, 363 (1960).

[8]W. Beusch, Helv. Phys. Acta 33, 363 (1960).

[9]G. J. McCallum, D. A. Bromley, and J. A. Kuehner, Nuclear Phys. 20, 382 (1960).

[10]J. Heintze and K. Knauf (to be published).

[11]A private communication by G. Sutter about a sim-

ilar experiment carried out at the Departement de Physique Nucléaire in Strasbourg, France, arrived when this report had already been prepared. The results seem to be in qualitative agreement with those presented here.

[12]T. Yuasa, J. Laberrigue-Frolow, and L. Feuvrais, J. phys. radium 18, 498 (1957).

[13]M. Deutsch, Nuclear Phys. 3, 83 (1957).

[14]B. Johansson, Nuclear Instr. 1, 274 (1957).

[15]K. Ford, Phys. Rev. 98, 1516 (1955).

[16]S. H. Vegors, Jr., L. L. Marsden, and R. L. Heath, Atomic Energy Commission Research and Development Report IDO-16370, 1958 (unpublished).

[17]W. Forsling (private communication).

EVIDENCE FOR LOW RATES FOR β DECAY OF Σ^- AND Λ HYPERONS*

William E. Humphrey, J. Kirz, and Arthur H. Rosenfeld
Lawrence Radiation Laboratory and Department of Physics, University of California, Berkeley, California

and

J. Leitner and Y. I. Rhee
University of Syracuse, Syracuse, New York

(Received April 6, 1961)

According to the theory by which strangeness-nonconserving Fermi interactions take place with the same coupling constant as strangeness-conserving weak interactions,[1] the hyperon decays,

$$\Sigma^- \to e^- + n + \bar{\nu} \tag{1a}$$

and

$$\Lambda \to e^- + p + \bar{\nu}, \tag{1b}$$

were expected to occur with branching fractions of 5.6% and 1.6%, respectively, with electron spectra rather close to phase space. Actually, experimental rates are already known to fall below these rates by about an order of magnitude,[2,3] and these data are further substantiated in this Letter.

The muonic decays $\Sigma^- \to \mu^- + n + \bar{\nu}$ and $\Lambda \to \mu^- + p + \bar{\nu}$ were expected with branching fractions of 2.5% and 0.3%, respectively, and are probably also lower by a factor of ten or more. These rare muonic decays are hard to separate from background, especially from normal pionic sigma decay followed by pion decay in flight; accordingly we shall not discuss muonic decay in this Letter.

The strangeness-conserving beta decay,

$$\Sigma^- \to e^- + \Lambda + \bar{\nu}, \tag{2}$$

is still expected to occur with a branching fraction of 2×10^{-4}.[4] The beta decay of Σ^+,

$$\Sigma^+ \to e^+ + n + \nu, \tag{1c}$$

is inhibited by the proposed $\Delta S/\Delta Q = +1$ rule.

Our $\Sigma^\pm$ and Λ particles were produced in the Berkeley 15-inch hydrogen bubble chamber by the reactions

$$K^- + p \to \Sigma^\pm + \pi^\mp, \tag{3}$$

$$K^- + p \to \Lambda + \pi^0, \tag{4}$$

$$K^- + p \to \Sigma^0 + \pi^0, \quad \Sigma^0 \to \Lambda + \gamma, \tag{4a}$$

where the K^- is captured at rest or interacts at very low energy. In order to be able to separate some of the β decays of Σ from the dominant pionic modes

$$\Sigma^\pm \to \pi^\pm + n, \tag{5}$$

we used the criterion that the visible decay particle (the electron candidate) should have a laboratory momentum $p \leq 100$ Mev/c,[3] and a track length ≥ 5 cm to assure reliable momentum measurements.

In order to eliminate two major sources of background we did not include in the sample Σ^- particles, which left either a very short or a very long track in the chamber.

(a) When a zero-length Σ^- undergoes β decay, the e^- could be confused with the e^- of the electron pair from the chain

$$K^- + p \to \Lambda + \pi^0, \quad \pi^0 \to e^+ + e^- + \gamma, \tag{6}$$

where $p(e^+)$ is close to that of the π^+ of Reaction (3). Similarly, Σ^+ of range < 1 mm were excluded.

(b) When a Σ^- undergoes β decay very near the end of its range, the e^- can be confused with a very close Compton electron from the chain initiated by Σ^- capture,

$$\Sigma^- + p \to \Sigma^0 + n; \quad \Sigma^0 \to \gamma + \Lambda; \quad \gamma \to \text{Compton}. \tag{7}$$

The decay mode

$$\Sigma^+ \rightarrow p + \pi^0 \qquad (8)$$

(where the proton track can be readily identified by ionization and range) was not examined. Its contribution to the branching fraction was taken into account, however.

Most of our Σ events were obtained with the 1960 K^- beam.[5] About 60 000 K^- particles (at approximately 2 per picture for 2×10^{11} protons per pulse) entered the chamber, with an average $p \approx 230$ Mev/c. These yielded 6700 Σ^- decays and 1500 Σ^+ decays through Channel (5), which satisfied the above criteria, and were also flat enough (dip ≤ 45 deg) to permit preselection on scanning projectors. Momentum templates and correction tables for dip, magnification, and similar effects were used to select the sample to be measured. The efficiency of this process is close to 100% at low electron momenta, but losses near 100 Mev/c reduce the over-all efficiency to about 85%.

In addition to this, a 1958 K^- experiment produced 1400 Σ^- decays and 300 Σ^+ decays through Channel (5) which satisfy our selection criteria.[6]

All these events have been measured; therefore, the efficiency for the search is close to 100%.

If we combine the efficiency with the fraction of the phase space for $0 \leq p_e \leq 100$ Mev/c (which is about 1/3), the effective branching-fraction denominator becomes $\frac{1}{3}(0.85\times6700+1400) = 2400$ for Σ^-, and $\frac{1}{3}(0.85\times1500+300) = 525$ for Σ^+ through Channel (5). If we include the Σ^+ decays through Channel (8), our effective denominator becomes 1050 for Σ^+.

Two further sources of background were considered:

(a) About 1 in 300 Σ^- particles interacts in flight, and by Process (7) or similar means produces an e^- within 5 mm. The probability for this is less than 10^{-6} if we exclude the cases in which a visible Λ decay makes the reaction easily detectable.

(b) If the chamber is not operating at optimum sensitivity, pions and muons with $p \approx 100$ Mev/c can be close to minimum-ionizing. Then, if the decay electron is not identified by range or delta rays, the decay modes,

$$\Sigma^\pm \rightarrow \pi^\pm + n + \gamma \qquad (9)$$

and

$$\Sigma^\pm \rightarrow \pi^\pm + n \text{ followed by } \pi^\pm \rightarrow \mu^\pm + \nu \qquad (10)$$

within a few millimeters, could simulate β decay with a small probability.

The results of our search are as follows:

We found three Σ^- decays which had charged decay particles with $p < 100$ Mev/c. One of these has a decay track of 91 ± 3 Mev/c, and could be a background event of the second type mentioned above, since the ionization does not rule out particles heavier than an electron. The second one is shown in Fig. 1; it has a decay electron

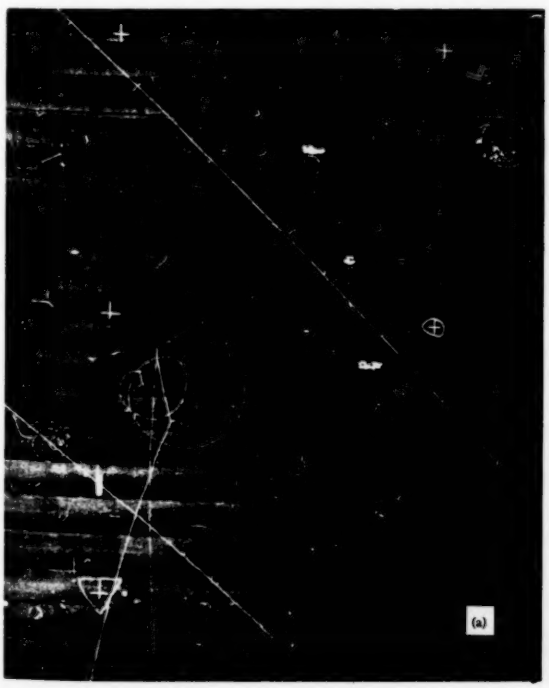

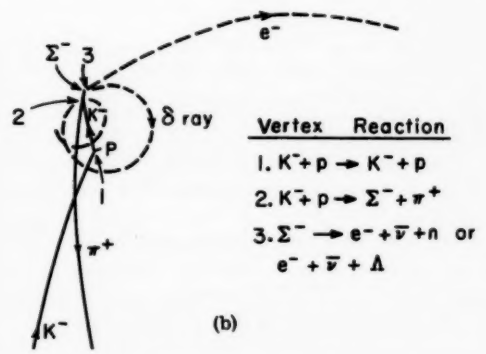

FIG 1. β decay of Σ^- produced in the reaction $K^- + p \rightarrow \Sigma^- + \pi^+$ [(a) bubble chamber photograph; (b) diagram]. The K^- particle scatters elastically before being captured. A δ ray of 5 Mev/c originates from the first 2.5 mm of the decay track. The momentum beyond the δ ray was measured as 43 ± 1.2 Mev/c. The length of the Σ^- track (2.2 ± 0.3 mm) indicates that the Σ^- did not stop before decay.

of 49 ± 2 Mev/c, and is therefore either a strangeness-nonconserving β decay (1a) or a strangeness-conserving β decay (2). The third candidate has a decay electron of 93 ± 5 Mev/c. This event could, however, be due to Chain (6), because the π^+ from Reaction (5) doubles back on the incoming K^- track, thereby obscuring the Σ^- production vertex.

No candidates for Σ^+ β decay were found.

Next we discuss the 900 visible Λ decays produced by the 1958 K^- beam. These were measured, and the ones that did not fit the kinematics for pionic decay were examined for coplanarity. Other than one event found by inspection,[7] no certain β decays were found.

Our efficiency for finding Λ β decays is about 70%. Therefore, the effective denominator (including the unseen $\Lambda \to n + \pi^0$ decays) is $(\frac{4}{3})900 \times 0.70 = 950$.

Our current information on β branching fractions is summarized in Table 1. The branching fractions calculated from this table are little more than lower limits. For every sure leptonic decay there are usually several "possibles." It might be reasonable to double these fractions, yielding $1/1000$ $\Sigma^- \to e^-$; $0/1000$ $\Sigma^+ \to e^+$; and $2/1000$ $\Lambda \to e^-$. This guess should then be credible within a factor of 2, again assuming that the electron spectrum does not deviate drastically from phase space.

Table I. Accumulated information on β branching fractions.

	Effective denominator			Numerator (β decays)		
	Σ^-	Σ^+	Λ	Σ^-	Σ^+	Λ
World survey of events reported up to November, 1958[a]	200	100	1500	1[b]		2
Dyer[c]	67	130	...	0	0	...
Berkeley propane bubble chamber[d]	2000	2000	10 000	1?	0	5
Baglin et al. (Freon chamber)[e]	150	...	4500	0	...	≈8
Helium chamber[f]	60	70	...	0	0	...
Franzini and Steinberger (propane chamber)[g]	...	...	...	1	...	...
This Letter	2400	1050	950	1+2?	0	0
Total	4900	3350	17000	2+n?	0	15

[a] See reference 7.

[b] J. Hornbostel and E. O. Salant, Phys. Rev. 102, 502 (1956). In this experiment only five normal Σ decays were found, and no detection efficiency for β decays was reported. The event listed is a probable β decay of a Σ particle of undetermined charge.

[c] John N. Dyer, thesis, University of California Radiation Laboratory Report UCRL-9450, November, 1960 (unpublished).

[d] Wilson M. Powell, Lawrence Radiation Laboratory (private communication). The Powell group did not scan specially for β decays. However, bremsstrahlung and curling up make a large fraction of the electrons easy to spot. The 2000 Σ^- and Σ^+ represent approximately 1/3 of the propane group's sample (we assume they also have a 1/3 probability of finding the β decay of a Σ). The possible $\Sigma^- \to e^- + n + \bar{\nu}$ decay could also be the decay of a K meson, since Σ production did not have an associated pion. The 10 000 Λ's represent about 1/2 of the group's sample of 14 000 corrected for the unseen $\pi^0 + n$ decays. The factor of 1/2 assumes that they can identify electrons below 85 Mev/c.

[e] P. Falk-Vairant, postdeadline paper, presented at the meeting of the American Physical Society, Berkeley, December 29-31, 1960. Our numbers come from a later Letter from Frank T. Solmitz from École Polytechnique on January 13, 1961.

[f] Martin M. Block, Duke University (private communication).

[g] P. Franzini and J. Steinberger, Phys. Rev. Letters 6, 281 (1961). This event is definitely a strangeness-nonconserving decay (1a). The e^- momentum rules out the possibility of $\Sigma^- \to \Lambda + e^- + \bar{\nu}$.

If we compare this with the original predictions by Feynman and Gell-Mann,[1] we have:

	Experiment	Theory
$\Sigma^- \to e^- + n + \bar{\nu}$	$\approx 0.1\%$	5.6%
$\Lambda \to e^- + p + \bar{\nu}$	$\approx 0.2\%$	1.6%
$\Sigma^+ \to e^+ + n + \nu$	≈ 0	0

The discrepancy is about 10 to 1 for Λ decay and perhaps more for Σ decay; we conclude that β decays of hyperons cannot be explained by forms of Fermi interaction such as that of Feynman and Gell-Mann having the same coupling constant at each permitted vertex.

We wish to thank Dr. Donald H. Miller and Dr. Ronald R. Ross for valuable discussions and suggestions. The efficient work of our scanners, especially David J. Church and Lawrence A. Drews, is greatly appreciated.

*Work done under the auspices of the U. S. Atomic Energy Commission and the Office of Naval Research.

[1]R. P. Feynman and M. Gell-Mann, Phys. Rev. 109, 193 (1958).

[2]F. Eisler, R. Plano, A. Prodell, N. Samios, J. Steinberger, M. Conversi, P. Franzini, I. Manelli, R. Santangelo, and V. Silvestrini, Phys. Rev. 112, 979 (1958).

[3]J. Leitner, P. Nordin, A. H. Rosenfeld, F. T. Solmitz, and R. D. Tripp, Phys. Rev. Letters 3, 186 (1959).

[4]Note that for 1/3 of these decays the Λ will subsequently decay via its neutral channel, and the over-all event then becomes indistinguishable from the low-energy electron cases of reaction (1a).

[5]Pierre Bastien, Orin Dahl, Joseph J. Murray, Mason Watson, Ray G. Ammar, and Peter Schlein, in Proceedings of the 1960 International Conference on Instrumentation for High-Energy Physics (Interscience Publishers, Inc., New York, 1961), p. 299.

[6]Some of the events included in this sample have already been reported in reference 3.

[7]P. Nordin, J. Orear, L. Reed, A. H. Rosenfeld, F. T. Solmitz, H. D. Taft, and R. D. Tripp, Phys. Rev. Letters 1, 380 (1958). The survey in that paper did not include the Λ denominator we are now reporting, although it did include the one β decay in the numerator.

$\pi^- - p$ ELASTIC SCATTERING AT 550, 600, 720, 900, AND 1020 Mev

Calvin D. Wood, Thomas J. Devlin, Jerome A. Helland, Michael J. Longo, Burton J. Moyer, and Victor Perez-Mendez

Lawrence Radiation Laboratory, University of California, Berkeley, California

(Received April 10, 1961)

This Letter contains the results of measurements of differential cross sections taken in the energy region of the second and third peaks of the $\pi^- - p$ total scattering cross section.[1,2] The data were obtained by using an array of recoil proton scintillation counters in coincidence with pion detectors to identify elastic events. Details of the experimental procedure and the data analysis will be published separately.[3]

It should be here stated that we were unable to arrive at an independent normalization for the data, because of pion beam monitoring difficulties, although the shapes of the curves were rather well determined and repeatable. Therefore, we normalized our data to the total elastic cross sections as determined by other workers and summarized by Falk-Vairant and Valladas,[4] keeping the point at $\cos\theta^* = 1$ fixed at the value determined by dispersion relations[5] and the optical theorem (where θ^* is the c.m. scattering angle for the pion). Hence, the normalization is known only to about ± 12 to 15%. A future run is planned to measure the absolute normalization.

The errors quoted were obtained from a statistical analysis of the repeatability of repeated runs. The only region of the curve where the errors are significantly different from pure statistics (i.e., different by more than a factor of two) is that in which the recoil proton had nearly the same laboratory-system angle as the scattered pion. Corrections due to accidental and inelastic counts were 2% or less for all channels and all energies.

The results are listed in Table I, where θ^* is the center-of-mass angle of the scattered pion and $d\sigma/d\Omega$ is the differential cross section (in mb/sr). The corresponding graphs appear in Fig. 1.

In Fig. 2 we present a plot of the energy dependence of the coefficients of the various cosine power series adjusted to our data, and also to the data of Goodwin et al.,[6] Shonle,[7] Bergia et al.,[8]

Table I. Angular distributions from $\pi^- + p \rightarrow \pi^- + p$. The normalization of the curves is known only to about 12 to 15% (see text for explanation).

$E = 550$ Mev		$E = 600$ Mev		$E = 720$ Mev		$E = 900$ Mev		$E = 1020$ Mev	
$\cos\theta^*$	$d\sigma/d\Omega^*$ (mb/sr)	$\cos\theta^*$	$d\sigma/d\Omega^*$ (mb/sr)	$\cos\theta^*$	$d\sigma/d\Omega^*$ (mb/sr)	$\cos\theta^*$	$d\sigma/d\Omega^*$ (mb/sr)	$\cos\theta^*$	$d\sigma/d\Omega^*$ (mb/sr)
1.0	4.65 ±0.24	1.0	6.19 ±0.21	1.0	5.46 ±0.24	1.0	17.82 ±0.56	1.0	12.91 ±0.40
0.621	2.63 ±0.14	0.608	2.69 ±0.05	0.577	1.44 ±0.032	0.782	3.92 ±0.050	0.766	3.00 ±0.064
0.542	2.16 ±0.08	0.527	2.29 ±0.035	0.492	1.17 ±0.034	0.534	0.405±0.017	0.506	0.345±0.019
0.377	1.74 ±0.16	0.359	1.54 ±0.27	0.318	0.86 ±0.22	0.443	0.203±0.027	0.412	0.200±0.034
0.168	1.16 ±0.20	0.148	0.79 ±0.11	0.102	0.717±0.095	0.260	0.218±0.063	0.224	0.204±0.046
0.027	0.577±0.040	0.006	0.332±0.021	-0.041	0.302±0.017	0.039	0.273±0.026	0.001	0.365±0.025
-0.107	0.302±0.028	-0.128	0.167±0.013	-0.174	0.308±0.014	-0.103	0.351±0.022	-0.141	0.351±0.035
-0.249	0.172±0.028	-0.269	0.124±0.013	-0.312	0.438±0.034	-0.234	0.461±0.019	-0.270	0.392±0.022
-0.451	0.230±0.023	-0.467	0.254±0.017	-0.503	0.780±0.029	-0.367	0.726±0.022	-0.400	0.441±0.026
-0.669	0.730±0.043	-0.681	0.674±0.023	-0.705	1.13 ±0.023	-0.549	1.409±0.031	-0.575	0.745±0.050
-0.787	1.13 ±0.05	-0.795	0.911±0.030	-0.812	1.09 ±0.027	-0.735	2.069±0.034	-0.752	1.102±0.044
-0.876	1.41 ±0.06	-0.880	1.20 ±0.046	-0.891	0.985±0.042	-0.832	2.019±0.044	-0.843	1.030±0.043
-0.946	1.53 ±0.15	-0.948	1.27 ±0.055	-0.953	0.550±0.068	-0.903	1.635±0.046	-0.910	0.792±0.043
						-0.958	0.790±0.049	-0.961	0.297±0.041

and Chrétien et al.[9] The initials standing by the data points indicate their origins. From this behavior of the coefficients we make the following inferences.

1. The prominence of a_3 between 300 and 550 Mev may be ascribed to P-D interference. If so, it may be due to the overlap of the high-energy tail of the 200-Mev $P_{3/2}$ resonance with a D-state interaction building up with increasing energy.

2. The small magnitudes of a_3 and a_4 at 600 Mev indicate that if a D-state interaction exists at 600 Mev it has angular momentum 3/2. If at 600 Mev no states higher than $D_{3/2}$ interact strongly, and if the $P_{3/2}$ interaction has sufficiently decreased, we can understand the small $\cos^3\theta$ and $\cos^4\theta$ contributions and the prominence of a_2;

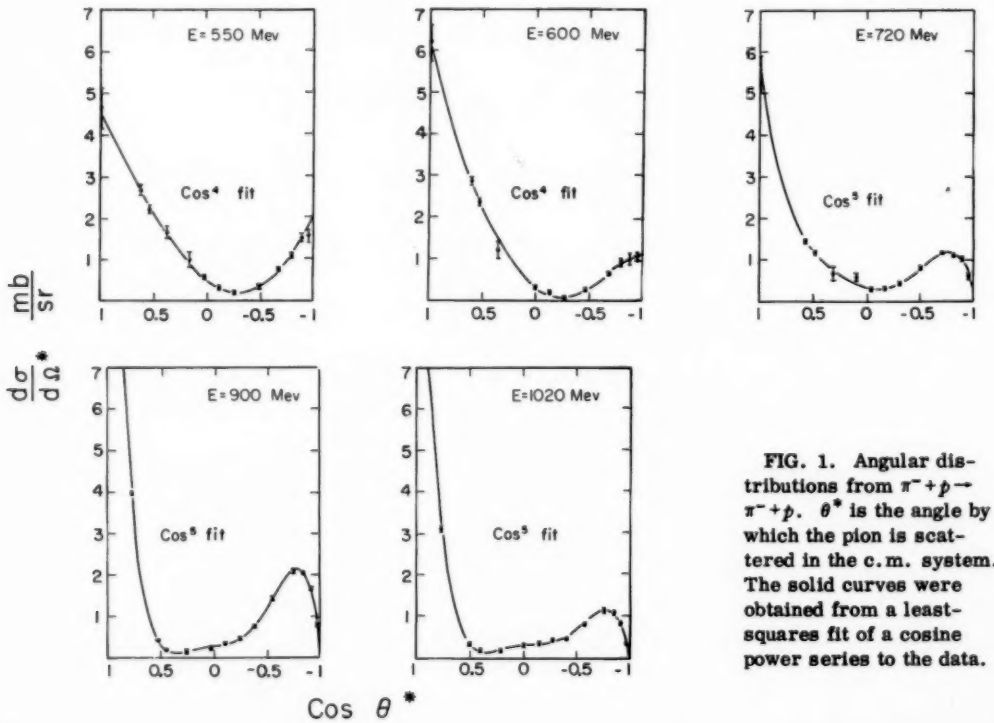

FIG. 1. Angular distributions from $\pi^- + p \rightarrow \pi^- + p$. θ^* is the angle by which the pion is scattered in the c.m. system. The solid curves were obtained from a least-squares fit of a cosine power series to the data.

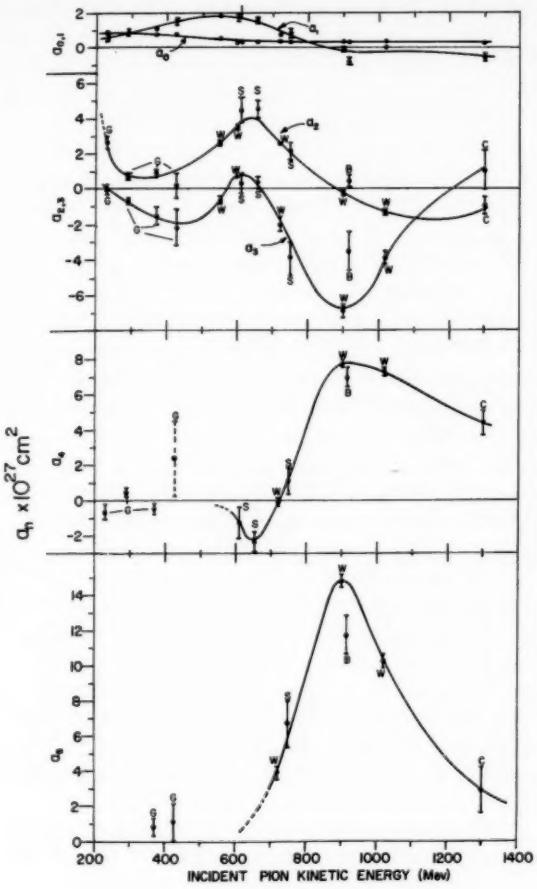

FIG. 2. Coefficients a_l from the expansion $d\sigma/d\Omega^* = \sum_{l=0}^{l_{max}} (a_l \cos^l\theta^*)$ which was fitted to the data by the method of least squares.

a superposition of principally $S_{1/2}$ and $D_{3/2}$ waves would give just this.

3. At 900 Mev we require strong values of a_3, a_4, and a_5; but no powers higher than $\cos^5\theta$ are required to fit the data. These facts call for a prominent $F_{5/2}$ interaction together with strong D-state interaction. We cannot fit the 900-Mev data without a superposition of F and D waves (and possibly of P waves as well). The hump in the vicinity of $\cos\theta^* = -0.8$, which appears to be at a maximum at 900 Mev, is due to D and F (and possibly also P) spin-flip amplitudes in superposition.

4. The strong forward peaking, particularly at 900 Mev, implies that absorptive processes may be prominent in these "resonances." At 900 Mev a simple diffraction model with an absorbing volume whose radius is 1.2 fermis can describe quite well the small-angle data.

More extensive analysis of these results is in progress, including phase-shift calculations, and further experimental work is planned, including polarization measurements. In agreement with the assignments of Peierls,[10] we infer strong $D_{3/2}$ interaction at 600 Mev, and strong $F_{5/2}$ interaction at 900 Mev; but our data indicate a more complicated picture than simple resonances in these states.

We gratefully acknowledge our indebtedness to Professor A. C. Helmholz for encouragement and discussion, to Richard Eandi, Donald Hagge, and Dale Dickinson for their valuable assistance in all phases of the experiment, and to the Bevatron staff and crew.

[1]J. C. Brisson, J. Detoef, P. Falk-Vairant, L. Van Rossum, G. Valladas, and L. C. L. Yuan, Phys. Rev. Letters 3, 561 (1959). [Also see their report in the Proceedings of the 1960 Annual International Conference on High-Energy Physics at Rochester (Interscience Publishers, Inc., New York, 1960).]

[2]T. J. Devlin, B. C. Barish, W. N. Hess, V. Perez-Mendez, and J. Solomon, Phys. Rev. Letters 4, 242 (1960).

[3]C. D. Wood, T. J. Devlin, J. A. Helland, M. J. Longo, B. J. Moyer, and V. Perez-Mendez, Phys. Rev. (to be published).

[4]P. Falk-Vairant and G. Valladas, in Proceedings of the 1960 Annual International Conference on High-Energy Physics at Rochester (Interscience Publishers, Inc., New York, 1960), p. 38.

[5]J. W. Cronin, Phys. Rev. 118, 824 (1960).

[6]L. K. Goodwin, R. W. Kenney, and V. Perez-Mendez, Phys. Rev. Letters 3, 522 (1959); Phys. Rev. (to be published).

[7]J. I. Shonle, Phys. Rev. Letters 5, 156 (1960).

[8]S. Bergia, L. Bertocchi, V. Borelli, G. Brautti, L. Chersovani, L. Lavatelli, A. Minguzzi-Ranzi, R. Tosi, P. Waloschek, and V. Zoboli, Nuovo cimento 15, 551 (1960).

[9]M. Chrétien, J. Leitner, N. P. Samios, M. Schwarz, and J. Steinberger, Phys. Rev. 108, 383 (1957).

[10]R. F. Peierls, Phys. Rev. 118, 325 (1960).

LOSS OF C^{11} FROM PLASTIC FOILS AND ITS EFFECT ON CROSS-SECTION MEASUREMENTS*

J. B. Cumming, A. M. Poskanzer, and J. Hudis

Chemistry Department, Brookhaven National Laboratory, Upton, New York

(Received April 6, 1961)

In the course of measurements of the ratio of the cross sections for the $C^{12}(p, pn)C^{11}$ and $Al^{27}(p, 3pn)Na^{24}$ reactions using stacked polyethylene and aluminum foils, it was discovered that up to 15% of the C^{11} activity may be lost by the plastic foils during irradiation. We ascribe the observed results to hot atom reactions of the recoiling C^{11} atoms leading to gaseous products which diffuse out of the target. This phenomenon seriously affects the use of the C^{11} production rate in thin plastic foils to monitor high-energy proton beams.

Our observations to date may be summarized as follows:

1. Production rate relative to 95-mg/cm² plastic scintillator. We have bombarded stacks of polyethylene, "oriented" polystyrene, graphite, and 95-mg/cm² polystyrene plastic scintillator in the external 3-Bev proton beam of the Cosmotron and have observed that the apparent production rate of C^{11} per (gram/cm²) of carbon varied significantly with both the thickness and chemical composition of the target material. The target diameter was sufficiently large to intercept most of the beam so as to reduce the effects of misalignment of the foils. The target stacks were relatively thin (< 0.5 g/cm)² to minimize production of secondary particles and the foils were sandwiched in such a manner as to compensate for nuclear recoil losses. The results of these measurements are shown in Fig. 1. It appears that the loss from polystyrene is less than from polyethylene of equal thickness. However, one should not assume that other batches of these materials will behave precisely the same. It was also observed that the apparent loss of C^{11} activity from 9.5-mg/cm² polyethylene was the same for foils irradiated in vacuum as in air.

2. Observation of C^{11} activity in the gas phase. Foils were irradiated in an aluminum tank containing 1 atmosphere of helium. After irradiation, the gas was expanded into a proportional counter. In one experiment the tank contained two 95-mg/cm² plastic scintillators. The C^{11} in the gas phase corresponded to a loss of (0.8 ± 0.1)% of the activity produced in the scintillators. A similar experiment with no plastic in the tank gave a blank of ~5% of the above value. The data in Fig. 1 have been normalized to this value.

Polystyrene foils, 7.7 mg/cm² thick, produced a C^{11} activity in the gas phase equivalent to a loss of (1.7 ± 0.2)%. One irradiation of 9.5-mg/cm² polyethylene foils with cyclotron neutrons (20-Mev H^2 + Be) to produce C^{11} by the $(n, 2n)$ reaction gave a gaseous activity corresponding to a loss from the foils of (8 ± 1)%. The activity of the foils measured relative to a 95-mg/cm² scintillator indicated a loss of (12 ± 2)%. The accuracy of the present experiments does not indicate whether or not all of the activity lost from the foils is retained in the gas phase.

3. Irradiation at low temperature. The 9.5-mg/cm² polyethylene foils were irradiated in sealed polyethylene envelopes at liquid nitrogen temperatures. A half hour after irradiation it was observed that, when a foil was warmed to room temperature, (9 ± 1)% of the activity was lost with a half-time of ≤2 min. If the foil was warmed in a sealed vial, no loss of activity was

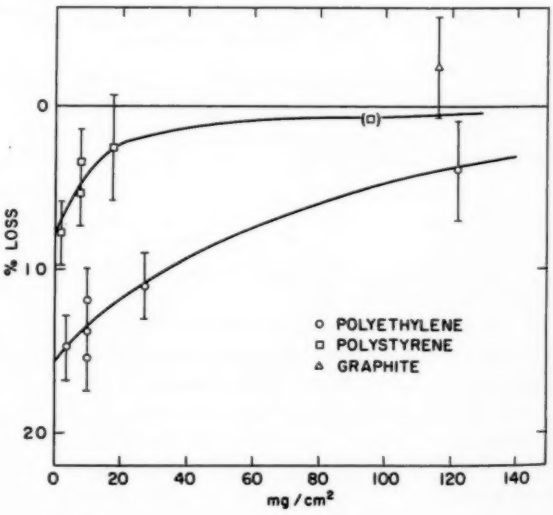

FIG. 1. The percent loss of C^{11} from various target materials as a function of the thickness of the material. The measurements were made relative to a 95-mg/cm² plastic scintillator and normalized to a loss of 0.8% for this point. The normalized point is indicated by parentheses in the figure.

observed until the vial was opened.

4. Composition of the radioactive gas. Gas chromatography with charcoal and silica gel columns was used to analyze[1] the chemical composition of the radioactive gas liberated from 9.5-mg/cm^2 polyethylene. The composition was found to be 57% methane, 36% acetylene, 6% ethylene, and 1% ethane. No CO or CO_2 was observed.

Absolute measurements of the $C^{12}(p, pn)C^{11}$ cross section may have been affected by the loss of C^{11} in those cases where thin plastic targets were used. Recent measurements in the Bev region[2,3] have used polystyrene targets sufficiently thick so that the correction is less than 1%. The loss effect may also account for some of the discrepancies in the $C^{12}(p, pn)C^{11}/Al^{27}(p, 3pn)Na^{24}$ cross-section ratios which have been reported.

The authors wish to acknowledge helpful discussions with and the assistance of R. Cool, D. R. Christman, G. Friedlander, G. Harbottle, C. Paul, H. Stangl, and A. P. Wolf.

---

*Research performed under the auspices of the U. S. Atomic Energy Commission.

[1]See J. Yang and A. P. Wolf, J. Am. Chem. Soc. 82, 4488 (1960).

[2]J. B. Cumming, G. Friedlander, and C. Swartz, Phys. Rev. 111, 1368 (1958).

[3]N. Horowitz and J. J. Murray, Phys. Rev. 117, 1361 (1960).

EXTREMELY ENERGETIC COSMIC-RAY EVENT*

John Linsley, Livio Scarsi,† and Bruno Rossi
Laboratory for Nuclear Science, Massachusetts Institute of Technology, Cambridge, Massachusetts
(Received April 12, 1961)

This note is a preliminary report on an extremely large cosmic-ray air shower. The event was observed at the M.I.T. Volcano Ranch station, elevation 5800 ft, near Albuquerque, New Mexico. An array of scintillation counters was used to detect and measure air showers by the technique used in the earlier M.I.T. Agassiz experiment.[1] The main array was made up of 19 detectors arranged in a pattern of triangles as shown in Fig. 1. The area of each detector was 3.3 m^2, and the spacing of adjacent detectors was 442 m. The area enclosed by the array was 2 km^2, but the sensitive area for detecting very large showers was considerably greater. An additional detector shielded by 10 cm of lead sampled the penetrating component of showers.

The event to be described was one of two, nearly equal in size, which were the largest observed in the period of operation September, 1959, to May, 1960. The total on-time of the equipment during that interval was about 180 days. The particle densities (particles/m^2) registered at the various points of the array are given in Fig. 1. The shower core struck several hundred meters outside the array boundary.

We found the direction of the shower axis by making a least-squares fit of the observed arrival times to those expected for a plane shower front. The values 41°, 41°, and 70° were found for the zenith angle, declination, and right ascension, respectively. The deviations of the ob-

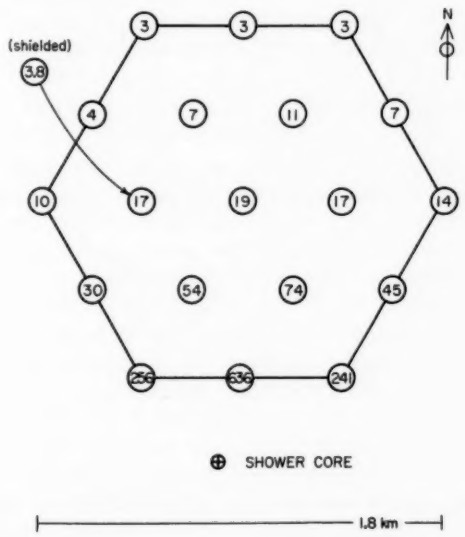

FIG. 1. Diagram of the Volcano Ranch 2-km^2 array, showing the location of the shower axis and measured densities in particles/m^2 for this event, No. 39565. The shielded detector was located very near the indicated main detector.

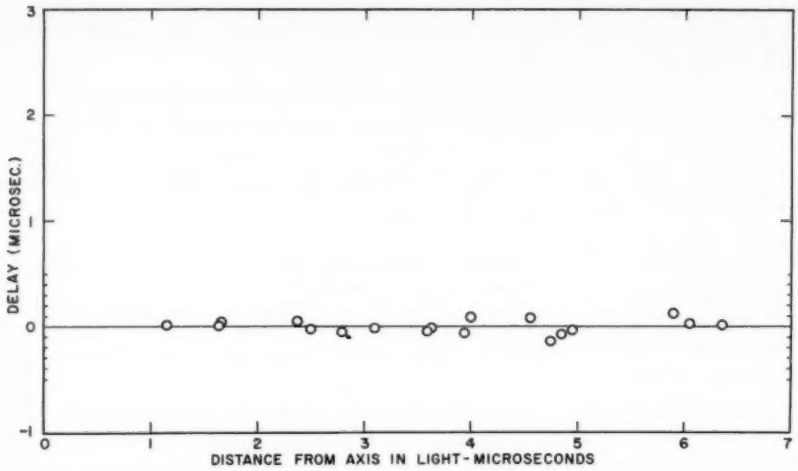

FIG. 2. Apparent delay of the extreme front of the shower, with respect to a plane which best fits the timing data, as a function of distance from the shower axis. Distance from the axis is given in light-microseconds (units of 300 m). Ordinate and abcissa have the same scale.

served data from the computed values are shown in Fig. 2 as a function of distance from the shower axis. The rms deviation is 0.07 μsec.

We found the location of the shower core by fitting the density observations to the following trial lateral distribution formula:

$$\Delta = 0.18(N/R_0^2)(R/R_0)^{-1.2}(1+R/R_0)^{-2.3}, \qquad (1)$$

where Δ is the total density of particles at a perpendicular distance R from the shower axis, $R_0 = 100$ m, and $N = \int_0^\infty 2\pi \Delta R dR$. This formula fits the experimental data obtained at Volcano Ranch for the range of shower sizes $5\times10^7 < N < 2\times10^8$, and the range of distances from the axis $100 < R < 1000$ m. In this case, the value obtained for N was 5.5×10^9. There are two sources of uncertainty in relating this number to the real shower size; i.e., to the actual total number of particles in the shower. The first is the uncertainty in core location resulting from statistical and instrumental errors in the data. We estimate the error from this source to be no greater than about 10%. The second is the uncertainty whether Eq. (1) is applicable for such a large shower, especially for distances less than 350 m from the axis. A preliminary inspection of several showers with $N > 8\times10^8$ which struck within the array indicates that for such showers the particle density increases more rapidly with decreasing distance from the axis than Eq. (1) predicts. This implies that the value given above for N is an underestimate of the actual size of this shower, perhaps by a factor of 2. We intend to discuss the problem of relating shower density measurements to shower size, for very large showers, in a later publication.

If the figure 5.5×10^9 is accepted, tentatively, as the size of this shower, it follows on any reasonable shower model that the energy of the primary particle was about 10^{19} ev. Taking the usual estimate 3×10^{-6} gauss for the galactic magnetic field, one finds the radius of curvature of the path of a proton of such energy to be about 10^4 light years. Since, according to current estimates, the radius of the galactic halo is only about five times this value, while the thickness of the galactic disk is about five or ten times smaller, it seems certain that the primary particle acquired its energy outside our galaxy.

An important question is whether the primary particle was a proton or a heavier nucleus. In this connection, we note that other results obtained at Volcano Ranch, not yet published, show that most, if not all, showers have nearly the same proportion of penetrating to nonpenetrating particles, when observed near maximum shower development. We interpret this to mean that most, if not all, air shower primaries in the energy range 10^{17} to 10^{18} ev have about the same mass, and are probably protons. It is not yet clear whether some apparent exceptions are real or spurious. In any case, the shower described here had a "normal" proportion of penetrating particles (see Fig. 1).

Turning again to the time measurements, we note that the times shown in Fig. 2 correspond, generally speaking, to the arrival of the first particle at each of the various detectors. The distinction is important, since we find that at large distances from the core, shower particles arrive over a time span of the order of microseconds. The distributions in arrival time of the

particles at the 8 detectors furthest from the axis of this shower are shown in Fig. 3. The distributions were obtained by an analysis of the shapes of the recorded pulses. The number of particles that make up each distribution is not great, and the (graphical) method used for deriving the true scintillation pulse from the recorded pulse has limited accuracy. However, some general features seem to emerge. (1) The "extreme front" of the shower, corresponding to the initial rise of the pulse, is well defined. (2) Many particles are delayed by as much as one or two μsec. (3) Few particles are delayed by more than twice the mean delay. While this type of direct evidence is not available except for a few exceptionally large showers, we find by statistical analysis that similar conclusions hold, on the average, for smaller showers.

Figure 2 can be considered a profile of the extreme front of this shower, and shows that the curvature of the extreme front is quite small. The precision of our method is sufficient to establish that the extreme front of an individual shower has a finite radius of curvature, R_C, if the value of R_C is less than about 7 km. For this shower the most likely value for R_C is 10 to 12 km, but any value in the range 7 km $< R_C < \infty$ will fit the data reasonably well. To date we have not found any shower for which we could establish that R_C is less than 7 km.

These timing results suggest a model in which an appreciable fraction of air shower particles that arrive at distances greater than 1500 m from the axis, at elevation 5800 ft, begin to diverge strongly from the shower axis at heights greater than 7 km above ground level. Thus, such particles may provide new information about the early stages of shower development.

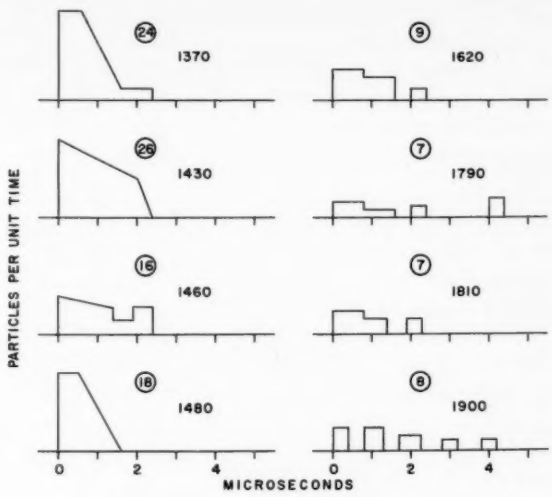

FIG. 3. Distributions in arrival time of shower particles at the eight detectors furthest from the shower axis. The number of particles included in each distribution (to which the areas have been normalized) is shown circled. Distances from the shower axis are also given.

*This work, carried out under grants from the National Science Foundation, was also supported in part by the U. S. Atomic Energy Commission, the Office of Naval Research, and the Air Force Office of Scientific Research.

†Present address: Istituto Nazionale di Fisica Nucleare, Milan, Italy.

[1]G. Clark, J. Earl, W. Kraushaar, J. Linsley, B. Rossi, and F. Scherb, Nature 180, 353 (1957); Suppl. Nuovo cimento 8, 623 (1958).

DELAYED PROPAGATION OF SOLAR COSMIC RAYS ON SEPTEMBER 3, 1960*

J. R. Winckler, P. D. Bhavsar, A. J. Masley, and T. C. May
University of Minnesota, Minneapolis, Minnesota
(Received April 3, 1961)

We should like to describe observations of a solar cosmic-ray increase which is remarkable for the large delay time in the arrival of the particles. Furthermore, the delays are energy dependent and are probably produced by a partially known sequence of events in interplanetary space. The present case is of particular interest because the delays extended to high energies detectable by balloons and by ground-level monitoring instruments and because the event was well documented by balloons at several latitudes during and after the flare and by rocket flights.[1]

In Table I we describe the sequence of solar-terrestrial events before, during, and after the cosmic-ray flare. Although there were several smaller flares during this period, only major flares of importance 3 are listed in the table. The flare at 0040 U.T. on September 3 was the only flare which was accompanied by a Type IV radio emission and, therefore, we believe that it was the source of the solar cosmic rays. This flare was in a region just appearing on the east limb of the sun, but was preceded by several large flares in a region on the face of the disk. An artist's conception of the situation in interplanetary space is shown in Fig. 1. This figure applies at the time of the cosmic-ray flare. The solar cloud from the 0706 U.T. flare on September 2 was in transit near the earth, while the cloud from the 2234 U.T. flare on September 2 had just left the sun. Judging by the Forbush decrease in galactic cosmic rays, which began at 0230 U.T. on September 4, the first cloud was magnetic in character. The second cloud did not produce a Forbush decrease but did produce a very strong geomagnetic storm on the earth. Note from the table that the delay between the first and second magnetic storms is the same as the delay between the flares which we have tentatively assigned as their sources.

The cosmic-ray data summarized in Fig. 2 result from high-altitude balloons flown at Fort Churchill, Manitoba, Canada, and at Minneapolis, and from the ground-level neutron monitor at

Table I. Solar-terrestrial time table.

Date, time (U.T.)	Event	Comment on tentative identification
Sept. 2, 0706	Class 3 flare	Solar coordinates N19 W25; source of magnetic cloud; S. C. and Forbush decrease.
Sept. 2, 2234	Class 3 flare	Solar coordinates N21 W31; source of apparent nonmagnetic cloud but strong magnetic storm; no Type IV radio emission.
Sept. 3, 0040	Class 3 flare	Solar coordinates N17 E90; source of cosmic rays; accompanied by Type IV.
Sept. 3, 0112	Class 3 flare	Cosmic-ray flare maximum; x-ray burst (local).
Sept. 4, 0230	S. C.	Begin magnetic storm from 0700 flare Sept. 2.
Sept. 4, 0230	Forbush decrease	Indicates magnetic character of solar cloud.
Sept. 4, 1830	S. C.	Begin magnetic storm from 2230 flare Sept. 2; no Forbush effect.

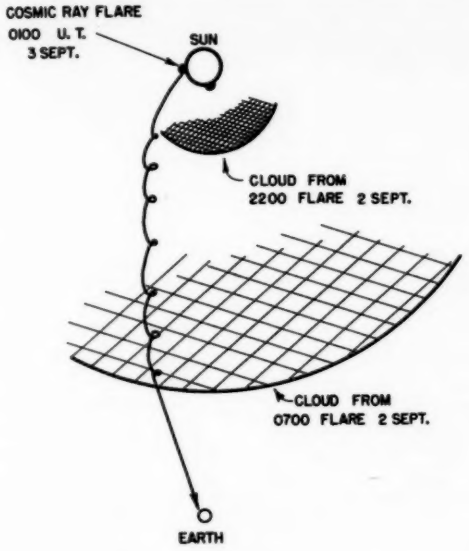

FIG. 1. Disturbances from two flares in the region approximately 30°W of central meridian were in transit at the time of the cosmic-ray flare. Particles from the cosmic-ray flare on the east limb were propagated through or around the magnetic cloud from the 0700 flare.

Deep River, Ontario, Canada.[2] The balloon instrumentation included integrating ionization chambers, Geiger counters, coincidence telescopes, and nuclear emulsions. The results of these instruments have been examined in detail and clearly show that all of the rate increases in Fig. 2 result from the solar cosmic-ray particles with the exception of the flare-coincident x-ray burst. The data are consistent with these particles being principally protons similar in some respects to other cases of solar flare protons observed with balloons.[3] For simplicity, in Fig. 2, we show only the ionization chamber records. The cosmic-ray flare is marked on the balloon records in Minneapolis by a large x-ray burst coincident with flare maximum. No x rays were observed at Fort Churchill, however. We conclude that this x-ray burst was the result of electrons precipitated from the geomagnetic field during the flare, and was not the direct solar bremsstrahlung which has been observed several times recently.[4] Following the flare, the cosmic-ray particles slowly increased in rate at all locations. Because the rates of the balloon instruments for solar cosmic rays are sensitive to altitude, a balloon depth schedule is included above and below the top section of Fig. 2 for the appropriate balloon flights. Two simultaneous flights are shown at Minneapolis at different depths. Since geomagnetic conditions were quiet during this period, we can with fair confidence assume that the geomagnetic cutoff at Minneapolis was operative and was about 250 Mev.[5] The energy cutoff at Fort Churchill is determined by the balloon depth, which varied between 5 and 15 g/cm^2 atmospheric depth during the flight. The corresponding energies are 75 Mev and 125 Mev. The characteristic energy of the sea-level neutron monitor is estimated to be between 500 and 600 Mev.

Two effects are seen to be operative. First of all, the time delay of the maximum cosmic-ray intensity at earth measured from the time of the flare is smallest for the high-energy detector and largest for the lowest energy detector at Churchill. The times at which the intensity maxima occurred on the neutron monitor, Minneapolis balloon, and Churchill balloon are marked by vertical lines on Fig. 2. Second, the low-energy particle intensity increases with time with respect to the high-energy particles. Since the Churchill balloon is continuously sensitive down to about 125 Mev or less, the changing character of the spectrum can be examined by plotting the ratio of ionization rate to counting rate for the Churchill flight. This is shown in the lower portion of Fig. 2. The I/I_{min} ratio at Churchill increases with time from a value like that for galactic cosmic rays (2 times minimum) to a value of about 4.2 times minimum ionization, showing the relative increase of low-energy particles. The ratio at Minneapolis, however, first decreases and then follows a slight increase with time, but maintains a value consistent with a spectrum of protons cut off below 250 Mev. Also shown on Fig. 2 is the time of the sudden commencement caused by the Class 3 flare at 0700 U.T. on September 2, and the beginning of the Forbush decrease shown by the sea-level neutron monitor. Two rocket ascents were made at Fort Churchill by the NASA Solar Beam Research Group.[1] These flights were made in the decay phase of the radiation as seen by the balloon flights.

From the balloon counter data at Churchill and Minneapolis, and from the Churchill rockets, we have attempted to construct the spectra in space at various times during the event. In the left section of Fig. 3 is shown the growth of intensity, and in the right section the initial decay. These spectra agree reasonably well with the mean ion-

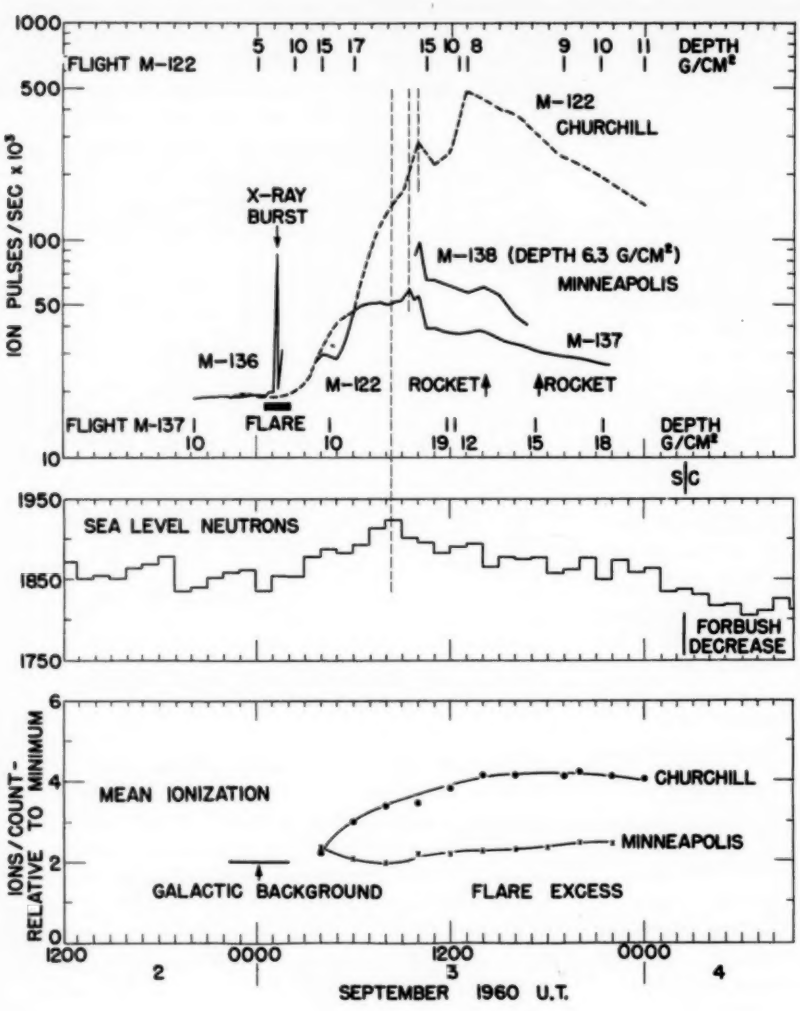

FIG. 2. Upper: total ionization rates at Fort Churchill and Minneapolis in the initial period when normal geomagnetic cutoffs were in effect. Center: flare increase seen on sea-level neutrons (courtesy Carmichael and Steljes). Lower: mean ionization showing growth of particles below 250 Mev with time at Fort Churchill.

ization measurements at Churchill in Fig. 2. Qualitatively, the spectrum steepens with time through both the rise and the fall of intensity. If we assume that the solar cosmic rays are injected into the solar system in a time of one hour or less during the flare, then the observed spectral changes can only be due to the energy dispersion between the sun and the earth. This dispersion increases the transit times twentyfold or more over the direct time of flight. We assume that this dispersion effect is associated with the unusual configuration of solar plasma and magnetic fields between the sun and the earth. The flare cosmic rays would be forced to travel through or around this region. It would indeed be difficult to relate in a detailed manner the spatial phenomena to the appearance of the spectra shown. However, the time dependence of the spectra is like that which would be obtained from a diffusion law with an energy-dependent mean free path. It seems quite possible that a kind of pseudodiffusion might take place in which the radius of curvature of the proton was a characteristic length in the diffusion process. Another kind of process which might produce an energy dispersion of this kind is the precession of particles in a nonuniform magnetic field, analogous to the precession of the Van Allen particles around the dipole field of the earth.

Although the polar ionospheric effects due to the very low-energy solar cosmic rays frequently show a delay,[6,7] balloon detectors have

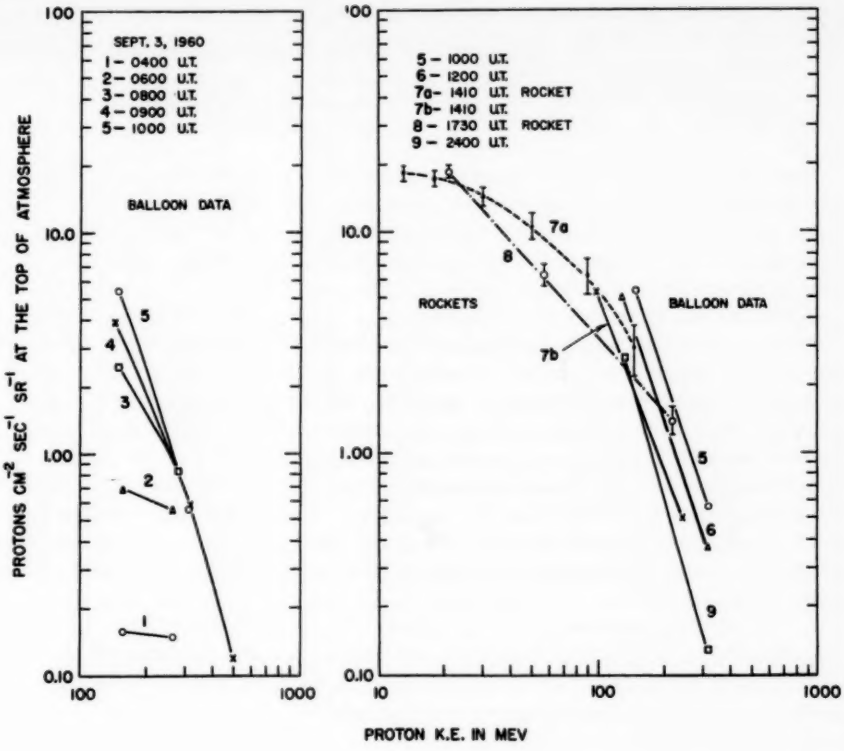

FIG. 3. Left: spectra during growth of event from simultaneous balloon measurements at Fort Churchill and Minneapolis. Right: spectra during initial decay of event from balloon and rocket data. (Rocket results from Fichtel, Davis, and Ogilvie, NASA Solar Beam Group.)

shown the prompt arrival of low-energy (100-Mev) particles. An event on August 22, 1958, reported earlier,[8] was observed by similar balloon equipment at Churchill and Minneapolis which measured the full intensity with a delay comparable to the direct transit time from the sun of 100-Mev protons. The August 22 event originated on the solar central meridian, at a time when no known recent solar events had disturbed the earth-sun region.

Many further balloon flights were made during this event at both Churchill and Minneapolis, and these will be described in more detail in a later communication. When the magnetic field became disturbed on September 4 and subsequently, it was again observed that the normal Störmer cutoffs at Minneapolis were altered and that very low-energy particles were admitted. In fact, at this time the flux values were the same at Churchill and Minneapolis, showing that the low-energy limit was determined by the atmospheric cutoff and not by the geomagnetic field. The event decayed slowly and was observed until September 6 by the Churchill balloon flights.

The field operation at Fort Churchill was at this time conducted by Ralph Fuchs and John Anderson of the University of Minnesota. We are greatly appreciative of the hospitality of the Canadian Defence Research Northern Laboratory during the summer of 1960.

*This research was sponsored by the National Science Foundation and the National Aeronautics and Space Administration.

[1]L. R. Davis, K. W. Ogilvie, H. M. Caulk, and J. M. Williams, Program of Joint Meeting of the Union Radio-Scientifique Internationale and the Institute for Radio Engineers, Boulder Laboratories, National Bureau of Standards, Boulder, Colorado, December, 1960 (unpublished), p. 42; and J. R. Winckler, ibid., p. 42.

[2]Data obtained courtesy of H. Carmichael through World Data Center A for Cosmic Rays.

[3]J. R. Winckler and P. D. Bhavsar, J. Geophys. Research 65, 2637 (1960); and E. P. Ney, J. R. Winckler, and P. S. Freier, Phys. Rev. Letters 3, 183 (1959).

[4]J. R. Winckler, T. C. May, and A. J. Masley, J. Geophys. Research 66, 316 (1961).

[5]F. B. McDonald and W. R. Webber, Phys. Rev. 115, 194 (1959).

[6]T. Obayashi and Y. Hakura, J. Geophys. Research 65, 3143 (1960).

[7]G. C. Reid and H. Leinbach, J. Geophys. Research 64, 1801 (1959).

[8]K. A. Anderson, R. Arnoldy, R. Hoffman, L. Peterson, and J. R. Winckler, J. Geophys. Research 64, 1133 (1959).

ROCKET OBSERVATIONS OF SOLAR PROTONS ON SEPTEMBER 3, 1960

L. R. Davis, C. E. Fichtel, D. E. Guss,* and K. W. Ogilvie*
National Aeronautics and Space Administration, Goddard Space Flight Center, Greenbelt, Maryland
(Received March 31, 1961)

It is now well established that high-energy nuclei arrive at the earth following some major solar flares. These solar particle beams have been observed using ground-level monitors, balloon-borne counters, and nuclear emulsions, and counters in satellites and space probes.

To obtain a more detailed picture of the character of solar particle beams in the range of energies between 2 Mev and 250 Mev, sounding rockets were used to carry charged-particle detectors well above the earth's atmosphere during several of these events. The rockets were launched from Fort Churchill, Manitoba, Canada, geomagnetic coordinates 60.7°N, 324.4°E where the magnetic field of the earth does not prevent the entry of low-energy particles. A typical flight trajectory for the Nike-Cajun sounding rocket is shown in Fig. 1. The rockets carried a Geiger counter, scintillation detector, nuclear emulsions, and a magnetometer to provide rocket aspect as a function of time.

Beginning on June 6, 1960, a 24-hour-a-day stand-by for a solar particle beam was begun at the Rocket Research Facility at Fort Churchill. Arrangements had been made with several solar observatories and riometer stations to send immediate notification of a major solar flare or polar cap absorption event. When the experiment was concluded at the end of November, ten firings had been made into four solar particle beams, and four other firings for comparison purposes had been made during quiet periods and periods of auroral absorption.

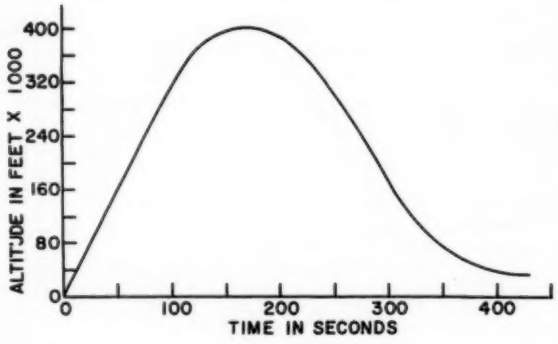

FIG. 1. SBE Nike-Cajun trajectory.

During the solar particle event, which began on September 3, 1960, at 2100 U.T., and is generally credited to a flare of magnitude 3 (solar coordinates 20°N, 87°E) occurring at 0040 U.T. on September 3, two rockets were shot. The exact firing times are given in Table I. Reduction and interpretation of the scintillation counter results for these two firings is not complete, but the Geiger counter results and emulsion results are reduced and will be presented here. The counter data were reduced by Davis and Ogilvie, and the emulsion data by Guss and Fichtel. The results are presented together because they refer to the same event and the same conclusions can be drawn from both.

The Geiger counter used was an Anton 302, placed so that its axis was parallel to the axis of the rocket, and mounted close to its wall on one side. The solid angle to the front, of almost 2 steradians, was shielded by the equivalent of 0.65 g/cm^2 of aluminum, and that to the rear by a variable but larger amount. Outside the atmosphere, the regular precessional motion of the rocket places a variable amount of absorber between the protons and the sensitive volume. Assuming an isotropic distribution in the upper hemisphere, two points on the integral energy spectrum of the particles may be obtained from

Table I. Rocket firing data.

Rocket designation	Firing time	Performance	Emulsions recovered
NASA 1019	1408 U.T.	Max altitude 130 km	yes
NASA 1020	1730 U.T.	Max altitude 130 km	no

the counting rates observed with the Geiger counter pointing first upwards and then down. The angular distribution of Geiger counter rate is consistent with the assumption of isotropy in the upper hemisphere. The only particles we have considered approaching the apparatus from below, are those which mirror so close under it that their range allows them to make the journey back up again. This correction increases the effective solid angle by about 10%. Another flux value may be found by summing up contributions to the solid angle, when the apparatus is at a depth of approximately 10 g on the way up. The appropriate energy is found by weighting the contribution of each sector by the reciprocal of the proton energy which can just penetrate to it.

The flux values in Table II show that in the energy region 22 to 67 Mev, the flux was the same at 1730 U.T. as at 1408 U.T., but a reduction had taken place in the 200-Mev region. This is in general agreement with the sea-level neutron monitor observations at Deep River, Ontario, which was showing an increased rate at the time of the first rocket firing.

The emulsion section of the payload consisted of a 1-in. by 4-in. diameter cylindrical stack of 600-micron thick Ilford G-5 nuclear emulsions, with the plane of the emulsions perpendicular to the rocket axis. The stack was shielded from the ambient radiation by 0.175 g/cm^2 of aluminum and 0.013 g/cm^2 of reflective aluminum foil and Mylar.

To obtain the proton energy spectrum, the emulsions were scanned so that all tracks from protons with kinetic energies between 13 Mev and 250 Mev within a given solid angle would be recorded. The proton energies were determined from range measurements in the energy interval between 13 Mev and 90 Mev and from grain density measurements in the energy interval between 90 Mev and 250 Mev. In the latter interval, it is not possible to determine the direction of motion of the particles, and a penetration correction must be made for those particles which cross the scan line by first traversing the emulsion.

The analysis of the Geiger counter data from this flight is consistent with the assumption that the solar beam particles were isotropic over slightly more than the upper hemisphere and zero over the remainder of the lower hemisphere, and this was assumed in obtaining the unidirectional fluxes from the emulsion data.

With the above assumption, the observed spectrum was corrected in the following way for ascent, descent, and the ionization loss in the atmosphere of mirrored particles to yield the integral spectrum under zero atmosphere. The observed differential spectrum was corrected for background and approximately corrected for penetration. An integral spectrum was then formed by normalizing to the flux at 250 Mev observed by Winckler et al.[1] at the same time at balloon altitudes. Because of the relatively small flux of protons with energies greater than 250 Mev, a change of the integral flux at that point would not appreciably alter the shape of the integral spectrum at lower energies, as may be seen from Fig. 2. The resulting spectrum was taken as a first approximation to the integral spectrum at the top of the atmosphere. Using this, the spectra at various absorber depths were computed, and the contributions, including penetration, at each absorber depth, were added to give a spectrum which was compared to the observed spectrum. From this comparison, a better estimate of the spectrum at zero atmosphere was made and the procedure repeated until agreement was reached.

The integral energy spectrum (a) and the differential energy spectrum (b) for protons at zero atmosphere found from the emuision data, are

Table II. Proton flux measurements during polar cap absorption on September 3, 1960.

Energy (Mev)	Integral flux (particles/cm^2 sec sr)	Time (U.T.)	Ft. Churchill riometer absorption at 30 Mc/sec
22	18.5 ±1	1408	1.4
67	7.3 ±0.5		
177	3.8 ±1.0		
22	19.7 ±1	1730	1.4
67	6.5 ±1		
220	1.3 ±0.6		

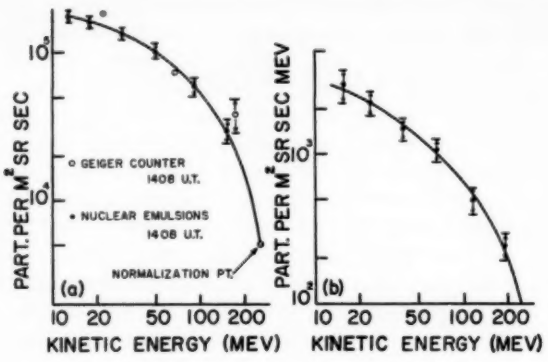

FIG. 2. Proton energy spectrum from solar particle beam of September 3, 1960. (a) Integral spectrum; (b) differential spectrum. NASA rocket 1019.

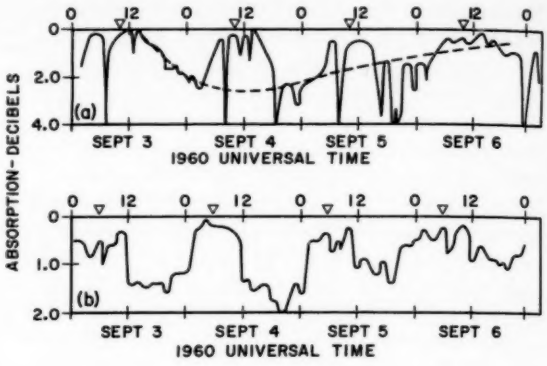

FIG. 3. Riometer absorption produced by the solar particle beam of September 3, 1960. (a) 27.6-Mc/sec riometer at College, Alaska; (b) 30-Mc/sec riometer at Fort Churchill, Canada.

shown in Fig. 2. The errors on the emulsion points include the uncertainty of the ascent correction as well as the statistical uncertainty associated with each point. The slope of the energy spectrum in the 13-Mev to 50-Mev region is very much smaller than that at higher energies. Although there are no previous experimental data in this low-energy region to indicate what slope is expected, this result is consistent with the discussion to be given below. We also show the points obtained at the same time by means of the Geiger counter. These were calculated completely independently of the emulsion flux values and spectral slope, and represent good agreement with them.

Figure 3 shows the absorption detected on the riometers at Fort Churchill[2] and at College, Alaska,[3] for the September 3 event. (Little and Leinbach[4] discuss riometers and the nighttime recovery effect due to recombination of ions in the atmosphere.) Although the event was only a moderate one in the low-energy region for which riometers are most sensitive, it was detected by the neutron monitor at Deep River, so a relatively large high-energy component was present, at least early in the event. From Fig. 3, one sees that the low-energy flux was characterized by a slow rise time to maximum intensity and a very long period where the riometer absorption was near maximum at about 2 db. Winckler et al.[1] have pointed out that these facts, combined with their own results and solar observations, strongly suggest a rigidity- or energy-dependent diffusion mechanism whereby low-energy particles reach the earth less efficiently in the early part of the event, so the flux of protons in the tens of kinetic energy range would be depressed more than those in the 100-Mev or greater range. The emulsion and Geiger counter spectra are consistent with this.

---

*National Aeronautics and Space Administration-National Academy of Sciences Postdoctoral Resident Research Associate.

[1]J. R. Winckler, P. D. Bhavsar, A. J. Masely, and T. C. May, preceding Letter [Phys. Rev. Letters 6, 488 (1961)].

[2]Courtesy of Defence Research Telecommunications Establishment, Shirley Bay, Ontario, Canada.

[3]Courtesy of H. Leinbach, University of Alaska, College, Alaska.

[4]C. G. Little and H. Leinbach, Proc. Inst. Radio Engrs. 46, 334 (1958).

HEAVY NUCLEI IN SOLAR COSMIC RAYS

C. E. Fichtel and D. E. Guss*
National Aeronautics and Space Administration, Goddard Space Flight Center, Greenbelt, Maryland
(Received March 31, 1961)

This Letter concerns the first successful attempt to detect heavy nuclei in a solar cosmic-ray event. The analysis to be reported here was made in a set of nuclear emulsions flown at 1408 U.T. on September 3, 1960, from Fort Churchill, Manitoba, Canada, in a Nike-Cajun research rocket payload during a solar particle event. A short description of the solar cosmic-ray event, the rocket, and the solar beam program is given in a preceding paper,[1] and will not be repeated here.

In order to determine whether or not heavy particles were present in the solar particle beam under consideration, a complete scan of the periphery of the four-inch diameter nuclear emulsion disks was made for delta-ray tracks, which had residual observable ranges in the emulsion of five-hundred microns or more and were within a specified solid angle. After the elimination of the tracks which could be identified as slow alpha particles, the remaining tracks fell into two groups; those which had a residual range of the order of several millimeters or less, and those which had ranges in the emulsion of many centimeters or more. In the latter group, seventeen tracks were found in the September 3 flight; this number corresponds to about $(80 \pm 21)\%$ of the expected cosmic-ray background of approximately 18 particles/(m^2 sr sec) seen at balloon altitudes at this time in the solar cycle. The 80% figure is reasonable because of the limited statistics and the low scanning efficiency for relativistic Li, Be, and B particles.

Since the amount of material above a normal balloon flight is equivalent in stopping power to one or two centimeters of emulsion, the heavy particles in the former group, those with ranges less than one centimeter, would not have reached balloon altitudes. Hence, it is necessary to determine whether this group of particles represents the normal cosmic-ray low-energy heavy spectrum or that of this solar cosmic-ray event. There was an identical firing on June 6, 1960, with the same Nike-Cajun payload system to obtain background data for the subsequent shots. In an equivalent scan of the nuclear emulsion plates flown on June 6, there were no heavy particles with residual ranges less than one centimeter. On the basis of finding no particles in this group, the calculated probability that the flux of heavy nuclei exceeded 3 particles/(cm^2 sr sec) in this range interval during the time of the June firing is less than approximately 0.05. Since no major decline in solar activity or increase in cosmic-ray intensity was detected during the period from June to September, 1960, the flux of galactic cosmic-ray heavy nuclei with potential ranges in nuclear emulsion of less than one centimeter during the September flight may be assumed to be essentially zero, or a few particles/(m^2 sr sec) at most.

The particles of interest, then, are those which had the short ranges, since, on the basis of the discussion of the preceding paragraph, these are the true solar particles. In order to determine the charge of the nuclei, the delta-ray method was used, since it gives a more reliable estimate of the charge than the thin-down or effective track width measurements. The variation of the delta-ray density with β was found to agree well with Mott's formula,

$$N_\delta = C\frac{Z^2}{\beta^2}\left\{\frac{m}{E_m} - \frac{1-\beta^2}{2\beta^2} - (1-\beta^2)\ln\left[\frac{m}{E_m}\left(\frac{2\beta^2}{1-\beta^2}\right)\right]\right\}, \quad (1)$$

with m/E_m equal to 13. This equation has previously been shown to be a good representation of the experimentally observed delta-ray distribution.[2,3] A graph showing the curves for N_δ as a function of range and the experimental points for the thirty-five low-energy heavy nuclei is shown in Fig. 1. The spread in points is approximately as expected for the limited statistics, due to the short ranges in most cases and the general limitations of charge resolution. For a discussion of further details of charge identification, charge calibration, and the expected distributions due to errors, see Aizu et al.[3] and Fichtel.[4]

Knowing the charge, range, and, thereby, the rigidity of each particle, a comparison can be made to the proton flux in a given rigidity range. The particles of medium charge, $6 \leq Z \leq 8$, have been chosen for this purpose because they are

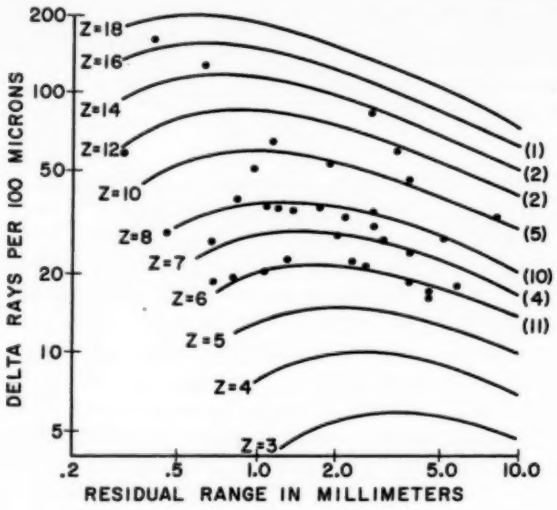

FIG. 1. Charge distribution of heavy solar cosmic rays detected in the nuclear emulsions flown on the Nike-Cajun rocket fired at 1408 U.T., September 3, 1960, at Fort Churchill, Canada. A brief discussion of the equation used for the curves giving N_δ as a function of Z and R is given in the text.

the most abundant and they are not widely separated in charge. After determining the rigidity of each particle from its range and the estimate of its charge, there were found to be 24 particles in the medium group with rigidities greater than 570 Mev/c corresponding to a flux of 20 ± 4 particles/(m^2 sr sec). The 570-Mev/c lower limit was set so that, under the given amount of material and within the given solid angle, all particles in the accepted group would have a residual observable path in the the emulsion of at least five-hundred microns. Due to the separation of tracks on a basis of range, there is an implied upper limit of approximately 1000 Mev/c. From the nuclear emulsion work presented in the previous Letter,[1] the flux of protons with rigidities greater than 570 Mev/c is $(2.5\pm0.7)\times10^4$ particles/(m^2 sr sec). The following ratio can then be obtained:

$$\frac{F(6\leq Z\leq 8,\ R>570\ \text{Mev}/c)}{F(Z=1,\ R>570\ \text{Mev}/c)}=(0.8\pm0.3)\times10^{-3}. \quad (2)$$

For the same energy per nucleon or the same energy per charge, the medium to proton ratio is appreciably smaller.

The ratio given by Eq. (2) can be compared to the cosmic-ray ratio of medium particles to protons of $(9.3\pm0.7)\times10^{-3}$ for the same rigidity cutoff.[5] In the sun, the medium to proton ratio has been estimated to be in the range of 1.0×10^{-3} to 2.1×10^{-3}, with one of the more recent determinations being 1.5×10^{-3}.[6] Within the uncertainties, then, the medium to proton ratio observed above a given rigidity cutoff in this sample of solar cosmic rays is slightly smaller than that observed in the sun, but an order of magnitude smaller than the galactic cosmic-ray ratio.

Although the statistics are poor, a little more detailed examination of the charge distribution to observe the more general features is justifiable. The fact that C and O nuclei occur in nearly equal numbers is consistent with their relative abundances in the sun. Due to the limitations on the charge determination, the number of nuclei classified as N should only be taken as an upper limit. Further, the observed absence of Li, Be, and B is reasonable on the basis of the abundances of these elements in the sun, where it is estimated that, as a group, they are less abundant than hydrogen by a factor of 10^{-9}, or more.[6] There is no spectral evidence to indicate what the abundance of Ne in the sun should be; however, on the basis of stellar models there is no reason to expect the abundance of Ne relative to C, N, and O to be very different from the cosmic abundance[7]; hence, the number of Ne nuclei observed, namely five, is reasonable. Nuclei with charges greater than ten were detected, and the number found is not too surprising on the basis of their relative abundance in the sun; however, one must remember that the acceleration process for the larger charges may differ appreciably from that of the medium group.

Sufficient statistics are not available in the September 3 event to permit a quantitative determination of the rigidity spectrum of the heavy particles; however, qualitatively it is not inconsistent with the proton rigidity spectrum in the same region. Some of the more probable acceleration mechanisms suggested for solar cosmic rays would lead to either the same rigidity dependence, the same energy per nucleon spectrum, or the same energy per charge relationship. However, there are also other considerations, such as favorable or unfavorable acceleration of heavies, partial ionization of the heavies during acceleration, and variations between events, such as those observed for the He to proton ratio.[8] Thus, although the bare medium to proton ratio found in this experiment may appear to give some support to theories suggesting that ordinary stars

cannot be the sole primary source of cosmic rays, the considerations mentioned above demand that the question of the origin of cosmic rays be left open at this time.

---

*National Aeronautics and Space Administration–National Academy of Sciences Postdoctoral Resident Research Associate.

[1]L. R. Davis, C. E. Fichtel, D. E. Guss, and K. W. Ogilvie, preceding Letter [Phys. Rev. Letters 6, 492 (1961)].

[2]E. Tamai, Phys. Rev. 117, 1345 (1960).

[3]H. Aizu, Y. Fujimoto, S. Hasegawa, M. Koshiba, I. Mito, J. Nishimura, K. Yokoi, and M. Schein, Phys. Rev. 116, 436 (1959).

[4]C. E. Fichtel, PhD. thesis, Washington University, 1959 (unpublished).

[5]C. J. Waddington, Progr. in Nuclear Phys. 8, 3 (1960).

[6]L. Goldberg, E. Müller, and L. Aller, Astrophys. J. Suppl. 45, Vol. V, 1 (1960).

[7]H. E. Suess and H. C. Urey, Revs. Modern Phys. 28, 53 (1956).

[8]S. Biswas, P. S. Freier, E. P. Ney, and W. Stein, Midwest Cosmic-Ray Conference papers, March, 1960 (unpublished).

LOW-ENERGY PION-PION S-WAVE PHASE SHIFTS*

Bipin R. Desai

Lawrence Radiation Laboratory, University of California, Berkeley, California

(Received February 8, 1961; revised manuscript received March 31, 1961)

Evidence for a P-wave $\pi\pi$ resonance has recently been found by Anderson et al. in an experiment on peripheral $\pi^- p$ collisions[1]; the resonance position and width are in rough accord with predictions based on nucleon electromagnetic structure.[2] It now becomes possible to make certain assertions about the S-wave $\pi\pi$ phase shifts on the basis of the crossing relations developed by Chew and Mandelstam.[3,4] Recently it has been suggested by Truong[5] that the anomalous peak in the double-pion production in $p+d$ collisions—$p+d\rightarrow He^3+\pi^+ +\pi^-$—observed by Abashian et al.[6] may perhaps be due to the large enhancement brought about by the interaction of the S-wave pions in the $I=0$ state, I being the isotopic spin. In this connection, therefore, it is of interest to see whether we can obtain from our solutions large $I=0$ S-wave amplitudes.

Crossing symmetry gives relations between the derivatives of the S- and P-wave amplitudes at the symmetry point, which are exact if we consider all higher partial waves to be small.[3,4] At this symmetry point, where $\nu=\nu_0=-2/3$ (ν being the square of the c.m. momentum of a pion), the two S amplitudes are given in terms of the pion-pion coupling constant, λ, and the first derivatives of the S amplitudes are given by the value of the P amplitude. In addition, there is a single relation connecting the second derivatives of the S waves to the first P-wave derivative. A two-parameter form for the P resonance has been given by Frazer and Fulco, the parameters being ν_R and Γ, which are related to the position and the width of the resonance.[2] To fit the experiment of reference 1, we need $\nu_R=3.5$ and $\Gamma=0.3$. Such a two-parameter form should be sufficient, we believe, to give a rough first approximation to the P amplitude and its first derivative at ν_0 if the contribution from the left cut is no larger than estimated by Chew and Mandelstam.[4,7] The above crossing relations then largely determine the S-wave amplitudes at low energies in terms of the three parameters λ, ν_R, and Γ.

The crossing relations at ν_0 are[4,8]

$$a_0=\tfrac{5}{2}a_2=-5\lambda, \tag{1}$$

$$a_0'=-2a_2'=6a_1, \tag{2}$$

and

$$a_0''-\tfrac{5}{2}a_2''=-12a_1', \tag{3}$$

where a_0 and a_2 are the S amplitudes at ν_0 for isotopic spin 0 and 2, respectively, and a_1 is the P amplitude. The primes indicate derivatives at ν_0. A correction for the D waves has already been made in the second-derivative relation, (3), given above.

If we indicate by $A_0^I(\nu)$ the S amplitude at an energy ν for a given isotopic spin I (=0 or 2), we can write it in the familiar form,[3]

$$A_0^I(\nu)=N_0^I(\nu)/D_0^I(\nu), \tag{4}$$

where $N_0^I(\nu)$ and $D_0^I(\nu)$ are the numerator and

the denominator functions, respectively. In the approximation in which the left-hand cut is replaced by a pole, Chew and Mandelstam obtained the formulas[4]:

$$N_0^I(\nu) = a_I + (\nu - \nu_0)\frac{\omega_{SI} + \nu_0}{\omega_{SI} + \nu} B_I, \quad (5)$$

and

$$D_0^I(\nu) = 1 - (\nu - \nu_0)[K(-\nu, -\nu_0)a_I + (\omega_{SI} + \nu_0)K(\omega_{SI}, -\nu)B_I], \quad (6)$$

where ω_{SI} gives the position of the pole, B_I is proportional to the residue, and K is a known function defined in reference 3.

The corresponding one-pole approximation for $A_1^1(\nu)/\nu$ – the P resonance ($I=1$) at an energy ν – was written in the two-parameter resonance form by Frazer and Fulco as[2]

$$\frac{A_1^1(\nu)}{\nu} = \frac{\Gamma}{\nu_R - \nu[1 - \Gamma\alpha(\nu)] - i\Gamma[\nu^3/(\nu+1)]^{1/2}}, \quad (7)$$

where $\alpha(\nu)$ is a known function. Given ν_R and Γ, we obviously can calculate the values of a_1 and a_1' needed in Eqs. (2) and (3) above. For example, we find $a_1 = 0.074$ and $a_1' = 0.014$ for $\nu_R = 3.5$ and $\Gamma = 0.3$.[1,9] We have five conditions embodied in the crossing relations (1), (2), and (3) and six parameters to determine in our S-wave effective-range formulas: a_0, a_2, ω_{S0}, ω_{S2}, B_0, and B_2. To achieve a sixth condition, we notice from the above relations that for an a_1 value such as the one given above, the potential for the $I=0$ state has a long-range repulsion and a short-range attraction. So long as the inner attraction is strong, we find that the interaction is not sensitive to the range of the outer repulsion. We shall, therefore, fix a priori the value of ω_{S0} which is proportional to the range of the repulsive potential. A reasonable estimate of $\omega_{S0} \simeq (2a_1/a_1') - \nu_0$ is given by the approximate crossing conditions of Chew and Mandelstam.[4] Using this estimate, we obtain $\omega_{S0} \simeq 11$ for the a_1 and a_1' values given above. For the $I=2$ state, the outer potential is attractive, and we may expect the interaction to be sensitive to the range. We shall, therefore, use relation (3) to determine ω_{S2}. It turns out that for the above values of a_1, a_1', and ω_{S0}, no solutions exist for ω_{S2} when we have $\lambda \geq +0.03$.

The curves for $a_I[\nu/(\nu+1)]^{1/2}\cot\delta_0^I$, where δ_0^I is the S-wave phase shift for a given isotopic spin I, are given in Figs. 1 and 2 for various values of λ

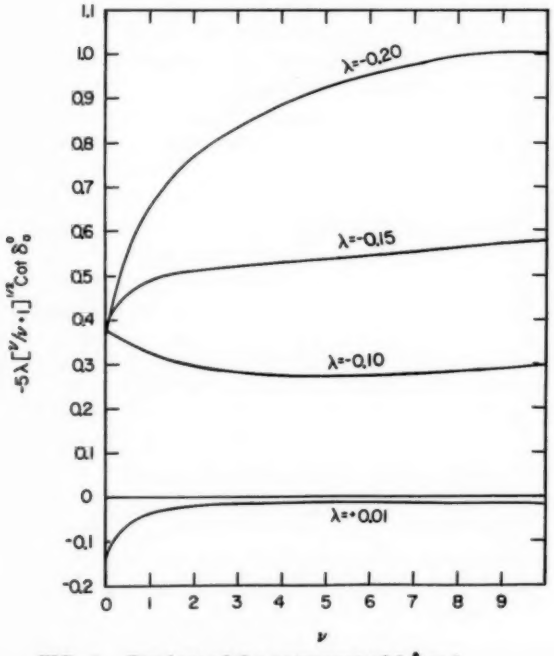

FIG. 1. Product of the cotangent of δ_0^0 and $-5\lambda[\nu/(\nu+1)]^{1/2}$ for the λ values -0.20, -0.15, -0.10, and $+0.01$ with $\omega_{S0} = 11$.

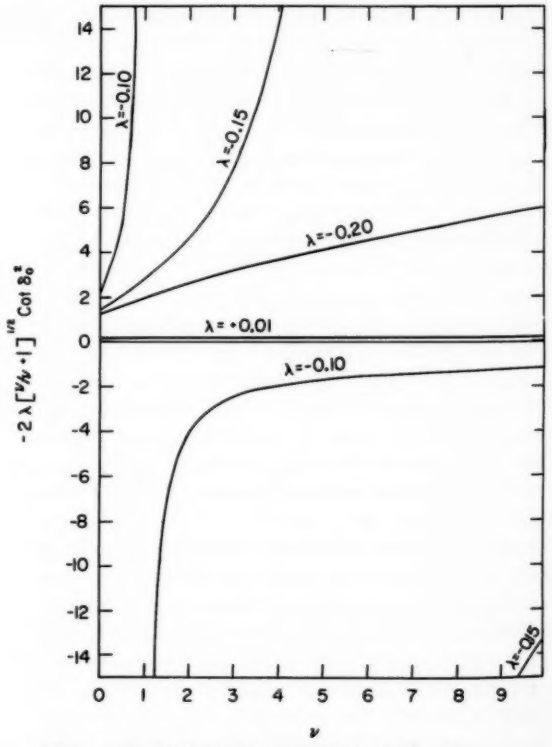

FIG. 2. Product of the cotangent of δ_0^2 and $-2\lambda[\nu/(\nu+1)]^{1/2}$ for the (λ, ω_{S2}) values $(-0.20, 2.2)$, $(-0.15, 2.3)$, $(-0.10, 2.7)$, and $(+0.01, 6.5)$.

with $a_1 = 0.074$, $a_1' = 0.014$, and $\omega_{S0} = 11$. We find that the interaction in the $I = 0$ state is attractive and much stronger than in the $I = 2$ state, for both positive and negative values of λ.[10] In general, we observe that the results we obtain here are quite different from the ones in the S-dominant case.[11]

Knowing the results of double-pion production in $p + d$ collisions, $p + d \to \mathrm{He}^3 = \pi^+ + \pi^-$, we can obtain additional information about the $I = 0$, S amplitude.[5,6] The enhancement factors $|D_0^0(0)/D_0^0(\nu)|^2$ – normalized to unity at $\nu = 0$ – for the $I = 0$ state for different values of λ are given in Table I, together with the corresponding scattering lengths a_{S0}.[13] It is found that for λ in the interval $(-0.15, -0.20)$ corresponding to the scattering length in the interval $(2, 3)$, the enhancement factor, together with the usual phase space, gives a good fit to the experimental data after the $I = 1$ component of the 2π system is subtracted out.[14] We may further add that in this region of λ values, our assumption of considering the interaction to be insensitive to ω_{S0} is particularly good, since we now have a rather strong inner attraction.

On the basis of the τ-decay spectrum,[15] some authors have observed that the $I = 2$ state should be more attractive than the $I = 0$ state,[16,5] a result which is impossible to obtain within the present framework. The discrepancy may perhaps lie in the assumptions usually made in the τ-decay analysis: (a) considering the three-body problem in terms of simple two-body forces, and (b) considering only the symmetric $I = 1$ final state.

Table I. Values of $|D_0^0(0)/D_0^0(\nu)|^2$ for $I = 0$ and for different λ, a_{S0} values.

ν	$\lambda = -0.20$ $a_{S0} = 2.81$	$\lambda = -0.15$ $a_{S0} = 1.96$	$\lambda = -0.10$ $a_{S0} = 1.32$	$\lambda = +0.01$ $a_{S0} = 0.35$
0	1	1	1	1
0.1	0.491	0.659	0.822	1.088
0.2	0.337	0.503	0.704	1.166
0.3	0.262	0.413	0.619	1.229
0.4	0.217	0.354	0.554	1.273
0.5	0.188	0.311	0.502	1.298
0.6	0.167	0.280	0.461	1.302
0.7	0.149	0.255	0.425	1.288
0.8	0.138	0.235	0.396	1.257
0.9	0.128	0.219	0.370	1.214
1.0	0.120	0.205	0.348	1.164

The author wishes to thank Professor Geoffrey F. Chew for suggesting this investigation and for his advice.

*Work done under auspices of the U. S. Atomic Energy Commission.

[1]J. A. Anderson, V. X. Bang, P. G. Burke, D. D. Carmony, and N. Schmitz, Phys. Rev. Letters 6, 365 (1961) (references to earlier experimental work are given here); and P. G. Burke, talk presented at the 1960 Conference on Strong Interactions, University of California, Berkeley, December, 1960 [Revs. Modern Phys. (to be published)]. The resonance energy is observed to be ~4.5. (We use $\hbar = c = \mu = 1$, where μ is the pion mass.)

[2]Existence of a P-wave $\pi\pi$ resonance on the basis of nucleon electromagnetic structure was first conjectured by W. R. Frazer and J. R. Fulco, Phys. Rev. Letters 2, 364 (1959); and Phys. Rev. 117, 1603 (1960). In their analysis, these authors attempted to represent the entire anomalous isotopic-vector magnetic moment in terms of the $\pi\pi$ P-wave resonance, and on this basis predicted a resonance energy at about 3.5. However, the actually observed nucleon form factor has a small (~20%) high-momentum component of a sign opposite to the 2π contribution as pointed out by J. Bowcock, W. N. Cottingham, and D. Lurié, Nuovo cimento 16, 918 (1960), and Phys. Rev. Letters 5, 386 (1960). [See also S. C. Frautschi, Phys. Rev. Letters 5, 159 (1960).] When this effect is included, the resonance energy is correctly predicted to be ~4.5.

[3]G. F. Chew and S. Mandelstam, Phys. Rev. 119, 467 (1960).

[4]G. F. Chew and S. Mandelstam, Lawrence Radiation Laboratory Report UCRL-9126, March, 1960 [Nuovo cimento (to be published)]. See also G. F. Chew, Proceedings of the 1960 Annual International Conference on High-Energy Physics at Rochester (Interscience Publishers, New York, 1960). It is assumed that the reader is familiar with the principles discussed here and in reference 3.

[5]T. N. Truong, Phys. Rev. Letters 6, 308 (1961).

[6]A. Abashian, N. E. Booth, and K. M. Crowe, Phys. Rev. Letters 5, 258 (1960); and A. Abashian, talk presented at the 1960 Conference on Strong Interactions, University of California, Berkeley, December, 1960 [Revs. Modern Phys. (to be published)].

[7]Recently, a four-parameter resonance form has been given by J. S. Ball and D. Y. Wong, Phys. Rev. Letters 6, 29 (1961). This resonance form cannot be represented, even roughly, by the Frazer-Fulco two-parameter function. We do not consider here the Ball-Wong form, because it corresponds to a nearby discontinuity on the left cut that is an order of magnitude larger than that estimated by Chew and Mandelstam.[4] Nevertheless, as future developments improve our understanding of the P wave, the calculations described here may correspondingly be improved. This

approach is in no way committed to the Frazer-Fulco form.

[8]A set of relations for the S and P amplitudes at zero energy have been recently given by J. G. Taylor, Phys. Rev. Letters 6, 237 (1961). These relations are incorrect inasmuch as the contribution of the higher partial waves in the crossed channel is neglected. For example, the relation $a_0^2/a_2^2=5/2$ is not consistent with perturbation theory, since we expect that in the limit of weak coupling the above ratio should be $\sim(5/2)^2$, the ratio at the symmetry point, and not 5/2.

[9]Notice that the position of the resonance is not ν_R as defined by the relation (7) but it is the value of ν for which the real part of the denominator in Eq. (7) vanishes and is higher than ν_R.

[10]A bound state appears for the $I=0$ state for $\lambda \simeq -0.50$.

[11]G. F. Chew, S. Mandelstam, and H. P. Noyes, Phys. Rev. 119, 478 (1960).

[12]Such behavior was already indicated by G. F. Chew, Proceedings of the 1960 Annual International Conference on High-Energy Physics at Rochester (Interscience Publishers, New York, 1960).

[13]A good approximation to the enhancement factor for small ν values is

$$\left\{\left[1+a_{SI}\frac{2}{\pi}\left(\frac{\nu}{\nu+1}\right)^{1/2}\ln[\nu^{1/2}+(\nu+1)^{1/2}]\right]^2+a_{SI}^2\frac{\nu}{\nu+1}\right\}^{-1},$$

where a_{SI} is the scattering length for the S wave with isotopic spin I.

[14]A. Abashian and N. E. Booth, Lawrence Radiation Laboratory, University of California, Berkeley (private communication). I am told by these authors that the experiment is being analyzed further.

[15]R. Dalitz, Phys. Rev. 94, 1046 (1954); E. Fabri, Nuovo cimento 11, 479 (1954); S. McKenna, S. Natali, M. O'Connell, J. Tietge, and N. C. Varshneya, Nuovo cimento 10, 763 (1958).

[16]B. S. Thomas and W. G. Holladay, Phys. Rev. 115, 1329 (1959); N. N. Khuri and S. B. Treiman, Phys. Rev. 119, 1115 (1960); R. F. Sawyer and K. C. Wali, Phys. Rev. 119, 1429 (1960). See also A. N. Mitra and E. Lomon, Proceedings of the 1960 Annual International Conference on High-Energy Physics at Rochester (Interscience Publishers, New York, 1960).

LOW-ENERGY $\bar{K}$-NUCLEON INTERACTION*

R. C. King,† R. E. Lanou, Jr., and S. F. Tuan
Department of Physics, Brown University, Providence, Rhode Island
(Received April 3, 1961)

The recent discovery[1] of Y^* has emphasized the need for more complete information on the $\bar{K}$-nucleon interaction; in particular the need to differentiate between the $(a+)$ (constructive Coulomb-nuclear interference) solution and the $(a-)$ (destructive Coulomb-nuclear interference) solution which gives rise to the K^--p quasi-bound-state resonance.[2] In principle it is possible from low-energy K^--p scattering data to make this important distinction.[3-5] The interference effect should manifest itself experimentally through both the total elastic scattering cross section[4,6] and more directly in the differential elastic scattering cross section at small angles.[4,7] It is the purpose of this note to point out that, when the errors inherent in the S-wave zero-range approximation scattering lengths are included in theoretical calculations, certain ambiguities arise on comparison with experimental data which make it important to exercise great care in deciding which type of interference is correct.

Use has been made of the K-matrix formalism of Dalitz and Tuan[8] to include in the zero-range analysis of K^--p interactions at low energy the effects of $\bar{K}^0$-K^- mass difference and the long-range Coulomb interaction. The differential cross section for elastic scattering of K^- mesons incident on protons is

$$\frac{d\sigma_{el}}{d\Omega}=\left|\frac{\csc^2(\theta/2)}{2Bk^2}\exp\left[\frac{2i}{kB}\ln\sin(\theta/2)\right]+\frac{C^2[x-ik_0(x^2-y^2)]}{D}\right|^2, \quad (1)$$

where x and y are related to the complex scattering lengths $A_T=a_T+ib_T$ in the $T=1$ and $T=0$ channels by $x=\frac{1}{2}(A_0+A_1)$, $y=\frac{1}{2}(A_1-A_0)$; k and k_0 are the wave numbers in the K^--p and $\bar{K}^0$-n channels, B is the Bohr radius for the K^--p system ($B=83.4$ fermis), $C^2=(2\pi/kB)\times[1-\exp(-2\pi/kB)]^{-1}$ is the S-wave Coulomb penetration factor, and D is given by

$$D=(1-ixk_0)[1-ixC^2k(1-i\lambda)]+C^2kk_0(1-i\lambda)y^2,$$

in which $\lambda=(-2/kBC^2)[\ln(2kR)+\mathrm{Re}\psi(i/kB)+2\gamma]$, where $\gamma=0.5772$ (Euler's constant) and ψ is the logarithmic derivative of the gamma function. R is taken to be the K-meson Compton wave-

length ($R = 0.4$ fermi).

The complex scattering lengths used in our calculations are those due to Dalitz,[9] in which an estimate of their uncertainties has been made. The scattering lengths corresponding to the so-called $(a+)$ and $(a-)$ solutions are given by

$$(a+)\begin{cases} A_0 = 0.05(\pm 0.2) + i\,1.10(^{+0.2}_{-0.3}), \\ A_1 = 1.45(\pm 0.2) + i\,0.35(^{+0.09}_{-0.07}); \end{cases}$$

$$(a-)\begin{cases} A_0 = -0.75(^{+0.35}_{-0.45}) + i\,2.00(\pm 0.35), \\ A_1 = -0.85(\pm 0.15) + i\,0.21(\pm 0.04). \end{cases} \quad (2)$$

The dominant term of the elastic differential scattering cross section [Eq. (1)], except for small-angle scattering, is the nuclear term, which, it may be shown, is most sensitive to changes in $|x|$ as opposed to changes in x, y, or $|y|$. Thus, maximizing (minimizing) $|A_0 + A_1|$ will maximize (minimize) the differential cross section. Making use of this, the resulting maximum and minimum cross sections have been calculated and are denoted by $+\delta(a\pm)$ and $-\delta(a\pm)$, respectively, for the $(a\pm)$ solutions. In addition, results corresponding to the "mean value" for $(a+)$ and $(a-)$ solutions have been calculated. The effect of these uncertainties is illustrated in Fig. 1 which gives the center-of-mass angular distribution at a K^--meson laboratory momentum of 172 Mev/c. A comparison is then made with hydrogen bubble-chamber experimental data,[7] indicating that within the limits of present experimental uncertainties it is impossible to differentiate conclusively between constructive $(a+)$ and destructive $(a-)$ Coulomb-nuclear interference solutions.

The experimental data for total scattering cross sections represent integrals over angles excluding a certain range of small-angle scattering. Therefore, to make a direct comparison between theory and experiment, the theoretical cross sections must be calculated by integrating between limits which are determined by the par-

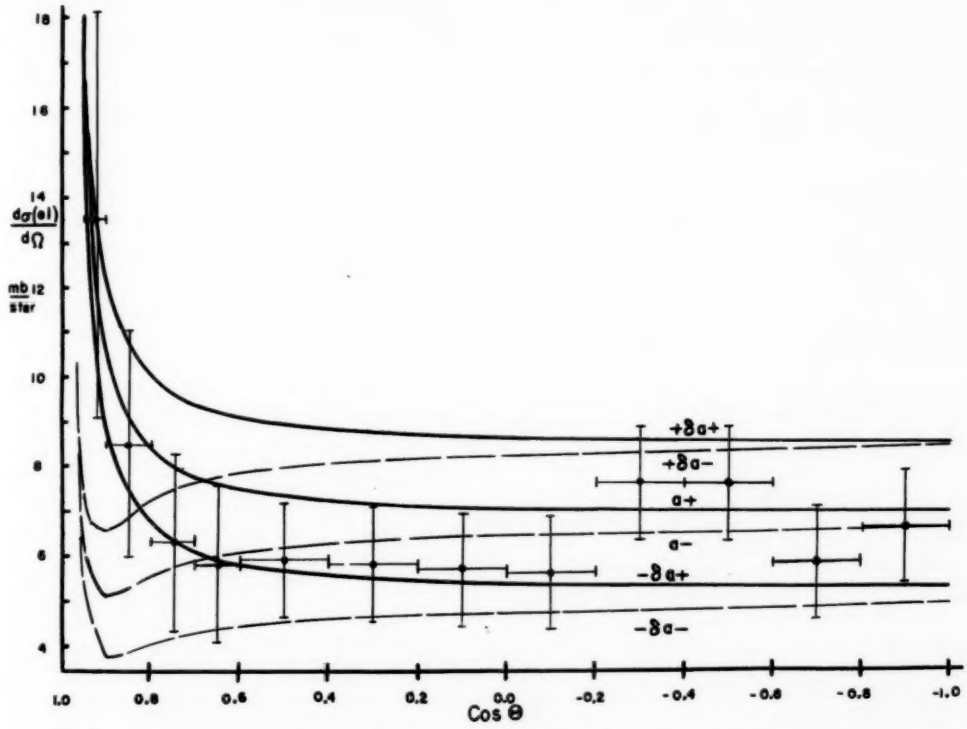

FIG. 1. Center-of-mass angular distribution for K^--p elastic scattering at laboratory momentum 172 Mev/c. The solid curves correspond to the $(a+)$ constructive interference solutions, and the dashed curves correspond to the $(a-)$ destructive interference solutions. Curves labelled $+\delta(a\pm)$ and $-\delta(a\pm)$ represent, respectively, the maximum and minimum cross sections for the $(a\pm)$ solutions. The experimental points are hydrogen bubble-chamber data of reference 7.

ticular experiment under consideration. The different nature of the experimental techniques used in emulsion and bubble-chamber experiments require different limits of integration. The emulsion events[6,10] are selected by the requirement of a proton recoil of a certain minimum length; this results in a certain minimum incident K^- momentum below which no events are observed. The bubble-chamber events,[7] on the other hand, are not subject to the same criterion but are selected by visibility of scatter; this results in a certain minimum angle of detection at all momenta of incident K^- mesons. These differences in technique result in slightly different theoretical total elastic cross-section curves for the two cases. (The behavior at low K^- momentum shows this difference most strikingly, but it is of no importance in deciding between the solutions.)

Denoting the limiting angle of scattering by θ_m, the total elastic scattering cross section is given by

$$\sigma_{el} = \int_{\theta_m}^{\pi} 2\pi \frac{d\sigma_{el}}{d\Omega} \sin\theta d\theta,$$

and hence

$$\sigma_{el} = 2\pi|\gamma|^2(1+\cos\theta_m) + \frac{4\pi}{\alpha^2}\cot^2(\theta_m/2) + \mathrm{Re}\frac{16\pi\gamma}{\alpha\beta^*}\{1-\exp[\beta^* \ln\sin(\theta_m/2)]\}, \quad (3)$$

where the asterisk denotes complex conjugate, $\alpha = 2Bk^2$, $\beta = 2i/kB$, and $\gamma = (C^2/D)[x - ik_0(x^2 - y^2)]$.

For the emulsion data the criterion for cutoff is that the laboratory momentum of the recoil proton be at least 30 Mev/c (corresponding to a range of 5 μ in emulsions).[4,6,10] For the bubble-chamber data, a cutoff corresponding to a center-of-mass scattering angle given by $\cos\theta_m = 0.7$ was used consistently for all energies of incident K^- meson.[7]

It is to be noted that the dominant term in the above expression (3) is the first, so that the limiting values for the total elastic scattering cross sections consistent with the Dalitz parameters are once again given by the $+\delta(a\pm)$ and $-\delta(a\pm)$ solutions. For these solutions and the mean value $(a\pm)$ solutions the calculated total elastic scattering cross section is compared with bubble-chamber data[7] [Fig. 2(a)] and emulsion data[6,10] [Fig. 2(b)].

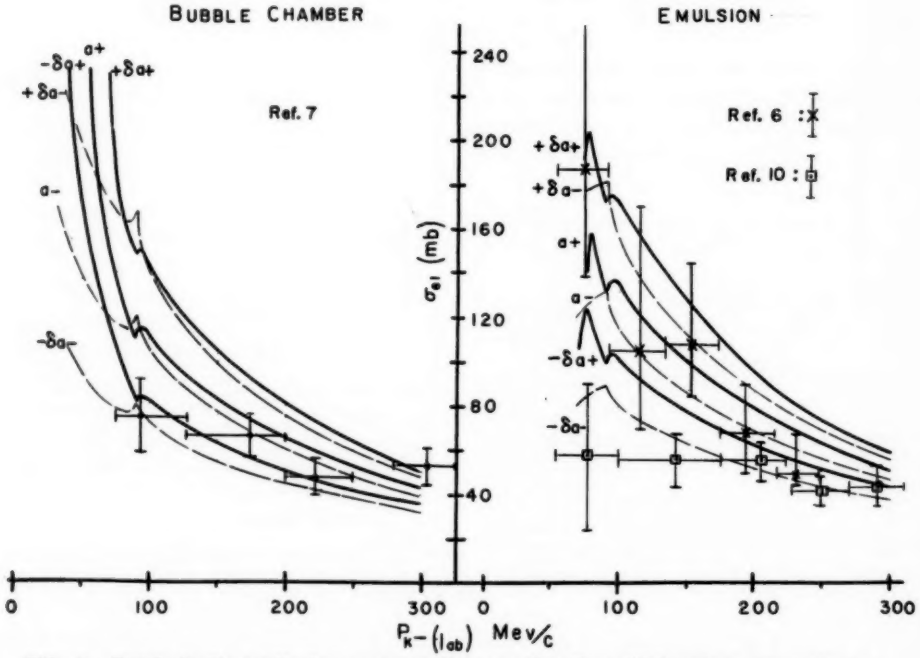

FIG. 2. Total elastic scattering cross section as a function of laboratory momentum. Curve notation as in Fig. 1. (a) Cutoff $\cos\theta_m = 0.7$; the experimental points are hydrogen bubble-chamber data. See reference 7. (b) Cutoff angle θ_m corresponding to a proton recoil momentum of 30 Mev/c. The experimental points are emulsion data of references 6 and 10.

On the basis of earlier values of the Dalitz parameters, Jackson and Wyld[4] calculated the expected variation of total elastic scattering cross section with momentum and concluded after comparison with emulsion data[10] that the Coulomb-nuclear interference is destructive. Using the same theoretical curves, Davis et al.[6] concluded that both emulsion data and bubble-chamber data suggested constructive interference. It is clear, however, from our calculations, using the latest values of the Dalitz parameters together with their errors, that no conclusive differentiation may be made between constructive ($a+$) and destructive ($a-$) interference on the basis of currently known experimental data.

Since the Dalitz parameters[9] are obtained by making use, among other things, of the experimental information on the total elastic scattering cross section at 172 Mev/c and the zero-range approximation neglecting Coulomb effects in the K^--p channel, the absolute magnitude of any cross sections predicted by formulas (1) and (3) will be approximately normalized to the experimental data at 172 Mev/c. Consequently, it is only the shape of both the angular distribution curves and the total cross section versus momentum curves which may be used to differentiate between the constructive and destructive solutions. Our results indicate that except in a narrow region on either side of the charge-exchange threshold, at which momentum cusp behavior is observed, the shape of the total cross sections are essentially the same for both types of solution. Thus, we make once again the oft-stated observation[3,4] that it is the differential cross section which would provide a more direct method of differentiating between ($a+$) and ($a-$) solutions. The shapes of angular distributions for both the ($a+$) and the ($a-$) curves are virtually independent of the exact values of these parameters and are sufficiently different to suggest that a conclusion might be arrived at, given a greater amount of experimental data in the essential range of $\cos\theta$ from 0.75 to 0.95.

In conclusion, we wish to emphasize (1) the need of obtaining accurate measurements of the cross sections for Λ^0 and Σ^0 reactions at the energy range of interest [p_k(lab) ~ 200 Mev/c]. A clean separation of Λ from Σ^0 events will then supplant the necessity of introducing the extrapolated assumption of constancy for the ratio[3,9,11] $\epsilon = [\Lambda/(\Sigma+\Lambda)]_{T=1} \sim 0.5$ in the low-energy region, currently employed in obtaining the theoretical solutions. (2) Our analysis has concentrated on the evaluation of relevant scattering and angular distribution information to differentiate between ($a+$) and ($a-$), which is of special interest (in terms of its relationship to the $T=1$ excited hyperon Y^*) because of the $T=1$ resonance present in the ($a-$)-type solution[3] below K^--p threshold. This should in no way obviate the over-all necessity of distinguishing between (a)-type solutions and (b)-type solutions. An experiment on K_2^0-p scattering would give information concerning this possibility.[12]

We would like to thank Professor R. H. Dalitz, Professor A. H. Rosenfeld, Professor R. Tripp, and Dr. R. Ross for very helpful and informative discussions and communications about the current status of low-energy K^--p interactions.

---

*This work was supported by the U. S. Atomic Energy Commission.

†University Fellow.

[1]M. H. Alston, L. W. Alvarez, P. Eberhard, M. L. Good, W. Graziano, H. K. Ticho, and S. G. Wojcicki, Phys. Rev. Letters 5, 520 (1960); M. Ferro-Luzzi, Revs. Modern Phys. (to be published); O. Dahl, N. Horwitz, D. H. Miller, J. J. Murray, and P. G. White, Phys. Rev. Letters 6, 142 (1961); H. J. Martin, L. B. Leipuner, W. Chinowsky, F. T. Shively, and R. K. Adair, Phys. Rev. Letters 6, 283 (1961).

[2]R. H. Dalitz, Phys. Rev. Letters 6, 239 (1961); J. Franklin and S. F. Tuan, Nuovo cimento (to be published).

[3]R. H. Dalitz and S. F. Tuan, Ann. Phys. 8, 100 (1959). See also S. F. Tuan, Nuovo cimento 18, 1301 (1960); M. Ross and G. Shaw, Phys. Rev. Letters 5, 579 (1960).

[4]J. D. Jackson and H. W. Wyld, Phys. Rev. Letters 2, 355 (1959).

[5]R. Karplus, L. Kerth, and T. Kycia, Phys. Rev. Letters 2, 510 (1959).

[6]D. H. Davis, R. D. Hill, B. D. Jones, B. Sanjeevaiah, J. Zabrzewski, and J. P. Lagnaux, Phys. Rev. Letters 6, 132 (1961).

[7]L. W. Alvarez, University of California Lawrence Radiation Laboratory Report UCRL-9354, 1960 (unpublished). For the total elastic cross sections, UCRL-9354 presents the experimental points in the form $(20/17)\int_{\cos^{-1}0.7}^{\pi} 2\pi(d\sigma/d\Omega)\sin\theta d\theta$; we have removed the factor of 20/17 for standardization of emulsion and bubble-chamber results.

[8]R. H. Dalitz and S. F. Tuan, Phys. Rev. Letters 2, 425 (1959); Ann. Phys. 10, 307 (1960). See also reference 4, where Jackson and Wyld had obtained equivalent results employing the R-matrix formalism of Wigner and Eisenbud; we have adopted here the notations of Dalitz and Tuan as quoted in the references given above.

[9]R. H. Dalitz, Revs. Modern Phys. (to be published). Also private communication.

[10]W. Alles, N. N. Biswas, M. Ceccarelli, and J.

Crussard, Nuovo cimento 6, 571 (1957).

[11]Preliminary results on the $\Lambda^0/(\Sigma^0+\Lambda^0)$ ratio at 200 Mev/c suggest a fit with either of (a+) or (a-) solutions, with no indication of rapid variation for $(\Sigma/\Lambda)_{T=1}$ above K^--p threshold. (Private communication from Professor R. H. Dalitz on recent Berkeley experiments.)

[12]One such experiment is in progress in the Brookhaven National Laboratory Bubble-Chamber Group (W. J. Willis, private communication).

$\Delta I = 1/2$ RULE IN Σ DECAY: A PROBLEM OF SIGN*

S. P. Rosen
Midwestern Universities Research Association, Madison, Wisconsin
(Received April 10, 1961)

Several authors[1,2] have pointed out that a certain admixture of $\Delta I = 1/2$ and $3/2$ has the same physical consequences in Λ decay as the $\Delta I = 1/2$ rule, and only differs from it in the sign of the $(p\pi^-)$ amplitudes relative to the $(n\pi^0)$ amplitudes. Since this sign does have physical consequences in another process, namely the nonmesonic decay of Λ hypernuclei,[2,3] the experimental data on Λ decay[4] are not conclusive evidence in favor of the $\Delta I = 1/2$ rule. The purpose of this note is to indicate a similar situation in Σ decay.

Each mode of Σ decay,

$$\Sigma^+ \to p + \pi^0, \quad \Sigma^+ \to n + \pi^+, \quad \Sigma^- \to n + \pi^-, \tag{1}$$

is described by a pair of S- and P-wave amplitudes,[5]

$$N_k \equiv \begin{Bmatrix} S_k \\ P_k \end{Bmatrix}, \quad (k \equiv 0, +, -) \tag{2}$$

and the effective interaction Hamiltonian is written as

$$\mathcal{H} = a\mathcal{H}_{1/2} + b\mathcal{H}_{3/2} + c\mathcal{H}_{5/2}, \tag{3}$$

where $\mathcal{H}_{n/2}$ behaves as a quantity with isotopic spin $n/2$ ($n = 1, 3, 5$). Since $\mathcal{H}$ is assumed to be invariant under CP, the constants a, b, and c are real, and the phases of S_k and P_k can be expressed in terms of the appropriate pion-nucleon phase shifts. From matrix elements of $\mathcal{H}$ between states of isotopic spin 1 and 3/2, we obtain the relation

$$\sqrt{2}N_0 + N_+ = dN_-, \tag{4}$$

where

$$d = \left\{ \frac{a - b(8/5)^{1/2} + c(3/5)^{1/2}}{a + b(2/5)^{1/2} + c(1/15)^{1/2}} \right\}. \tag{5}$$

The physical properties of Σ decay[6] are not affected by the transformation

$$N_- \to -N_-, \tag{6}$$

and, consequently, cannot be used to determine the sign of d in Eq. (4). Now, it is obvious from (5) that if d is negative, at least one of b and c must be comparable in magnitude with a. Therefore, the validity of the $\Delta I = 1/2$ rule depends upon a sign that has no physical significance in Σ decay itself.

To emphasize this point, let us suppose that the N_k are real, and represented by vectors in an S-P diagram.[5] Recent experiments indicate that the rates for the three decay modes are approximately equal,[7] i.e.,

$$|N_0| \approx |N_+| \approx |N_-|, \tag{7}$$

and also that $\sqrt{2}N_0$, N_+, N_- form a right-angled triangle[8]; therefore, from (4), either

$$d = +1, \tag{8a}$$

or

$$d = -1. \tag{8b}$$

If c is zero, then b is zero when $d = +1$ and $a\sqrt{(10)}$ when $d = -1$. Due to the uncertainty in the sign of N_-, no choice between (8a) and (8b), and consequently no definite conclusion about the $\Delta I = 1/2$ rule, can be made.

This problem of sign can be approached in the following way.[9] When $\mathcal{H}$ is written in the form

$$\mathcal{H} = N_0\bar{\Sigma}^+ p\pi^0 + N_+\bar{\Sigma}^+ n\pi^+ + N_-\bar{\Sigma}^- n\pi^- + \text{H.c.}, \tag{9}$$

it is easy to see that a change in the signs of N_- and the Σ^- field,

$$N_- \to -N_-, \quad \Sigma^- \to -\Sigma^-, \tag{10}$$

leaves $\mathcal{H}$ invariant. Therefore, insofar as the transformation (10) is permissible, the signs of

N_0 and N_+ relative to N_- are not observable. Since the charge independence of the strong interaction Hamiltonian, $\mathcal{H}_S$, requires that the signs of Σ^+, Σ^-, and all other particle fields be fixed,[10] transformations of the type (10) cannot be applied to $\mathcal{H}_S$. We may, therefore, conclude that the relative signs of N_0, N_+, N_-, are observable, but only in processes where $\mathcal{H}_S$ plays an essential role.

An example of this type of process is the nonmesonic decay of hypernuclei. The matrix elements for

$$\Lambda + n \rightarrow n + n \tag{11}$$

and

$$\Lambda + p \rightarrow n + p \tag{12}$$

include contributions from the schemes,[9]

$$\Lambda + \begin{Bmatrix} n \\ p \end{Bmatrix} \rightarrow \Sigma^{\pm} + \pi^{\mp} + \begin{Bmatrix} n \\ p \end{Bmatrix}$$

$$\rightarrow n' + \pi^{\pm} + \pi^{\mp} + \begin{Bmatrix} n \\ p \end{Bmatrix} \rightarrow n' + \begin{Bmatrix} n'' \\ p'' \end{Bmatrix},$$

$$\Lambda + p \rightarrow \Sigma^+ + \pi^- + p \rightarrow p' + \pi^0 + \pi^- + p \rightarrow p' + n'', \tag{13}$$

and, therefore, the rates for (11) and (12) are, in principle, affected by the relative signs of N_0, N_+, N_-, as well as by those of the Λ-decay amplitudes.[2,3] In practice, due to the role of the strong interactions in schemes like (13), it may not be feasible to determine these signs from the known rates of hypernuclear decay, and a more clear-cut method will have to be devised.

We now see that the $\Delta I = 1/2$ rule presents a problem of sign in Σ decay similar to that in Λ decay. There is, however, one important difference; namely that, whereas in Λ decay this sign determines the admixture of different ΔI uniquely,[1] in Σ decay it does not [see Eq. (4)]. It is, perhaps, ironic that the process which could throw further light on this question, i.e., the pionic decay of Σ^0, is not accessible to experiment.

It is a great pleasure to thank D. B. Lichtenberg for his helpful correspondence on the observability of signs.

---

*Supported by the U. S. Atomic Energy Commission.

[1]S. Okubo, R. E. Marshak, and E. C. G. Sudarshan, Phys. Rev. 113, 944 (1958).

[2]R. H. Dalitz, Revs. Modern Phys. 31, 823 (1959).

[3]M. Ruderman and R. Karplus, Phys. Rev. 102, 247 (1956); F. Cerulus, Nuovo cimento 5, 1685 (1957).

[4]Summarized by M. Schwartz, Proceedings of the 1960 Annual International Conference on High-Energy Physics at Rochester (Interscience Publishers, Inc., New York, 1960), p. 726.

[5]M. Gell-Mann and A. H. Rosenfeld, Ann. Rev. Nuclear Sci. 7, 407 (1957).

[6]T. D. Lee and C. N. Yang, Phys. Rev. 108, 1645 (1957); R. Gatto, Nuclear Phys. 5, 183 (1958).

[7]Tables compiled by D. A. Glaser, M. L. Good, and D. R. O. Morrison, 1958 Annual International Conference on High-Energy Physics at CERN (CERN Scientific Information Service, Geneva, 1958), p. 270.

[8]B. Cork, L. Kerth, W. A. Wenzel, J. W. Cronin, and R. W. Cool, Phys. Rev. 120, 1000 (1960). This paper gives references to earlier data.

[9]D. B. Lichtenberg (private communication).

[10]In order to form isoscalars from strongly interacting fields, some convention about their behavior in isotopic spin space must be adopted. For example, either $(\Sigma^+, \Sigma^0, \Sigma^-)$ or $(\Sigma^+, \Sigma^0, -\Sigma^-)$ may be chosen as the spherical components of an isovector $\vec{\Sigma}$; the choice, once having been made, must be used consistently. Thus the transformation $\Sigma^- \rightarrow -\Sigma^-$ is ruled out; however, $\vec{\Sigma} \rightarrow -\vec{\Sigma}$ is not.

ERRATA

ODD ΛΣ PARITY AND THE NATURE OF THE πΛΣ COUPLING. Y. Nambu and J. J. Sakurai [Phys. Rev. Letters 6, 377 (1961)].

We would like to emphasize that the parity combination

$$P(\Lambda\Sigma) = -1,\ P(K\Lambda N) = -1,\ P(K\Sigma N) = +1$$

[where $P(\Lambda\Sigma)$ stands for the relative ΛΣ parity, etc.] has been previously considered by S. Barshay [Phys. Rev. Letters 1, 97 (1958); Nuclear Phys. 13, 435 (1959)].

LARGE ANISOTROPIC KNIGHT SHIFTS IN INTERMETALLIC COMPOUNDS. R. G. Barnes, W. H. Jones, Jr., and T. P. Graham [Phys. Rev. Letters 6, 221 (1961)].

Our Letter overlooked the fact that Jaccarino, Matthias, Peter, Suhl, and Wernick[9] had reported quantitative values with respect to the anisotropic Knight shifts of Al^{27} in certain Laves phase compounds. The last sentence of the second-last paragraph should be replaced by: "On the other hand, as has also been remarked by Jaccarino et al.,[9] a major part of the large anisotropy in the case of $TmAl_2$ very likely arises from the nonisotropic part of the *s-f* exchange interaction, the isotropic part of which has been shown[9] to account for the large Knight shifts in the rare-earth-aluminum compounds. The latter authors also reported observing anisotropic shifts in the rare-earth-aluminum Laves phase compounds."

ABSTRACTS

In this section are printed the abstracts of Articles that have been forwarded to The American Institute of Physics for publication in THE PHYSICAL REVIEW. In quoting information obtained from this section before the appearance of the corresponding Article, reference should be made to "Physical Review (to be published)" rather than to this Journal.

LIGHT AS A PLASMA PROBE. Michel Baranger, Carnegie Institute of Technology, Pittsburgh, Pennsylvania, and Bernard Mozer, Brookhaven National Laboratory, Upton, New York (Received February 27, 1961).

The effect of longitudinal plasma oscillations on atomic spectra is examined. It is shown that they should give rise to satellite lines, disposed symmetrically in pairs about a forbidden line and separated from it by Ω_p, the plasma frequency. Discussion is given of the circumstances under which these satellites should be strong enough to be observed. Their observation would amount to a measurement of the frequency and intensity of plasma oscillations.

SPACE DISPERSIVE PROPERTIES OF PLASMA. Jacob Neufeld, Health Physics Division, Oak Ridge National Laboratory, Oak Ridge, Tennessee (Received November 1, 1960).

The "space dispersion," i.e., the occurrence of the term $\vec{k}$ in the dielectric constant $\epsilon(\omega, \vec{k})$, can be attributed either to the Doppler effect or to the magnitude of the term ak that may appear in the formulation of the problem. (a is a characteristic distance such as the Debye length.) Using an approach based on the Doppler effect, the macroscopic parameters of a plasma have been represented in the form of four-dimensional tensors of the fourth order (similar to those introduced by Mandelstam and Tamm). The phenomenological description of plasma has also been formulated in a three-dimensional space by means of two macroscopic parameters: the electric susceptibility χ_e and the "proper magnetic susceptibility" χ_μ/μ. Expressions for these parameters have been given for the general case of a plasma having an electron velocity distribution $f(\vec{v})d\vec{v}$ and for a few typical specific cases. Both parameters are functions of the frequency and of the wave vector. This formulation brings into evidence the fact that a plasma is a magnetically polarizable medium and the term χ_μ/μ vanishes only if the electron velocity distribution is isotropic. In the current literature on the subject the existence of the term χ_μ/μ has not been taken into account, since, by using a "modified representation" of the dielectric constant, the magnetic properties of plasma have not been brought into evidence. In the "modified representation" the dielectric constant ϵ_M is defined by the relationship $\vec{k}\times\vec{B} = -(\omega/c)\epsilon_M\vec{E}$, whereas in the conventional representation the same relationship has the form $\vec{k}\times\vec{B} = -(\omega/c)\epsilon\vec{E} + 4\pi(\chi_\mu/\mu)\vec{k}\times\vec{B}$ (where $\epsilon = 1 + 4\pi\chi_e$). A general formalism has been developed for deriving the electric and magnetic plasma parameters directly from the Boltzmann-Vlasov equations.

MOBILITY OF ION IN A SYSTEM OF INTERACTING BOSE PARTICLES. Ryuzo Abe* and Ko Aizu,† Department of Physics, Northwestern University, Evanston, Illinois (Received February 2, 1961).

The transport property of an ion in a dilute Bose-Einstein gas subject to an external electric field is investigated by means of the Boltzmann equation. The interaction Hamiltonian which describes the ion-phonon scattering processes is obtained by the use of the Bogoliubov transformation, and the cross section for the scattering of the ion by phonons is calculated. The solution of the Boltzmann equation is obtained by applying a variation principle, and the temperature dependence of the ion mobility is shown to be T^{-4} at very low temperatures. A comparison of the results with the experimental data in liquid helium and the Khalatnikov and Zharkov theory is given, and also the ion mobility in the Fermi system is briefly discussed.

*On leave of absence from Tokyo Institute of Technology, Tokyo, Japan.

†On leave of absence from Rikkyo University, Tokyo, Japan.

THEORY OF THE SLOW PINCH DISCHARGE. I. THE MAGNETOHYDRODYNAMIC STABILITY OF THE DISCHARGE CORE. A. A. Ware,* John Jay Hopkins Laboratory for Pure and Applied Science, General Atomic Division of General

Dynamics Corporation, San Diego, California (Received February 1, 1961).

Among the unexplained properties of the slow pinch discharge observed in Zeta, Sceptre, and other experiments is the the gross magnetohydrodynamic stability of the discharge. Since the pinch of the magnetic lines of force is approximately constant within the main core of these discharges, the energy principle is applied to such a configuration. The stability condition for interchange modes is $dp/dr \geq -2\gamma pB_\theta^2/r(B^2+\gamma p)$ and, for kink modes, dp/dr should be greater than an undetermined positive quantity. Comparison with experimental results suggests that interchange instabilities are occurring and limiting the negative pressure gradient to the above value, whereas the kink modes can be occurring with, at most, only small amplitude. Possible reasons are given to explain why the kink instability is not observed.

*On leave of absence from Associated Electrical Industries Research Laboratory, Aldermaston, Berkshire, United Kingdom.

PRIMITIVE THEORY OF FERRIMAGNETIC RESONANCE FREQUENCIES IN RARE EARTH GARNETS.

J. H. Van Vleck, Lyman Laboratory of Physics, Harvard University, Cambridge, Massachusetts (Received February 14, 1961).

The effective g factor for ferrimagnetic resonance frequencies in rare earth garnets is calculated by direct inspection of eigenvalues rather than study of the equations of motion. The rare earth ions are treated as captive in the exchange field from the iron, but subject to decomposition of their energy levels by crystalline fields and/or spin-orbit interaction. With a crystalline field, the problem is tractable in a simple way only if these decompositions are large or small compared to those which could be produced by the exchange field acting alone. Anisotropy, actually very important at low temperatures, is neglected except insofar as it can be represented by an anisotropy field. The concept of "fictitious spin" is useful, and the spectroscopic splitting factors turn out to be more relevant than the true gyromagnetic ratios. For europium garnet, our theory becomes essentially that of Wolf. It is shown that Kittel's formula, $g_{eff}=2(M_{Fe}+M_{RE})/M_{Fe}$, has approximate validity if most of the magnetic moment of the rare earth arises from nondiagonal matrix elements joining ionic energy levels with separations large compared with the Zeeman energy in the exchange field. The fact that in certain cases the experimental results are represented fairly well by Kittel's formula is hence not necessarily to be construed as evidence that the rare earth ion is highly damped by spin-lattice interaction as in his original model.

ABRUPT MAGNETIC TRANSITION IN $MnSn_2$.

J. S. Kouvel and C. C. Hartelius, General Electric Research Laboratory, Schenectady, New York (Received February 17, 1961).

The magnetic susceptibility and the electrical resistivity of the intermetallic compound $MnSn_2$ are found to decrease precipitously as the temperature is lowered through 73°K. Both these abrupt changes exhibit a small temperature hysteresis and are highly suggestive of a first-order transition. From 73°K down to 4.2°K, the susceptibility is essentially constant; above 73°K, the susceptibility rises slowly to a maximum (at 86°K) and then decreases in a manner consistent with the Curie-Weiss relation. It is tentatively concluded that the abrupt transition at 73°K involves only a partial disordering of an antiferromagnetic state.

ELECTRIC FIELD GRADIENTS IN POINT-ION AND UNIFORM-BACKGROUND LATTICES.

F. W. de Wette, Department of Physics, University of Illinois, Urbana, Illinois (Received February 10, 1961).

The lattice contribution to the field gradient in ionic crystals and metals is a quantity which has a well-defined value. However, for an actual evaluation the field gradient is usually broken up into a number of conditionally convergent series with poor convergence. Rapidly convergent expressions for these series and consequently for the field gradient can be obtained by applying the method of plane-wise summation.

This method is applied to the field gradient in ionic crystals with tetragonal and hexagonal symmetry and to the field gradient in tetragonal and hexagonal close-packed metal structures. As an example, an expression for the field gradient at the position of the anion is derived for ionic

crystals with the CdI_2 structure. This expression is numerically evaluated for $CoBr_2$, $FeBr_2$, $MgBr_2$, $MnBr_2$, CaI_2, CdI_2, CoI_2, FeI_2, GeI_2, MgI_2, and MnI_2. Rather extensive numerical results are also presented for both close-packed metal structures, including values for the field gradient in Li, Be, Zn, In, and Rh.

INFLUENCE OF WET AND DRY AMBIENTS ON FAST SURFACE STATES OF GERMANIUM. Y. Margoninski* and H. E. Farnsworth, Barus Physics Laboratory, Brown University, Providence, Rhode Island (Received January 1, 1961).

Simultaneous measurements of surface recombination velocity and added trapped charge density in the fast states as a function of surface potential were carried out on an n-type specimen, which was subjected to the following gaseous ambient cycles: (a) room air-vacuum, (b) dry air-vacuum, (c) dry oxygen-vacuum, (d) dry nitrogen-vacuum, (e) wet nitrogen-vacuum, and (f) wet oxygen-vacuum. The most important results of these measurements were: (1) Dry nitrogen had no influence whatsoever on any of the surface state parameters; (2) dry oxygen affected only the density of states and the unperturbed surface potential; (3) wet nitrogen and wet oxygen had almost the same and most pronounced effect on the fast surface states.

*On leave from the Department of Physics, Hebrew University, Jerusalem, Israel. Present address: Research Laboratory, Raytheon Company, Waltham, Massachusetts.

NONLINEARITY AND MICROWAVE LOSSES IN CUBIC STRONTIUM TITANATE. G. Rupprecht, R. O. Bell, and B. D. Silverman, Research Division, Raytheon Company, Waltham, Massachusetts (Received February 23, 1961).

The complex dielectric constant of single-crystal strontium titanate has been measured from 90°K to 230°K at microwave frequencies. The real part of the dielectric constant consists of a large field-independent contribution which obeys a Curie-Weiss law over the entire range of measurement plus a smaller anisotropic field-dependent contribution. These results are shown to be in qualitative agreement with the theory of ferroelectricity in perovskite structures as proposed by Slater. The observed loss tangent consists of a contribution which is quadratic in an applied biasing field plus a field-independent contribution. The field-independent loss tangent goes through a minimum at about 170°K with a much steeper slope on the low-temperature side of the minimum than on the high-temperature side. The origin of the behavior of the field-independent loss tangent is discussed.

MECHANISM OF IMPURITY CONDUCTION IN SEMICONDUCTORS. Jerzy Mycielski, Institute of Physics, Polish Academy of Sciences, Warsaw, Poland (Received February 27, 1961).

A new possible mechanism of impurity conduction in semiconductors at low temperatures is proposed. The conductivity is thought of as due to the carrier jumps over the Coulomb potential wall from the occupied impurity centers to the empty ones. The activation energy of conductivity and, in the case of strong carrier-phonon interaction, the conductivity itself are calculated and compared with Fritzsche's experimental data for the so-called "ϵ_2 anomaly" in p- and n-type germanium.

SELF-DIFFUSION COEFFICIENT IN SOLID ARGON. R. Fieschi, Istituto di Fisica dell'Università, Milano, Italia, Istituto Nazionale di Fisica Nucleare, Sezione di Milano, Italia, and Gruppo di Fisica dei Solidi del Consiglio Nazionale delle Ricerche, Milano, Italia, G. F. Nardelli, Comitato Nazionale Energia Nucleare, Centro di Ispra-Gruppo di Fisica dei Solidi, Milano, Italia, and A. Repanai Chiarotti, Istituto di Fisica dell'Università, Milano, Italia and Gruppo di Fisica dei Solidi del Consiglio Nazionale delle Ricerche, Milano, Italia (Received December 23, 1960).

Self-diffusion in argon crystals is discussed on the basis of the mobility of vacancies, and in the scheme of the "absolute rate theory." Detailed calculations are made for the heat of activation Q and for the pre-exponential factor D_0, including quantum corrections. The change of potential energy is evaluated first by minimizing the lattice energy with respect to the displacement of the four atoms around the diffusing particle, and next by calculating first-order elastic relaxation of the entire lattice. The change of vibrational properties is evaluated in the Einstein approximation. Including the contributions for the hole formation,

the values $D_0 = 4.20 \times 10^{-4}$ cm^2 sec^{-1} and $Q = 13.85 \times 10^{-2}$ ev are found, at $T = 80°K$; the zero-point energy contributes 5% to the heat of activation.

SPECIFIC HEATS OF DILUTE Cu-Co ALLOYS BETWEEN 1.5 AND 4.5°K. L. T. Crane and J. E. Zimmerman, Scientific Laboratory, Ford Motor Company, Dearborn, Michigan (Received February 24, 1961).

Specific heats of eight specimens of dilute copper-cobalt alloys were measured in the range of 1.5 to 4.5°K. Cobalt concentration of these samples lay between $\frac{1}{4}$ and $2\frac{1}{2}$ weight percent. At all concentrations the specific heat is greater than that of pure copper, with the excess being linear in temperature and quadratic in concentration for the lower concentrations at the higher temperatures. Near the lower end of this temperature range samples of greater than $1\frac{1}{4}$% cobalt also exhibit an additional anomaly which appears to have a characteristic temperature proportional to cobalt concentration. A comparison with the specific heats of dilute Cu-Mn alloys shows that the magnetic interactions in Cu-Co and Cu-Mn must differ greatly in character.

ALTERNATIVE APPROACH TO THE SOLUTION OF ADDED CARRIER TRANSPORT PROBLEMS IN SEMICONDUCTORS. J. P. McKelvey, R. L. Longini, and T. P. Brody, Westinghouse Research Laboratories, Pittsburgh, Pennsylvania (Received February 13, 1961).

A novel method of solving added carrier transport problems in semiconductors is presented. The usual procedure in treating problems of this type is to derive a continuity equation for charge carriers on the basis of carrier conservation, allowing for generation and recombination, and to solve this equation under appropriate boundary conditions. The resulting fluxes or currents are obtained from diffusion and drift current equations which involve the concentrations and concentration gradients. In the formulation presented here, equations embodying conservation of flux (again with due allowance for generation and recombination) which incorporate the proper boundary conditions from the outset are solved in the steady-state one-dimensional case to yield a Green's function for the desired carrier fluxes directly. The method is more general than the commonly used continuity equation formulation in that the physical dimensions of the system and the diffusion lengths are not restricted to be large compared to the mean free path; in particular it is unnecessary to assume Fick's law for diffusion processes. Otherwise the method is equivalent to the continuity equation analysis. An example involving carrier generation in a plane region bounded on one side by a surface of arbitrary reflection coefficient (or recombination velocity) and on the other by a collecting p-n junction is worked out. The results are shown to reduce to those obtained via the continuity equation in the appropriate limiting case.

DIELECTRIC PROPERTIES OF $BaTiO_3$ SINGLE CRYSTALS IN THE PARAELECTRIC STATE FROM 1 kc/sec TO 2000 Mc/sec. E. Stern and Allen Lurio, International Business Machines Watson Laboratory at Columbia University, New York, New York (Received January 27, 1961).

The dielectric constant of $BaTiO_3$ single crystals in the region above the 120°C Curie point has been measured at several frequencies in the range from 1 kc/sec to 2000 Mc/sec. In addition, the B coefficient in Devonshire's equation for the free energy has been studied at 500 Mc/sec. It is shown that the crystal is completely clamped with respect to the measuring field at 500 Mc/sec so that the coefficient of the P^4 term in Devonshire's equation is positive and agrees with the expected theoretical result of $B_F{}^C = 2.23 \times 10^{-13}$ cgs units.

LOW-TEMPERATURE RECOVERY OF RESISTIVITY IN ELECTRON-IRRADIATED GOLD. J. B. Ward* and J. W. Kauffman, Northwestern University, Evanston, Illinois (Received November 30, 1960; revised manuscript received April 3, 1961).

This paper describes the results of two electron irradiations of 99.999% purity, 0.008-in. diameter gold wire, at 13° and at 10.5°K, respectively, and subsequent isochronal anneals. The anneals were carried out in 1- or 2-degree steps from the lowest temperature up to 65°K, and, in addition, the second set of anneals was extended for one-hour periods at 125, 170, 225, and 260°K. Each of the anneals produced some recovery. The

plot of the slope of the isochronal recovery curve showed peaks, and indicated a Stage I in the annealing, extending up to 45°K, during which 28.5% of the resistivity increment annealed out. From 45 to 65°K (Stage II) no distinct processes were observed. Stage II apparently continues up to 240°K; from 45 to 250°K, 36% of the resistivity increment anneals out; 35.5% remained at this temperature.

By assigning a suitable frequency factor K_0 to each process in Stage I, and assuming that the processes are first order (corresponding to recombination of close pairs of vacancies and interstitials), it is possible to calculate the activation energies for each process. For $K_0 = 10^{10}$ to 10^{13} sec^{-1}, these ranged from 0.037 to 0.045 ev for the first peak to 0.11 to 0.13 ev for the fifth.

An explanation is suggested for the major differences between the annealing behavior of gold and copper.

*Now at the Department of Metallurgy, Royal School of Mines, Prince Consort Road, London, S. W. 7, England.

TUNNELING FROM AN INDEPENDENT-PARTICLE POINT OF VIEW. Walter A. Harrison, General Electric Research Laboratory, Schenectady, New York (Received February 20, 1961).

A method is developed for calculating wave functions through regions of varying band structure. This method is applied to tunneling problems using the transition-probability approach of Bardeen. It is found that the experiments of Giaever involving tunneling into superconductors cannot be understood strictly in terms of an independent quasi-particle model of the superconductor. The observed proportionality of the tunneling probability to the density of states depends upon the matrix elements being constant which, in turn, depends upon a many-particle feature of the problem. This feature does not carry over to fluctuations in the density of states arising from band structure, and contributions to the current are not expected to be proportional to the density of states in that case. Instead, a projection in wave-number space of the appropriate constant-energy surface enters. Tunneling systems are discussed which involve semiconductors, semimetals, and transition metals as well as simple metals. Finally, alterations in the properties arising from alterations in the nature of the boundary regions are discussed.

LONGITUDINAL MAGNETORESISTANCE IN n-TYPE GERMANIUM: EXPERIMENTAL. W. F. Love, University of Colorado, Boulder, Colorado, and W. F. Wei, Oklahoma State University, Stillwater, Oklahoma (Received February 16, 1961).

Measurements of the longitudinal magnetoresistance of single crystals of pure and doped n-type germanium oriented in the ⟨100⟩, ⟨110⟩, and ⟨111⟩ directions have been made in magnetic fields up to 300 kilogauss over the temperature interval 20°K-300°K. The magnetoresistance ratio, $\rho(H)/\rho(0)$, was found to vary linearly with magnetic field strength in the quantum limit. Magnetoresistance ratios less than one were observed and explained on the basis of the many-valley structure of the conduction band. The saturation of magnetoresistance predicted by classical transport theory was observed at the higher end of the temperature range and used to demonstrate a temperature variation of the anisotropy parameter K.

LONGITUDINAL MAGNETORESISTANCE IN n-TYPE GERMANIUM: THEORETICAL. S. C. Miller and M. A. Omar, University of Colorado, Boulder, Colorado (Received February 16, 1961).

The longitudinal magnetoresistance of n-type germanium is calculated for high magnetic fields where Landau levels are important. The scattering mechanisms considered are acoustic and ionized impurity scattering. Comparison is made with experiment for acoustic scattering and is found to be satisfactory for sufficiently high fields.

DEBYE-WALLER FACTOR IN MÖSSBAUER INTERFERENCE EXPERIMENTS. H. J. Lipkin, Department of Physics, The Weizmann Institute of Science, Rehovoth, Israel (Received February 23, 1961).

A simple calculation is presented of the effects of lattice dynamics on interference between Mössbauer processes and corresponding atomic processes; i.e., between Mössbauer and Rayleigh scattering, or between internal conversion of Mössbauer radiation and the photoelectric effect. When the energy of the emitted γ ray or electron is not measured, it is necessary to sum over all possible final states of the lattice. The interfer-

ence contribution is found to be attenuated by the same "Debye-Waller" factor as the ordinary Mössbauer contribution, depending only upon the momentum of the incident γ ray. If the energy of the emitted γ ray is measured (e.g., by a Bragg scattering experiment), the atomic contribution is attenuated by the usual x-ray Debye-Waller factor, depending upon the momentum transfer, the Mössbauer contribution by the square of the usual Mössbauer factor, and the interference term by the geometric mean of the atomic and Mössbauer factors.

MAGNETIC SHIELDING OF A NUCLEUS BY FREE ELECTRONS. Michael J. Stephen,* Solid State and Molecular Theory Group, Massachusetts Institute of Technology, Cambridge, Massachusetts (Received February 17, 1961).

The magnetic shielding constant of a nucleus by free electrons is evaluated by obtaining the classical partition function for a system of free electrons in a uniform magnetic field perturbed by the field of a nuclear magnet. Both diamagnetic and paramagnetic terms are included in the Hamiltonian. For a highly degenerate gas the shielding constant has oscillatory terms similar to those in the magnetic susceptibility of a free-electron gas. The possibility of observing these terms is discussed.

*Now at the Mathematics Institute, Oxford, England.

POLARIZATION OF NEUTRONS BY PROTONS COUPLED AND POLARIZED IN THE CRYSTALLINE STRUCTURE OF A FERROMAGNETIC ALLOY. N. Mitrofanov and J. J. van Loef, Instituto de Fisica y Matematicas, Universidad de Chile, Santiago, Chile (Received January 26, 1961).

A new effect has been detected: Protons which are interstitially dissolved in a palladium/nickel ferromagnetic alloy (54% Pd, 46% Ni) can be polarized and coupled at room temperature in the presence of an external magnetic field. In order to verify that this proton polarization is a real effect, experiments were performed in which the transmission of thermal neutrons through Pd-Ni samples was measured with and without the magnetic field. Samples with varying concentrations of hydrogen were tested. In the presence of the magnetic field, the thermal neutrons transmitted by the sample appear to be partially polarized, which can be explained by the coupling and polarizing of the protons.

The single transmission coefficient has been measured. For the 160-g Pd-Ni sample containing 70 mg of dissolved hydrogen, it was $3.4\% \pm 0.7\%$. From this result, it can be concluded that the protons are coupled and polarized by indirect spin-exchange forces. The estimated coupling energy corresponds to an internal effective field of about 10^9 gauss.

INFRARED CYCLOTRON RESONANCE IN *n*-TYPE InAs AND InP. E. D. Palik and R. F. Wallis, U. S. Naval Research Laboratory, Washington, D. C. (Received February 23, 1961).

Cyclotron resonance of conduction electrons in InAs and InP has been measured in the far infrared spectral region. The effective masses obtained for InAs show a variation with magnetic field indicative of the nonparabolic nature of the conduction band of this material.

ADIABATIC DEMAGNETIZATION WITH YTTRIUM-RARE EARTH ALLOYS. David T. Nelson* and Sam Legvold, Institute for Atomic Research and Department of Physics, Iowa State University, Ames, Iowa (Received February 27, 1961).

Alloys of yttrium with 0.3 and 1.0 atomic percent gadolinium, 1.0 at.% dysprosium, and 0.6 and 1.0 at.% holmium have been investigated to determine their usefulness as the working substance for adiabatic demagnetization. In addition, single crystals of 0.6 and 1.0 at.% holmium-yttrium alloys were studied. Those alloys which exhibited paramagnetic susceptibility behavior in the temperature range 1.2 to 4.2°K were demagnetized adiabatically from about 11 koe and 1.25°K. The lowest temperature attained was 0.76°K for the single crystal of 1.0 at.% holmium with the magnetic field parallel to the *a* axis of the hexagonal crystal. Magnetization measurements obtained for the single crystals in the temperature range 1.2 to 4.2°K indicated strong anisotropy with the *a* axis as the easy axis of magnetization. Hysteresis was observed in the magnetization of the 1.0 at.% holmium single crystal with the *a*

axis parallel to the field. Entropy removal during magnetization was calculated from the magnetization data for the single crystals and found to be only about 15% of that expected if the alloy behaved like an ideal paramagnetic substance.

*Present address: Department of Physics, Luther College, Decorah, Iowa.

NUCLEAR MAGNETIC RESONANCE IN $(NH_4)_2$-$(BeF_4)_x(SO_4)_{1-x}$ AND OTHER FERROELECTRIC SYSTEMS. Gerald Burns, International Business Machines Research Laboratory, Yorktown Heights, New York (Received January 31, 1961).

The temperature dependence of fluorine and proton nuclear magnetic resonance (NMR) in polycrystalline samples of the solid solution $(NH_4)_2(BeF_4)_x(SO_4)_{1-x}$ has been measured for several x. This solid solution is ferroelectric for high and low x and is paraelectric in between. A sharp transition in the second moment of the F^{19} resonance was observed but found to be independent of x, while the ferroelectric properties are dependent on x. The proton NMR showed the nonequivalence of the NH_4 groups, but again the temperature dependence could not be correlated with the ferroelectric properties. Thus, the ferroelectric behavior of this system cannot be associated with the appealing hypothesis of the freezing in of the vibrating NH_4 or BeF_4 groups.

The temperature dependence of the proton NMR was also observed in the ferroelectric compounds $(NH_4)_2Cd_2(SO_4)_3$ and NH_4HSO_4. Similar conclusions can be drawn from these measurements as those given above. In some of the alums, the crystallographic phase transition is again not accompanied by any change in the proton resonance line. However, in N_2H_5Al alum and NH_3OHAl alum, there is a very abrupt change in the NMR line at the temperature of the phase transition.

PHOTOELECTRIC EFFECT AND PAIR ANNIHILATION WITH LARGE MOMENTUM TRANSFER. David S. Moroi, Institute for Atomic Research and Department of Physics, Iowa State University, Ames, Iowa (Received April 15, 1960; revised manuscript received March 1, 1961).

Photoelectric effect and pair annihilation in hydrogen with large momentum transfer are studied, taking into account the recoil and anomalous magnetic moment of the proton, in an effort to see whether these processes can be used to probe quantum electrodynamics at small distances. A negative result is obtained. It turns out that for an incident energy of 100 Mev, the important term containing the electron propagator, which is sensitive to small-distance modifications, is about 0.5% of the term which is insensitive to them.

The proton structure is described by two covariant form factors determined by the electron-proton scattering. The differential cross sections are calculated in the Born approximation in the laboratory system, neglecting the binding energy of the hydrogen atom. The results are analyzed in the extreme relativistic energy range and in the special case that the outgoing electron (photon) comes off perpendicular to the incident beam. The total cross sections are calculated in the high-energy approximation, simply to check the present method of calculation.

The differential cross sections are very small, $\sim 10^{-42}$ - 10^{-40} cm^2/sr. The same calculations, if applied to an atom with higher atomic number Z, give the differential cross sections for the above processes larger by a factor $2Z^5$, if one neglects screening. For a Au target the differential cross sections are then of the order of 10^{-33} - 10^{-31} cm^2/sr. However, this extension of the calculations introduces a considerable error in the differential cross sections, because the influences of the Coulomb field and anomalous magnetic moment of a nucleus to the electron-wave functions are neglected. It will serve only as an estimate of the order of magnitude of the differential cross sections.

EFFECT OF VIRTUAL EXCITATIONS ON THE ELASTIC SCATTERING OF ELECTRONS AND POSITRONS BY ATOMIC HYDROGEN. Kenneth Smith, Argonne National Laboratory, Argonne, Illinois, and P. G. Burke, Lawrence Radiation Laboratory, University of California, Berkeley, California (Received February 23, 1961).

Total cross sections for the elastic scattering of electrons and positrons (neglecting positronium formation) from the 1s state of atomic hydrogen have been calculated allowing for virtual excitation to the 2s and 3s states. The S-, P-, and D-wave contributions to $Q_{1s\text{-}1s}$ have been computed for incident energies below 10 ev.

The results for positron scattering show that

virtual excitation to the 2s and 3s states only slightly affects the phase shifts calculated in the static approximation. The influence of the 2s state appears to be much more important for electrons. The scattering lengths of these exploratory calculations are compared with the results of other calculations.

MICROWAVE ZEEMAN SPECTRUM OF ATOMIC CHLORINE. V. Beltran-Lopez and H. G. Robinson, Gibbs Physics Laboratory, Yale University, New Haven, Connecticut (Received February 17, 1961).

The microwave spectrum of atomic chlorine has been observed at 9190 Mc/sec in the products of a radio-frequency electrodeless discharge. Of the twelve allowed transitions per isotope, $\Delta M_I = 0$, $\Delta M_J = \pm 1$, five arising from Cl^{35} and two from Cl^{37} have been measured. Using a nonrelativistic Hamiltonian, analysis of the data yields $-g_J(Cl;{}^2P_{3/2})/g_p = 438.50415 \pm 0.00063$, where g_p is the proton gyromagnetic ratio in a cylindrical sample of mineral oil. This result can be transformed to $g_J(Cl;{}^2P_{3/2})/g_J(D) = 0.666201 \pm 0.000002$. A calculation of the $g_J(Cl)$ isotope effect shows that it should not be observable in the present experiment. Estimates of the atom-atom and atom-molecule hard-sphere collision cross sections are made from measurements of linewidth and line intensity.

NUCLEAR ENERGY LEVELS OF F^{19}, F^{21}, Ne^{22}, and Ne^{24}. M. G. Silbert and Nelson Jarmie, Los Alamos Scientific Laboratory, University of California, Los Alamos, New Mexico (Received February 20, 1961).

A 16-in. radius, 180° double-focussing magnetic spectrometer was used to investigate the nuclear energy levels of F^{19}, F^{21}, Ne^{22}, and Ne^{24} by analysis of protons and alpha particles produced by (t, p) and (t, α) reactions with natural neon and with Ne^{22} gas targets. Between excitation energies of 2.8 and 6.5 Mev, new levels in F^{19} were found at 5.102, 5.539, 5.628, 5.937, and 6.169 Mev. Previously reported levels at 3.29, 4.48, and 4.95 Mev were not observed. Up to an excitation energy of 4.3 Mev in F^{21}, new levels were seen at 3.451, 3.509, 3.635, 3.977, 4.056, and 4.158 Mev, while the four previously known lower states at 0.285, 1.104, 1.743, and 2.047 Mev were confirmed. The mass of F^{21} was determined to be 21.006624 ± 0.000011 amu (O^{16} standard); $(M-A) = 6.168 \pm 0.010$ Mev. In Ne^{22} thirty-eight excited states were observed up to an excitation of 9.4 Mev. Levels at 1.277, 3.343, and 4.473 Mev were confirmed, while a previously reported level at 4.9 Mev was not observed. Energy levels in Ne^{24}, up to an excitation energy of 6.4 Mev, were found at 1.986, 3.873, 3.962, 4.764, 4.886, 5.576, (5.641), and 6.030 Mev. The mass of Ne^{24} was determined to be 24.001238 ± 0.000011 amu (O^{16} standard); $(M-A) = 1.153 \pm 0.010$ Mev. Standard deviations in the values for the excitation energies vary from 0.015 to 0.025 Mev. Some representative cross sections are reported.

9.17-Mev STATE IN N^{14}. R. E. Segel, J. W. Daughtry, and J. W. Olness, Aeronautical Research Laboratory, Dayton, Ohio (Received February 27, 1961).

The angular distributions of the 9.17-Mev ground-state gamma ray and the gamma rays of the 2.73-6.44 Mev cascade resulting from the 1.75-Mev proton resonance on C^{13} ($N^{14*} = 9.17$ Mev) have been measured. The spins deduced from the angular distributions for the 9.17-Mev state and the 6.44-Mev state agree with previous assignments. The angular momenta admixtures required are found to be in disagreement with one shell model of N^{14} but it is shown that the model can be brought into accord with experiment by having the 9.17-Mev state wave function include a configuration with a nucleon in the f shell.

HYPERFINE STRUCTURE OF THE 24-kev TRANSITION IN Sn^{119}. O. C. Kistner, A. W. Sunyar,* and J. B. Swan,† Brookhaven National Laboratory, Upton, New York (Received February 28, 1961).

The Zeeman splittings of the two lower levels of Sn^{119} were measured by the method of recoilless emission and resonant absorption of the 24-kev γ radiation emitted in the decay of Sn^{119m}. The source consisted of Sn^{119m} diffused into 0.002-inch iron foil. Gray tin metal at a temperature of ~10°C was used as the absorber. The magnitude of the internal magnetic field at the source nuclei was sufficient to allow resolu-

tion of the six absorption peaks resulting from the $3/2^+ - 1/2^+$ $M1$ transition. Measurements were made with the internal fields aligned by application of a small external magnetic field; in this manner the central line of each triplet could be enhanced or suppressed by observing the radiation emitted either perpendicular or parallel to the external field. The splitting parameters obtained from the measurements yield a value of 0.672 ± 0.025 nm for the magnetic moment of the first excited state of Sn^{119}, and an effective magnetic field at the tin nuclei in the iron environment of 78.5 ± 2.0 koe. The chemical shift is such that the transition energy in the source is less than that in the absorber by $(4.24 \pm 0.04) \times 10^{-8}$ ev. Within the limits of measurement, no quadrupole coupling was observed.

*Now on leave at The Institute for Theoretical Physics, Copenhagen, Denmark.

†On leave from the University of Western Australia, Nedlands, Western Australia.

NUCLEAR ORIENTATION OF Dy^{155} AND Dy^{157}. Quirino O. Navarro and D. A. Shirley, Lawrence Radiation Laboratory and Department of Chemistry, University of California, Berkeley, California (Received February 20, 1961).

The isotopes Dy^{155} and Dy^{157} were aligned at low temperatures in a single crystal of neodymium ethylsulfate, using the magnetic hfs method. Angular distribution of gamma radiation following the decay of these isotopes was studied as a function of temperature in the region $0.02°K < T < 1°K$. Spin and parity assignments of 5/2 - were made to states at 227 kev in Tb^{155} and at 327 kev in Tb^{157}. Assuming $I = 3/2$ for both dysprosium isotopes as well as pure $L = 1$ beta decay to the 5/2 - states, nuclear moments of $|\mu_{155}| = 0.21 \pm 0.05$ nm and $|\mu_{157}| = 0.32 \pm 0.02$ nm were derived.

NUCLEAR ELECTRIC MONOPOLE TRANSITION IN Ca^{42}. N. Benczer-Koller,* M. Nessin, and T. H. Kruse, Columbia University, New York, New York (Received February 23, 1961).

The 0^+ assignment to the 1.836-Mev, second excited state in Ca^{42} has been confirmed by the observation of electric monopole electron-positron pairs and internal conversion electrons corresponding to the crossover transition to the ground state. The shape of the continuous positron spectrum from the $E0$ pairs, as well as the ratio $R = 9.0 \pm 1.8$ of pairs to $E0$ conversion electrons, are consistent with theoretical predictions for an $E0$ transition. 0.305-Mev internal conversion electrons were observed corresponding to the transition between the 1.836-Mev and the 2^+, 1.523-Mev, first excited state. The ratio of 1.836-Mev to 0.305-Mev electron yields is 1.03 $\pm$ 0.10. From these and other data the monopole strength parameter ρ was determined to be 0.41.

*Present address: Department of Physics, Rutgers University, New Brunswick, New Jersey.

PHOTODISINTEGRATION OF Be^9 FROM THRESHOLD TO 5 Mev. Mark J. Jakobson, Montana State University, Missoula, Montana (Received February 21, 1961).

A bremsstrahlung-photon difference method measurement of the $Be^9(\gamma, n)$ cross section indicates maxima in the cross section of 1.15 ± 0.15, 0.55 ± 0.1, 1.2 ± 0.2, and 1.0 ± 0.3 mb at energies of 1.70, 2.40, 2.95, and 4.6 Mev, respectively. The angular distribution of the neutrons corresponding to the 1.70- and 4.6-Mev peaks is spherically symmetric; $d\sigma/d\Omega = a + b \sin^2\theta$ $(a/b = 1.0 \pm 0.2)$ for the 2.95-Mev peak.

In^{116} ACTIVATION RATIOS. M. A. Greenfield, Department of Radiology, University of California, Los Angeles, California, and R. L. Koontz, Atomics International, Canoga Park, California (Received October 11, 1960; revised manuscript received March 27, 1961).

The data of Domanic and Sailor regarding the ratio of the 54-minute to the 13-second activities of In^{116} produced by neutron capture in In^{115}, previously published, have been corrected with experimentally determined self-absorption factors for 54-minute In^{116}. The results of these corrections have removed an anomaly observed between foils of different thicknesses, provided the foil is known to have been uniformly activated throughout its volume. The corrections appear to have removed a dependence of the ratio of activities on neutron energies from thermal to 2.66 ev. However, even after correction of the data there remains a substantial difference in

the value of the ratio of activities at 3.86 ev. The corrected value of the ratio at 3.86 ev is about one-half the value at the other energies investigated.

REACTIONS OF ALPHA PARTICLES WITH IRON-54 AND NICKEL-58. Frank S. Houck* and J. M. Miller, Chemistry Department, Columbia University, New York, New York and Chemistry Department, Brookhaven National Laboratory, Upton, New York (Received February 23, 1961).

The excitation functions for the (α, p), (α, n), (α, pn), $(\alpha, 2n)$, $(\alpha, 2pn)$, and $(\alpha, p2n)$ reactions of Fe^{54} and the $(\alpha, \alpha'p)$, $(\alpha, \alpha'n)$, $(\alpha, \alpha'pn)$, and $(\alpha, \alpha'2n)$ reactions of Ni^{58} have been determined for alpha-particle energies up to 40 Mev. A large preference for proton emission is observed. At the maxima in the excitation functions, these ratios were obtained: $\sigma(\alpha, p)/\sigma(\alpha, n) = 3.1$; $\sigma(\alpha, pn)/\sigma(\alpha, 2n) = 70$; $\sigma(\alpha, \alpha'p)/\sigma(\alpha, \alpha'n) = 6$; $\sigma(\alpha, 2pn)/\sigma(\alpha, p2n) = 6.3$ (at 40 Mev); and $\sigma(\alpha, \alpha'pn)/\sigma(\alpha, \alpha'2n) = 140$ (at 40 Mev). These results are discussed in terms of the compound-nucleus model. A value of $r_0 = 1.7$ f is required to fit the low-energy portion of the observed "total" cross section with total reaction cross section calculated from continuum theory.

*Present address: Operations Evaluation Group, Massachusetts Institute of Technology, Cambridge, Massachusetts.

NEUTRON TOTAL CROSS SECTIONS OF Be, B^{10}, B, C, AND O. D. B. Fossan,* R. L. Walter, W. E. Wilson, and H. H. Barschall, University of Wisconsin, Madison, Wisconsin (Received February 20, 1961).

Total cross sections of Be, B^{10}, B, C, and O have been measured for neutrons of energies between 3.4 and 16 Mev. Neutrons of energy spreads between 15 and 40 kev were produced by bombarding tritium targets with protons or deuterium targets with deuterons, the charged particles being accelerated in a tandem electrostatic accelerator. Sharp peaks in the total cross sections of B^{11}, C, and O yielded information about energy levels in B^{12}, C^{13}, and O^{17}. None of the total cross sections of the five nuclei investigated showed sharp peaks above energies corresponding to an excitation energy of the order of 12 Mev of the respective compound nucleus. The transition from sharp structure to a slowly varying cross section occurs quite abruptly except for the compound nucleus B^{11} which is excited to almost 12 Mev even for slow neutrons.

*Present address: University of Copenhagen, Copenhagen, Denmark.

HALF-LIFE OF SAMARIUM-147. P. M. Wright,* E. P. Steinberg, and L. E. Glendenin, Argonne National Laboratory, Argonne, Illinois (Received February 16, 1961).

A liquid scintillation counting technique has been applied to the determination of the half-life of Sm^{147} by specific alpha-activity measurement. A value of $(1.05 \pm 0.02) \times 10^{11}$ years is obtained.

*Permanent address: Chemistry Department, Wheaton College, Wheaton, Illinois.

EFFECT OF COMPETITION BETWEEN GAMMA-RAY AND PARTICLE EMISSION ON EXCITATION FUNCTIONS. James Robb Grover, Chemistry Department, Brookhaven National Laboratory, Upton, New York (Received February 23, 1961).

A procedure has been devised for calculating cross sections for nuclear reactions within about two Mev of threshold, where the effect of competition between gamma-ray and particle emission is often important. The requisite formulas depend upon assumptions embodied in the spin-dependent statistical theory of nuclear reactions, so the treatment is most valid for medium to heavy nuclei at moderate bombarding energies. Input data required by the formulas are (1) the level density parameter a, (2) an effective nuclear moment of inertia s, (3) the ratio of radiation width to level spacing (Γ_γ/D) evaluated at some convenient energy, spin, and parity in the excited nucleus immediately preceding the product, (4) transmission coefficients $T_l(\epsilon)$ for the range of energies and type of particle in the final evaporation step, and (5) the energies, spins, and parities of the first few excited states in the product nucleus. Using reasonable estimates for s, Γ_γ/D, and $T_l(\epsilon)$, experimental excitation functions near threshold for the reactions $Bi^{209}(p, 2n)Po^{208}$ and $Sm^{144}(\alpha, 3n)Gd^{145}$ were analyzed to find the corresponding values of a. The results are consistent with $a \sim 0.1A$ Mev^{-1} (A is the mass number), but inconsistent with $a \sim 2$ to 3 Mev^{-1} (in-

dependent of A), in contrast to the result often obtained when competition from gamma-ray emission is ignored. Also, a semiqualitative argument is given to suggest that competitive gamma-ray emission often seriously influences excitation functions even several Mev above threshold.

NEW YTTRIUM ISOMERS OF MASSES 86 AND 90. Larry Haskin, Department of Chemistry, University of Wisconsin, Madison, Wisconsin and Argonne National Laboratory, Argonne, Illinois, and Robert Vandenbosch, Argonne National Laboratory, Argonne, Illinois (Received February 16, 1961).

Cyclotron bombardment of Rb with alpha particles and Sr with deuterons have yielded two new yttrium activities. Y^{86m} decays with a half-life of 49.0 ± 1.5 min. The isomer is supported by a highly converted 7.2-kev isomeric transition followed by a 210-kev gamma ray having a conversion coefficient $e/\gamma = 0.06 \pm 0.01$. Y^{90m} has a half-life of 3.19 ± 0.06 hr, decaying to the Y^{90} ground state with emission of two gamma rays: 476 kev, $e/\gamma = 0.102 \pm 0.02$; and 203 kev, $e/\gamma = 0.036 \pm 0.007$. Spin and parity assignments are made for the Y^{90} levels.

STATES OF Be^{11}, B^{11}, AND C^{11}. P. F. Donovan, Bell Telephone Laboratories, Murray Hill, New Jersey and Brookhaven National Laboratory, Upton, New York, J. V. Kane and R. E. Pixley, Brookhaven National Laboratory, Upton, New York, and D. H. Wilkinson, Brookhaven National Laboratory, Upton, New York and Clarendon Laboratory, Oxford, England (Received February 21, 1961).

The gamma decay of the 4.46- and 5.03-Mev levels of B^{11} has been determined by (p,γ) coincidences using the reaction $Be^9(He^3,p)B^{11}$. The 5.03-Mev level is found to decay with a probability of 0.14 ± 0.03 via the state at 2.13 Mev; the intensity of the branch to the state at 4.46 Mev is less than 3×10^{-3}. The intensity of the branch from the 4.46-Mev level via that at 2.13 Mev is less than 5×10^{-3}. The data on these states are reviewed and it is concluded that the present results strongly favor the choices $J = 1/2-$, $5/2-$, and $3/2-$ for the states at 2.13, 4.46, and 5.03 Mev, respectively, without appeal to a model. It is, however, emphasized that the body of data as it stands at the moment might admit $J = 1/2+$ for the 2.13-Mev state and $J = 1/2-$ for the 5.03-Mev state. The previsions of the independent-particle model are then examined, and it is concluded that best general agreement between theory and experiment is achieved for $a/K \approx 4$-4.5. The likely relevance of the collective model is remarked upon. It is demonstrated with the aid of the reaction $B^{10}(p,\gamma)C^{11}$ that the ordering of the first three excited states of C^{11} is the same as in B^{11}. The beta decay of Be^{11} is reconsidered in the light of the increased firmness of the assignments in B^{11} and of the previsions of the independent-particle model; it is concluded that Be^{11} is most probably of even parity.

POSITRON SPECTRA OF Co^{56}. J. H. Hamilton, Physics Department, Vanderbilt University, Nashville, Tennessee, and L. M. Langer and D. R. Smith, Physics Department, Indiana University, Bloomington, Indiana (Received February 27, 1961).

The positron spectrum of Co^{56} has been carefully studied with a magnetic spectrometer. Two positron groups were observed. The maximum energies and intensities of the two groups are 1.464 ± 0.015 Mev and 0.440 ± 0.030 Mev and $\geq 90\%$ and $\leq 10\%$, respectively. No evidence for any other groups was found. In particular, an upper limit of 1% was set for the presence of any group with maximum energy 0.9-1.0 Mev. The high-energy spectrum has essentially an allowed shape. However, the inclusion of a shape factor such as $(1 + 0.3/W)$ offers a more consistent fit to all the data.

HYPERFINE STRUCTURE OF THE $(5p)^5(6s)\ ^3P_2$ STATE OF $_{54}Xe^{129}$ AND $_{54}Xe^{131}$. W. L. Faust and M. N. McDermott, Columbia Radiation Laboratory, Columbia University, New York, New York (Received February 17, 1961).

The hyperfine structures of the metastable $(5p)^5(6s)\ ^3P_2$ state of $_{54}Xe^{129}$ and $_{54}Xe^{131}$ have been measured by the atomic beam magnetic resonance method. The zero magnetic field intervals $f(F \rightarrow F')$ are: for Xe^{129}, $f(\frac{3}{2} \rightarrow \frac{5}{2}) = 5961.2577(9)$ Mc/sec; and for Xe^{131}, $f(\frac{5}{2} \rightarrow \frac{7}{2}) = 2693.6234(7)$ Mc/sec, $f(\frac{3}{2} \rightarrow \frac{5}{2}) = 1608.3475(8)$ Mc/sec, and $f(\frac{1}{2} \rightarrow \frac{3}{2}) = 838.7636(4)$ Mc/sec. The values of the

quadrupole and octupole moments of Xe^{131} without polarization corrections and without corrections for any effects of configuration mixing, are $Q = +0.120(12)$ b and $\Omega = +0.048(12)$ nm b. The hyperfine structure anomaly for the two isotopes due to the $s_{1/2}$ electron alone is $\Delta(s_{1/2}) = +0.0440(44)\%$, in disagreement with the prediction of the single-particle model.

DEUTERIUM AND BERYLLIUM $(n, 2n)$ CROSS SECTIONS BETWEEN 6 AND 10 Mev. H. C. Catron, M. D. Goldberg, R. W. Hill, J. M. Le Blanc, J. P. Stoering, C. J. Taylor, and M. A. Williamson, Lawrence Radiation Laboratory, University of California, Livermore, California (Received February 20, 1961).

The $(n, 2n)$ cross sections of deuterium and beryllium have been measured for incident neutron energies in the range from 6 to 10 Mev using a large liquid scintillator. The cross sections in barns obtained for deuterium were 0.067 ± 0.007 at 6.11 Mev, 0.073 ± 0.007 at 6.55 Mev, 0.088 ± 0.009 at 7.32 Mev, 0.11 ± 0.010 at 8.26 Mev, and 0.14 ± 0.015 at 10.2 Mev. The beryllium cross sections were 0.55 ± 0.08 at 6.55 Mev, 0.56 ± 0.07 at 7.32 Mev, and 0.63 ± 0.09 at 8.26 Mev.

INTERACTIONS OF 7.5-Mev PROTONS WITH COPPER AND VANADIUM. Bruce W. Shore,* Nathan S. Wall, and John W. Irvine, Jr., Department of Chemistry, Department of Physics, and Laboratory for Nuclear Science, Massachusetts Institute of Technology, Cambridge, Massachusetts (Received February 15, 1961).

The separate cross sections for interaction of 7.5-Mev protons have been measured for natural copper and vanadium. Angular distributions for elastic scattering are presented. The (inelastic scattering + alpha emission) cross sections are: copper, 266 mb, and vanadium, 134 mb. The (p, n) reaction cross sections are: Cu^{65}, 537 mb, and V^{51}, 555 mb. These data, along with separate measurements of polarization from copper, are compared with optical-model computations. The results indicate a volume-absorption potential rather than a surface-absorption potential.

*Now at Analytic Services, Alexandria, Virginia.

SURVEY OF INELASTIC SCATTERING OF DEUTERONS BY HEAVY ELEMENTS. Bernard L. Cohen and Robert E. Price, University of Pittsburgh, Pittsburgh, Pennsylvania (Received February 2, 1961).

Energy spectra of inelastically scattered deuterons from approximately 30 heavy elements are measured with about 80-kev resolution. Many new levels are reported, including a level in Pr^{141} whose discovery substantially alters the decay scheme of Nd^{141}. The gross structure of the spectra is studied and several regularities are noted. Angular distributions in Zr and the even isotopes of Sn indicate that the parity of the strongest levels in the anomalous peaks (~2.5 Mev) are negative, in agreement with the popular assumption that they are the 3^- collective vibrational level; however, there are also several strongly excited positive-parity levels in that region. The correlation between cross sections for exciting given levels by (d, d') and (d, p) or (d, t) reactions is studied. The correlation coefficients are generally slightly negative, but there are several cases where the same levels are strongly excited by all three reactions including one case (in Sn^{117}) where the principal $d_{5/2}$ single quasi-particle level is also the principal 2^+ vibrational level based on the $s_{1/2}$ ground state. A very strong positive correlation is found between cross sections for exciting given levels by Coulomb excitation and by direct-interaction inelastic scattering. The large peaks reported by Yntema and Zeidman in inelastic deuteron scattering from Rh, Ag, and Sn at 4-5 Mev and from Ta and Pt at about 3 Mev are not found here; explanations for this are offered.

MAGNETIC MOMENT OF THE PROTON IN UNITS OF THE NUCLEAR MAGNETON. H. S. Boyne and P. A. Franken, The University of Michigan, Ann Arbor, Michigan (Received February 3, 1961).

A new method for measuring the magnetic moment of the proton in units of the nuclear magneton is described. The method differs from the work of others in that the cyclotron frequency of free low-energy H_2^+ ions is measured with a low-power absorption technique as a function of magnetic field. The extrapolation technique of Franken and Liebes is utilized to correct for shifts produced by electrostatic

fields. The measurements yield $\mu_p(H_2O)/\mu_n = 2.792\,83 \pm 0.000\,06$. This determination is approximately 50 parts per million higher than the results of other workers.

TWICE FORBIDDEN BETA-RAY TRANSITION OF Co^{60}. D. C. Camp, L. M. Langer, and D. R. Smith, Physics Department, Indiana University, Bloomington, Indiana (Received February 27, 1961).

The high-energy beta-ray transition from the ground state of Co^{60} to the first excited state of Ni^{60} was studied in a magnetic spectrometer. The shape of the beta-ray spectrum is found to be consistent with that expected for a "unique" twice forbidden transition from a 5+ to a 2+ level. The relative intensity of this 1.48-Mev transition is found to be 0.12%. The comparative half-life is $\log(\langle S_2^3 \rangle f_0 t) = 11.8$ which is in close agreement with the values found for the other "unique" twice forbidden transitions of Be^{10} and Na^{22}.

COULOMB BARRIER IN A HIGHLY EXCITED NUCLEUS. D. W. Lang, Australian National University, Canberra, Australia (Received February 9, 1961).

Experiments involving alpha emission spectra from nickel and rhodium bombarded with protons are analyzed using the statistical model. It is shown, using values calculated by Igo for the cross sections for alpha absorption, that the experimental data are consistent with a constant value for the potential barrier.

EVIDENCE FOR SEQUENTIAL TWO-BODY DECAY IN THREE-BODY DECAY OF C^{12} AND B^{10}. E. H. Beckner, C. M. Jones, and G. C. Phillips, Rice University, Houston, Texas (Received February 27, 1961).

The reactions $B^{11}(p,\alpha)Be^8$ and $Be^9(p,d)Be^8$ have been studied by employing monoenergetic protons, thin targets, and a low-background magnetic spectrometer to resolve the disintegration products. The continuum spectra of alpha particles and deuterons produced, respectively, in the reactions have been compared to the generalized density-of-states function of Phillips, Griffy, and Biedenharn and good fits have been obtained. The density function was calculated from the experimental (α,α) scattering phase shifts. The calculated S-wave density function for Be^8 predicts a low-energy anomaly. This anomaly has been observed and confirms the assumption of the model used to calculate this spectral shape: three-body decay proceeding via a sequence of two-body decay modes.

NUCLEON-ANTINUCLEON MECHANISM FOR PION-PION SCATTERING RESONANCES. Johan G. Belinfante, Palmer Physical Laboratory, Princeton, New Jersey (Received February 27, 1961).

The Chew-Mandelstam N/D equations for pion-pion scattering were modified to include contributions from the nucleon-antinucleon intermediate state, which was estimated in perturbation theory as well as by limitations imposed by unitarity alone. It was found that the Frazer resonance could not be obtained by such a simple mechanism, starting from s-wave dominant solutions.

EXTENSION OF THE ISOBARIC NUCLEON MODEL FOR PION PRODUCTION IN PION-NUCLEON, NUCLEON-NUCLEON, AND ANTINUCLEON-NUCLEON INTERACTIONS. R. M. Sternheimer and S. J. Lindenbaum, Brookhaven National Laboratory, Upton, New York (Received February 28, 1961).

The isobaric nucleon model of pion production in nucleon-nucleon and pion-nucleon collisions has been extended to include the effect of the higher resonances in the isotopic spin $T = 1/2$ state of the pion-nucleon system, in addition to the effect of the well-known low-energy $T = 3/2$ resonance which has been previously investigated. The higher $T = 1/2$ resonances are centered at incident pion energies of 600 and 880 Mev, and thus correspond to isobar masses $m_I = 1.51$ and 1.68 Bev, respectively, as compared to $m_I = 1.23$ Bev for the $T = 3/2$ resonance. For the inelastic pion-nucleon interactions, calculations of the various pion and recoil-nucleon energy spectra have been carried out for incident pion energies

T_π, inc = 1.0, 1.4, and 2.0 Bev. We have considered both single- and double-pion production by the incident pion, corresponding to two-pion and three-pion final states, respectively. General equations for the center-of-mass energy spectra of the final-state pions and nucleons have been obtained for all single- and double-pion production reactions from both π^--p and π^+-p collisions. The results of the present extended isobar model at T_π, inc = 1.0 Bev are in reasonable agreement with the combined data from three experiments on π^--p interactions in the region of 1.0-Bev incident energy. The Q-value distributions for pion-nucleon and pion-pion pairs have been calculated for single-pion production at T_π, inc = 1.0 Bev. The present extension of the isobar model can also be used to treat up to four-pion final states in the π-N interactions, and up to eight-pion final states in N-N interactions.

For pion production in nucleon-nucleon collisions, we have obtained the branching ratios for all pion production reactions which involve the isobaric states N_1^*, N_{2a}^*, and N_{2b}^* corresponding to the $T = 3/2$ and $T = 1/2$ resonances. General equations for the energy spectra of the final-state pions and nucleons have been derived for all single- and double-pion production reactions from both p-p and n-p collisions. Calculations of the various pion and nucleon energy spectra have been carried out for incident nucleon energies of 2.3 and 3.0 Bev. For the processes of pion production in antinucleon-nucleon interactions which do not result in annihilation, it has been assumed that an anti-isobar $\bar{N}_\alpha^*$ can be produced, which is the antiparticle of the isobar N_α^*. Specific results have been obtained for both single- and double-pion production in $\bar{p}$-p, $\bar{p}$-n, and $\bar{n}$-p collisions.

K^--p AND K^--n CROSS SECTIONS IN THE MOMENTUM RANGE 1 TO 4 Bev/c.

V. Cook, Bruce Cork, T. F. Hoang, D. Keefe, L. T. Kerth, W. A. Wenzel, and T. F. Zipf, Lawrence Radiation Laboratory, University of California, Berkeley, California (Received February 27, 1961).

The energy dependence of the K^--nucleon total cross sections has been measured over the K^- momentum range 0.98 to 3.98 Bev/c. K^--n cross sections were obtained by deuterium-hydrogen subtraction, with a correction for screening effects. There is evidence for structure in the $T = 0$ K^--nucleon state in the momentum range 0.98 to 2.0 Bev/c. This structure is absent in the $T = 1$ state.

In addition, a measurement was made at 1.95 Bev/c of the angular distribution of the K^--p elastic scattering at small angles. The forward-scattering amplitude obtained from the data gives a ratio of real part to imaginary part, 0.5 ± 0.2, at 0°. The corresponding ratio for π^- mesons at this momentum was found to be $0.4^{+0.2}_{-0.4}$.

Measurements of the K^--p "elastic" charge exchange gives a cross section which falls about 10 mb at 1 Bev/c to at most a few mb at 4 Bev/c.

Momentum (Bev/c)	K^--p (mb)	K^--d (mb)	K^--n (mb)
0.98	47.1 ±1.2	74.3 ±0.8	31.2 ±1.6
1.10	43.6 ±1.6	...	...
1.23	33.8 ±0.9	60.7 ±0.5	29.4 ±1.1
1.35	31.2 ±0.9	...	...
1.48	32.5 ±0.8	56.6 ±0.5	26.4 ±1.0
1.60	32.5 ±0.8	...	...
1.73	32.5 ±0.6	54.9 ±0.5	24.3 ±0.8
1.95	30.5 ±0.4	51.3 ±0.7	22.7 ±0.9
2.48	26.9 ±0.5	47.8 ±0.6	22.6 ±0.9
2.97	25.3 ±0.4	46.2 ±0.4	22.4 ±0.7
3.98	25.4 ±0.7	44.7 ±0.5	20.5 ±0.9

ISOTOPIC COMPOSITION OF THE LOW-ENERGY HELIUM NUCLEI IN THE PRIMARY COSMIC RADIATION.

M. V. K. Appa Rao,* University of Rochester, Rochester, New York (Received February 13, 1961).

The isotopic composition of low-energy helium nuclei in the primary cosmic radiation has been determined by using the "constant sagitta" scattering method on tracks of helium nuclei stopping in a nuclear emulsion stack flown at a geomagnetic latitude $\lambda = 55°$N and at a mean atmospheric depth of 8.5 grams/cm^2; tracks with zenith angles less than 30° were accepted. The ratio of $He^3/(He^3+He^4)$ for the same energy per nucleon (between 200 and 400 Mev) is found to be 0.41 ± 0.09 at flight altitude. The correction for production of secondary He^3 in the residual atmosphere is calculated to be 4%. If one assumes no He^3 nuclei are present at the source, the observed ratio corresponds to a traversal of 14 ± 3 grams of interstellar matter by the low-energy helium nuclei. The value of $He^3/(He^3+He^4)$ corresponding to the same magnetic rigidity (between 1.3 and 1.6 Bv) is found to be 0.36 ± 0.11, which corresponds to a traversal of 12.2 ± 3.5 grams of interstellar mat-

ter. The observed ratio may indicate the presence of He^3 at the source of cosmic rays, or may be a reflection of local production within the solar system.

*On leave of absence from Tata Institute of Fundamental Research, Bombay 5, India.

COMPOSITE MODEL AND PARTIALLY CONSERVED CURRENTS IN WEAK INTERACTIONS. S. Okubo and R. E. Marshak,* CERN, Geneva, Switzerland (Received February 21, 1961).

It is shown that the idea of partially conserved currents has a natural basis in the composite model. Within this framework, the Goldberger-Treiman relation for the pion lifetime is discussed without recourse to dispersion theory.

*On leave from the University of Rochester, Rochester, New York.

RELATIVISTIC ELECTRON-PAIR SYSTEMS AND THE STRUCTURE OF NEUTRAL MESONS. Ernest J. Sternglass, Westinghouse Research Laboratories, Pittsburgh, Pennsylvania (Received February 13, 1961).

In an effort to obtain a semiclassical model for the neutral π meson, a Bohr-Sommerfeld type of system with the proton replaced by a positron is investigated in the limit of high velocities. It is found that as a result of the relativistic increase in the electromagnetic field between the two moving charges, a natural minimum approach distance occurs equal to one half of the classical "shell-electron" radius. At this separation, a new set of quantized states becomes possible which is found to be energetically unstable. The lowest state possesses an energy approximately equal to the π^0-meson energy. The relativistic states are characterized further by the greatly increased importance of perihelion precession, which accounts for one half of the total angular momentum in the extreme relativistic case. When the effect of precession on the intrinsic magnetic moment is taken into account, the total energy of the system is found to be $263\,m_0c^2$, in close agreement with the observed π^0-meson mass. The lifetime of the system against annihilation into two gamma rays is calculated on the basis of the close analogy to singlet positronium. Its value is found to be 2.06×10^{-16} sec, in good agreement with the latest value of the observed π^0-meson lifetime. The implications for the structure of other nuclear particles and their interactions are briefly discussed.

STRUCTURE OF RADIATIVE DECAY AMPLITUDES. H. Chew, Enrico Fermi Institute for Nuclear Studies and Department of Physics, University of Chicago, Chicago, Illinois (Received February 27, 1961).

It is shown that the matrix element for decay processes involving the emission of a single photon may be obtained from the matrix element for the corresponding nonradiative decay and the magnetic moments of the particles involved, up to terms that vanish as the photon frequency $K\to 0$. Detailed discussions are given for decays involving three and four spinless particles, as well as for four spin one-half particles. The results are similar to those obtained by Low for bremsstrahlung in scattering processes, but some novel features arise when the nonradiative decay is forbidden by selection rules.

LAGRANGIAN FORMALISM IN RELATIVISTIC DYNAMICS. G. Kalman, Department of Physics, Technion, Israel Institute of Technology, Haifa, Israel (Received April 28, 1960).

A covariant Lagrangian formalism is put forward with an explicit variation of the proper time in the action functional. This approach conforms with the geometrical interpretation in space-time. A general equation of motion is derived, which is not identical with the Euler-Lagrange equation. Momentum and mass are unambiguously defined through the requirement of translational invariance. The rest-mass is constant in the special case of electromagnetic field only. A conservation law for the combination of the momentum and the energy-momentum tensor of the free field is derived. No satisfactory Hamiltonian formalism can be established within the framework of the formalism.